DESIGN AND SYNTHESIS OF INHIBITORS OF DIHYDROFOLATE REDUCTASE

by

MICHELLE ANNE MEEK

A thesis submitted for the degree of

MASTER OF PHILOSOPHY

at

THE UNIVERSITY OF ASTON IN BIRMINGHAM

June 1988

Design and Synthesis of Inhibitors of Dihydrofolate Reductase

by

Michelle Anne Meek

Submitted for the degree of Master of Philosophy at Aston University, 1987.

The biochemical role of dihydrofolate reductase (DHFR) (EC 1.5.1.3) is discussed, together with the role of tetrahydrofolate in intermediary cellular metabolism. The development of classical folate analogues and non-classical, small molecule inhibitors, and some of the problems associated with their use in cancer chemotherapy is reviewed.

The novel lipophilic inhibitor of DHFR, methylbenzaprim, is the parent compound from which a series of analogues were synthesised. The preparative route to formation of these analogues involved the aromatic nucleophilic substitution of a series of substituted benzylamines onto m-nitropyrimethamine. The possibility of the preparation of an azido-substituted analogue of methylbenzaprim was also investigated.

The I_{50} values of methylbenzaprim and six analogues were determined against DHFR from rat liver. The K_{Iapp} and K_I values of six of these compounds were calculated using the equation for Zone B analysis. Some of the compounds exhibited K_I values comparable to that of methotrexate. These analogues were tested for *in vitro* cytotoxicity against murine leukaemia L1210 cells, and, from the results above, two compounds were screened for antitumour activity against the methotrexate-resistant M5076 reticulum cell sarcoma. The most lipophilic compound, the N-methylcarboxamide analogue of methylbenzaprim, exhibited activity against the M5076 sarcoma whilst the benzoic acid analogue was inactive.

The crystal structure of the parent compound, methylbenzaprim, was determined by direct methods. This revealed a space group of $P\bar{1}$ with four molecules in the unit cell and two independent molecules in the asymmetric unit. Quantum mechanical calculations were carried out, using the molecular orbital package MNDO, to study in closer detail the conformational and electronic characteristics of the molecule.

Keywords: Dihydrofolate Reductase
2,4-Diaminopyrimidines
Pyrimethamine
Lipophilic
Antitumour

To my parents

ACKNOWLEDGEMENTS

I would like to express my gratitude to Dr C Schwalbe, Dr P Lambert and Dr R Griffin for their guidance, support and friendship throughout this research project.

I would also like to thank Dr M Threadgill for his advice and help in the synthetic aspects of this research.

I also wish to thank Professor K Harrap, Dr H Calvert and Dr A Jackman at the Institute of Cancer Research, Sutton, Surrey for their help and co-operation with the biological studies.

I would like to acknowledge the University of Manchester Regional Computer Centre for the use of their facilities for the crystallographic computations.

I am grateful to the Science and Engineering Research Council for the financial support of this research project.

CONTENTS

LIST OF TABLES, FIGURES, PLATES AND SCHEMES

ABBREVIATIONS

ALL	acute lymphoblastic leukaemia
b.p.	boiling point
br.	broad
CNS	central nervous system
CSF	cerebrospinal fluid
D_m	measured density
D_x	calculated density
d	doublet
DHF	dihydrofolate
DHFR	dihydrofolate reductase
DNA	deoxyribonucleic acid
dTMP	deoxythymidine monophosphate
dUMP	deoxyuridine monophosphate
E	enzyme
E_t	total enzyme concentration
FAB	fast atom bombardment
h	hour(s)
I	inhibitor
I_t	total molar inhibitor concentration
i.m.	intramuscular
i.p.	intraperitoneal
i.r.	infra-red
K_I	inhibitor dissociation constant
K_{Iapp}	apparent inhibitor dissociation constant
K_m	Michaelis constant
MBP	methylbenzaprim
min	minute(s)
MNP	m-nitropyrimethamine

mRNA	messenger RNA
m.p.	melting point
m.s.	mass spectrum
NADPH	reduced form of nicotinamide adenine dinucleotide phosphate
n.m.r.	nuclear magnetic resonance
q	quartet
RNA	ribonucleic acid
s	singlet
S	substrate
sec	second(s)
t	triplet
THF	tetrahydrofolate
t.l.c.	thin layer chromatography
V	observed reaction velocity
V_i	inhibited reaction velocity
V_{max}	maximum reaction velocity
V_o	uninhibited reaction velocity
w/v	weight/volume
water	refers to double-distilled water

CHAPTER 1

INTRODUCTION

1.1 Biochemical Role of Dihydrofolate Reductase

An enzyme of vital importance in biochemistry and medicinal chemistry is dihydrofolate reductase (5,6,7,8-tetrahydrofolate:NADP+ oxidoreductase, EC 1.5.1.3, DHFR), which catalyses the NADPH-dependent reduction of 7,8-dihydrofolate (DHF) to 5,6,7,8-tetrahydrofolate (THF) (figure 1.1).

THF is essential in a series of enzymic reactions in cellular intermediary metabolism involving the transfer of a number of one-carbon groups[1]. These reactions at the oxidation levels of formate, formaldehyde and methanol, occur as steps in various metabolic sequences for the synthesis or degradation of purines, pyrimidines and amino-acids. THF forms adducts with the one-carbon fragments *via* covalent linkages at N-5 and N-10 which then enable the coenzyme to accept and donate these single carbon units to and from intermediates. Metabolites containing potential one-carbon units include: (1) inosinic acid, histidine, formiminoglutamate, formiminoglycine, *N*-formylglutamate, and formate at the formyl level; (2) serine, deoxycytidylate, glycine, and formaldehyde at the next lower oxidation state; and (3) methionine and thymidylate at the methyl level[2]. Figure 1.2 provides an outline of the metabolic interrelationships of the THF coenzymes[3].

An extremely important series of reactions is that of the thymidylate cycle, involving the enzymes serine hydroxymethyltransferase (SHMT), thymidylate synthase (TS) and (DHFR) (figure 1.3).

Figure 1.1 The reduction of 7,8-dihydrofolate to 5,6,7,8-tetrahydrofolate by DHFR

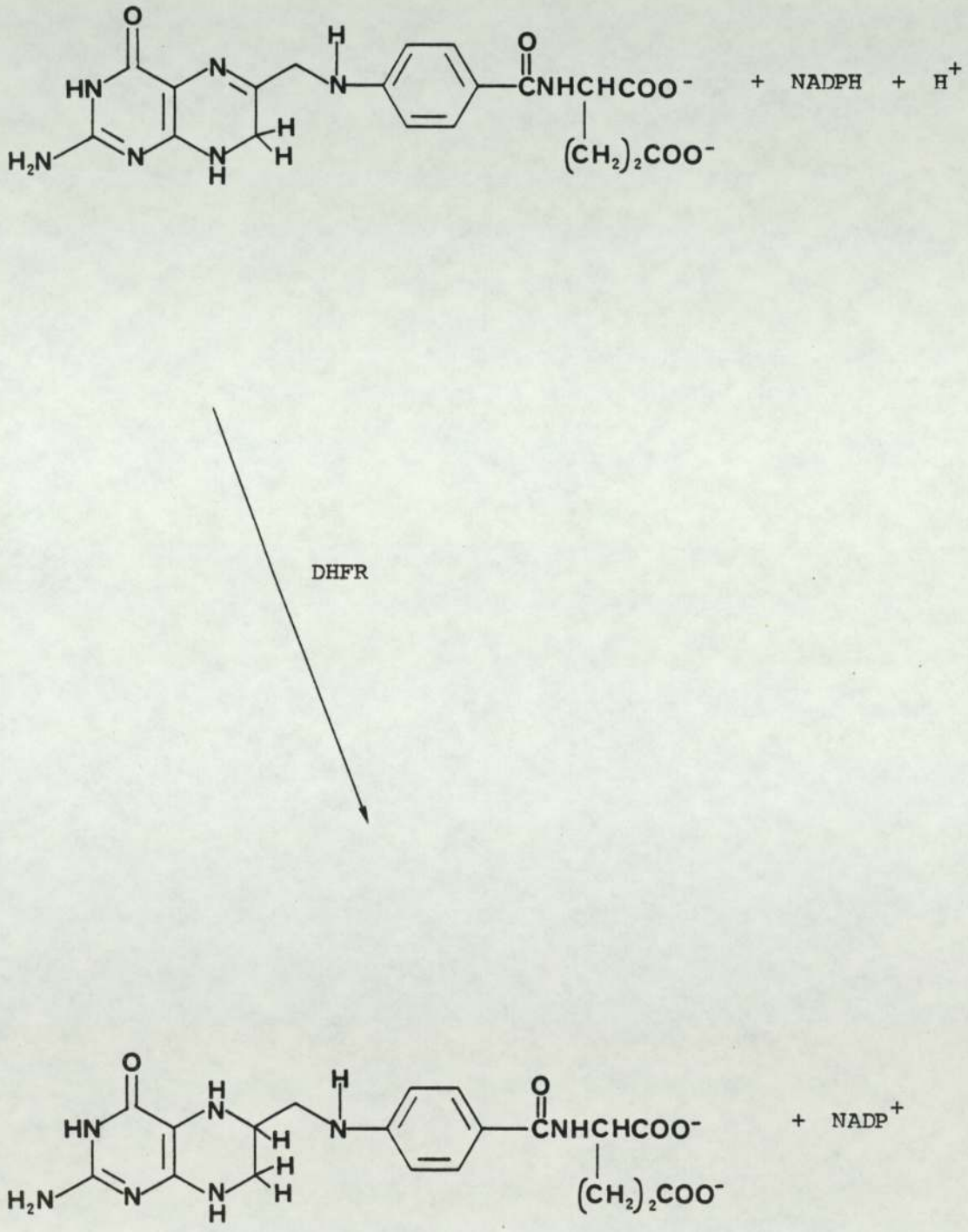

Figure 1.2 Metabolic interrelationships of tetrahydrofolate coenzymes

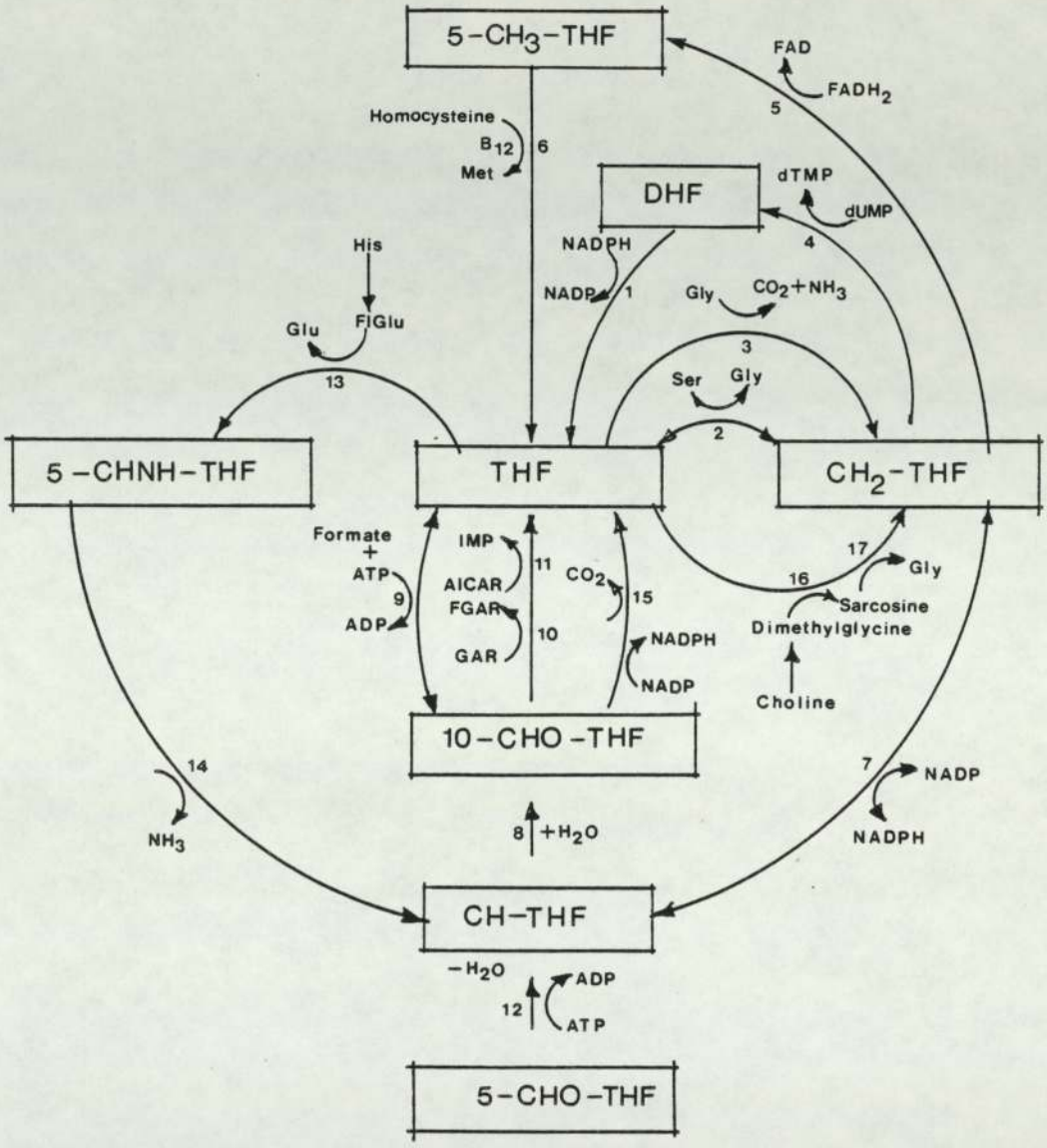

Abbreviations:
GAR glycinamide ribonucleotide
FGAR formylglycinamide ribonucleotide
AICAR aminoimidazolecarboxamide ribonucleotide
FIGlu formiminoglutamic acid
IMP inosinic acid
The enzymes catalysing the numbered reactions are listed in table 1.1.

Table 1.1 Enzymes involved in the metabolic interrelationships described in figure 1.2

1	Dihydrofolate reductase (EC 1.5.1.3)
2	Serine hydroxymethyltransferase (EC 2.1.2.1)
3	Glycine synthase (EC 2.1.2.10)
4	Thymidylate synthase (EC 2.1.1.45)
5	Methylenetetrahydrofolate reductase (EC 1.1.99.15)
6	5-Methyltetrahydrofolate-homocysteine methyltransferase) (EC 2.1.1.13)
7	Methylenetetrahydrofolate dehydrogenase (EC 1.5.1.5)
8	Methenyltetrahydrofolate cyclohydrolase (EC 3.5.4.9)
9	10-Formyltetrahydrofolate synthetase (EC 6.3.4.3)
10	Glycinamide ribonucleotide formyltransferase (EC 2.1.2.2)
11	Aminoimidazolecarboxamide ribonucleotide formyltransferase (EC 2.1.2.3)
12	5-Formyltetrahydrofolate cyclodehydrase (EC 6.3.3.2)
13	Formiminoglutamate:tetrahydrofolate formiminotransferase (EC 2.1.2.5)
14	Formiminotetrahydrofolate cyclodeaminase (EC 4.3.1.4)
15	10-Formyltetrahydrofolate dehydrogenase (EC 1.5.1.6)
16	Dimethylglycine dehydrogenase (EC 1.5.99.2)
17	Sarcosine dehydrogenase (EC 1.5.99.1)

Figure 1.3 Pathway showing regeneration of THF from DHF via a DHFR-catalysed reaction following the production of thymidylate

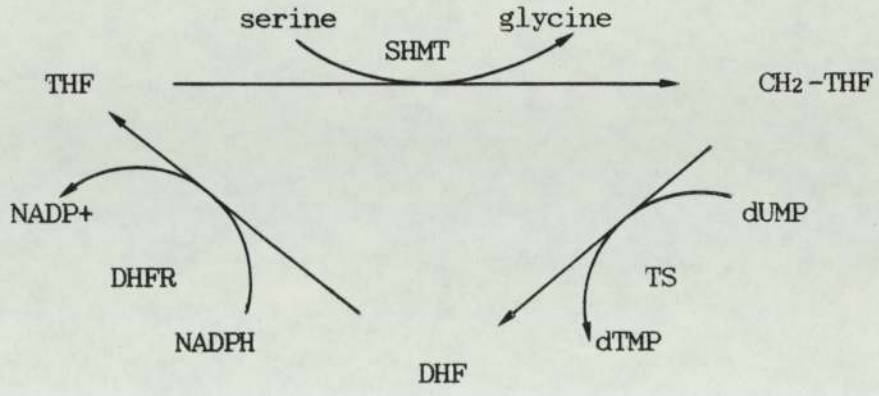

The biosynthesis of thymidylate, which is required in the synthesis of DNA, occurs from tetrahydrofolate via N^5,N^{10}-methylene tetrahydrofolate (CH_2-THF) in a reaction catalysed by thymidylate synthase[4,5]. Methylene tetrahydrofolate (CH_2-THF), in addition to providing a one-carbon unit to dUMP to form dTMP, acts as a reductant and is consequently oxidised to DHF. THF is then reformed by the reaction catalysed by DHFR shown in figure 1.3.

Consequently, a blockade of DHFR would result in accumulation of the metabolically inactive DHF, thus preventing the metabolism of essential one-carbon fragments. In this inhibited state, cells would then be unable to synthesise amino-acids such as serine and methionine, and nucleic acids such as purine and thymine, thus causing disruption of the synthesis of proteins, RNA and DNA. The biochemical reaction in figure 1.3 is the only known de novo source of thymidine, and so the blockade described above would cause disruption of DNA synthesis in a process described by Cohen[6] as "thymineless" death. Therefore DHFR is a prime target for inhibition by chemotherapeutic agents, as described below.

1.2 Inhibitors of Dihydrofolate Reductase

It was in 1946 that the structure of folic acid (1) was elucidated[7] and this was soon followed by the development of two important analogues of this vitamin. By replacing the 4-keto group of folic acid with a 4-amino group, Seeger et al, in 1947, produced aminopterin[8] (2), shortly followed in 1949 by its N-10 methyl derivative, methotrexate[9] (3). Both of these analogues of folic acid were found to be potent inhibitors of the growth of Streptococcus faecium (S.faecium). This work led on to the clinical studies by Farber et al[10], which showed that aminopterin produced temporary remissions in acute leukaemia in children, and Burchenal et al[11] who described the use of methotrexate in childhood leukaemia having obtained similar remissions.

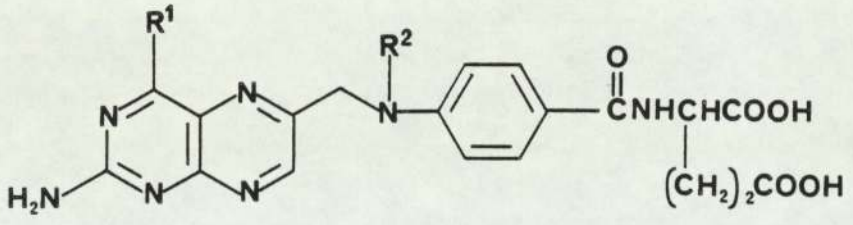

(1) folic acid $R^1 = OH$ $R^2 = H$ [as 4(3H)-one tautomer]

(2) aminopterin $R^1 = NH_2$ $R^2 = H$

(3) methotrexate $R^1 = NH_2$ $R^2 = CH_3$

It became clear by 1957[12,13,14] that dihydrofolate reductase is the target enzyme for these folate analogues. Hundreds of compounds have been synthesised since the 1940's in the search for effective antifolates. Detailed accounts of the development, therapeutic exploitation and mode of action of inhibitors of DHFR have been

published[15,16,17]. The search for species-specific drugs has had considerable success for antimicrobial chemotherapy with the use of trimethoprim (4)[18], and in the inhibition of plasmodial DHFR with the antimalarial pyrimethamine[19] (5).

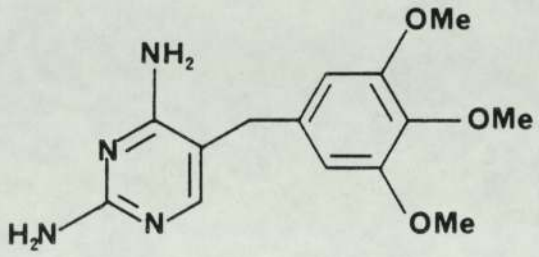

(4) Trimethoprim

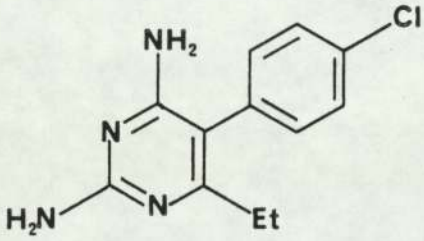

(5) Pyrimethamine

Similar selectivity has yet to be realised for anticancer agents, although methotrexate, which is used in the treatment of neoplastic and other proliferative diseases[20,21], is still one of the most widely used anticancer agents to date.

The many compounds that have been designed and synthesised as inhibitors of DHFR can be broadly divided into:-

(i)Folate analogues or classical inhibitors; and

(ii)Small molecule or non-classical inhibitors.

1.3. Folate Analogues or Classical Inhibitors of Dihydrofolate Reductase

Already mentioned is the 2,4-diamino analogue of folic acid, aminopterin[8] (2), and its N-10 methyl derivative methotrexate[9] (3), both of which are potent inhibitors of DHFR. Clinical studies showed that aminopterin is more toxic than methotrexate[22,23] and so it was removed from clinical use. Subsequently, it was shown that aminopterin was better transported into the gut cells of the mouse than methotrexate but not into tumour cells[24] which could explain its greater clinical toxicity.

Methotrexate is a stoichiometric inhibitor of DHFR[25] although it differs only slightly in structure from the natural substrates. Baker[16,26] presented evidence for the increased basicity at N-1 being crucial for the transition from substrate to potent inhibitor. This thinking was supported by the quantum chemical calculations of Perault and Pullman[27]. Over recent years x-ray crystallographic studies on the structures of several DHFRs have been carried out. These include those of the Escherichia coli (E.coli) binary complex with methotrexate and the Lactobacillus casei (L.casei, lc) ternary complex with methotrexate and NADPH[28-31], and that of the binary complex of chicken liver DHFR with a dihydrotriazine inhibitor bound to it[32]. These structures have provided important information about the binding of inhibitors to the enzyme. There was already much evidence to suggest that not only may methotrexate be protonated in the bound state but that it also binds somewhat differently to folic acid and DHF[33]. This evidence is supported by the crystallographic data of Bolin et al[30] which indicates a favourable charge-charge interaction between aspartate-26, lc and the protonated N-1 of methotrexate. Evidence for protonation is further supported by the

Figure 1.4 A schematic representation of hydrogen-bonding between DHFR from L.casei and the pteridine moieties of a) 7,8-DHF (hypothetical); and b) methotrexate

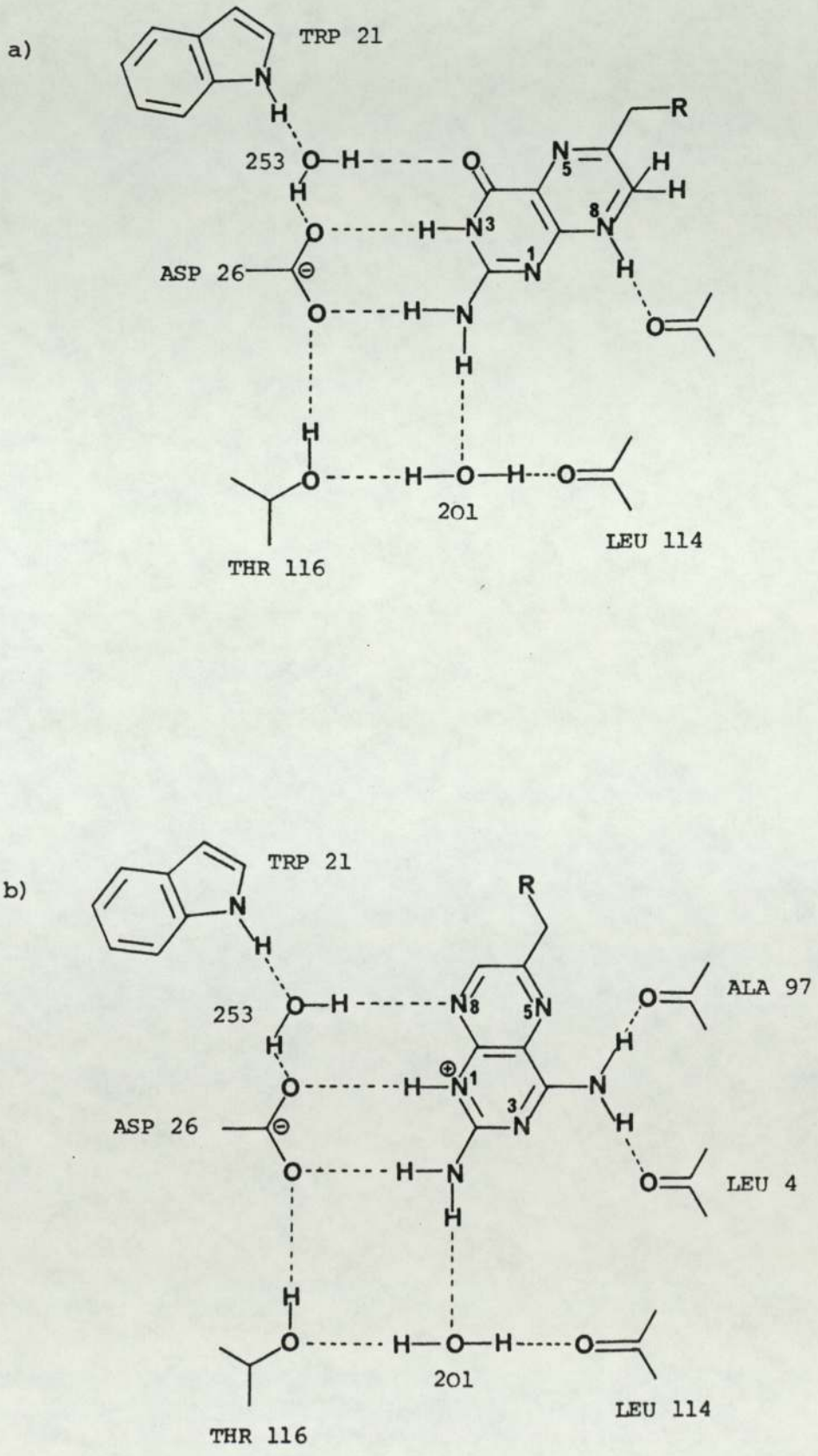

n.m.r data of Cocco et al[34]. Bolin et al[30] predicted a configuration of R at C-6 for THF if it is bound to DHFR in a similar conformation to methotrexate, but S if its pteridine ring is turned over. Fontecilla-Camps et al[35] and Charlton et al[36] provided evidence that folic acid and DHF must bind to the enzyme in a conformation that presents the opposite face of the pteridine ring to the nicotinamide cofactor, relative to the orientation of the pteridine ring of methotrexate bound to the enzyme. Figure 1.4 shows a model proposed by Bolin et al[30] for the binding of DHF and methotrexate such that there is a net loss of one protein ligand hydrogen-bond in the DHF complex relative to the binding of methotrexate in its complex as a result of replacing the 4-amino group of the inhibitor with the N-8 of the substrate. This fact, and the favourable charge-charge interaction between aspartate-26, lc and the N-1 protonated pteridine of methotrexate may be important factors in accounting for the differences in affinity between DHF and methotrexate.

A large number of folate analogues have been synthesised involving modifications of virtually every part of the folic acid molecule (figure 1.5):-

Figure 1.5

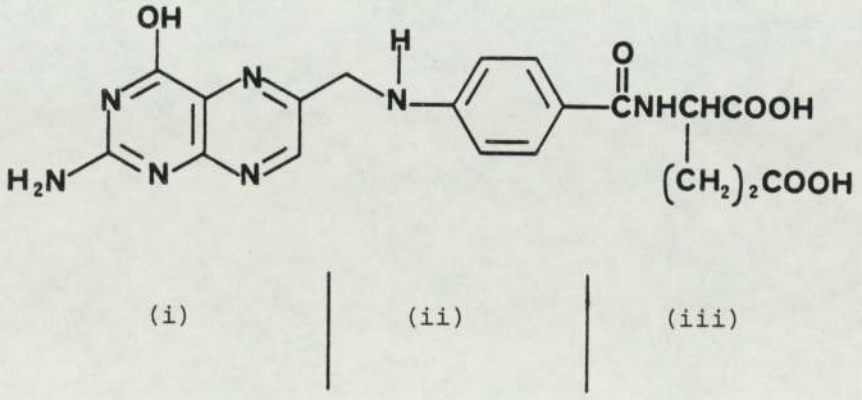

(i)the pteridine moiety;

(ii)the C9-N10 bridge and benzene ring; and

(iii)the glutamate moiety.

A detailed account of these modifications has been provided in a review by Montgomery and Piper[37].

The clinical response to methotrexate is closely related to the cellular uptake of the drug[38,39]. As methotrexate is a polar, lipid insoluble molecule it cannot be transported into cells by passive diffusion. It is transported *via* an active, carrier-mediated process shared by the reduced folates such as N^5-formyl-THF and N^5-methyl-THF[40,41].

As methotrexate is transported less well into normal murine cells than tumour cells it thus appears to exhibit relative selectivity for the tumour tissue[24,42]. Apart from employing methotrexate in various combination chemotherapy regimens[43], several other methods for improving the selectivity of methotrexate have been adopted. It was realised in the 1960's that methotrexate is a "schedule-dependent" drug, with an intermittent schedule of methotrexate treatment being a more effective maintenance therapy for acute lymphoblastic leukaemia (ALL) in remission than low dose daily treatment[44]. In 1949 Burchenal *et al*[45] found that the toxicity and biological activity of methotrexate are reversed by reduced folates such as N^5-formyl-THF (folinic acid, leucovorin, citrovorum factor) and THF. Goldin *et al*[46,47], in the early 1950's, recognised this as a way to improve selectivity with methotrexate. In the L1210 murine model the use of leucovorin allowed higher doses of methotrexate to be administered safely with improved therapeutic results. In ALL and lymphomas and some solid tumours, high dose methotrexate regimens with "leucovorin-rescue" appear safe and effective[48].

Other "rescue" techniques have been employed in an attempt to improve the selectivity of methotrexate. Studies of Borsa and Whitmore[49] indicated that thymidine could also partially prevent or reverse the effects of methotrexate. Nederbragt et al[50] have suggested that a thymidine-inosine combination may be more effective than leucovorin in providing selective protection.

The enzyme carboxypeptidase G_1 has been investigated in methotrexate rescue[51]. It cleaves glutamate residues from methotrexate and other folates and has been shown to rescue cells from methotrexate toxicity both in vitro and in vivo[38].

Asparaginase, an enzyme which has been found useful as an antitumour agent in the treatment of ALL for the induction of remission[52], has been investigated in the rescue of cells from the toxic effects of methotrexate. It has been shown that inhibitors of protein synthesis decrease the killing rate of agents that cause thymineless death[6]. Studies have demonstrated that two- to four-fold greater doses of methotrexate can be tolerated when asparaginase is given twenty four hours after administration of methotrexate than when methotrexate is given alone[53].

Due to the polar nature of methotrexate, it is prevented from penetrating into malignant cells that may be present in the cerebrospinal fluid (CSF) or brain[54]. There has been some success in achieving better CSF levels by using the high-dose methotrexate regimens with leucovorin[55], and intrathecal methotrexate is also used in an attempt to circumvent this problem. A number of analogues of methotrexate, including esters[56,57] and amides[58,59] have been synthesised with the aim of increasing lipid solubility and thus improving membrane transport but the results have been disappointing, with most derivatives being less active or only slightly more active than the parent amino-acid derivatives[56-59].

1.3.1 Resistance to Classical Antifolates

Despite being developed as an anticancer agent well over 30 years ago, methotrexate has remained the major antifolate in established clinical use in cancer chemotherapy. However, clinical resistance with methotrexate is a major problem which has not yet been adequately overcome. Tumours may be inherently resistant to methotrexate or they may acquire resistance as treatment progresses. Development of acquired resistance, for which examples will be given, has been attributed to[60]:-

(i) Increased levels of the drug-sensitive dihydrofolate reductase enzyme;

(ii) synthesis of an isoenzymatic form of this enzyme with decreased binding capacity for methotrexate;

(iii) impairment of the transport mechanism for the drug; and

(iv) defective polygammaglutamation of methotrexate.

It is clear that the increased levels of DHFR are due to selective amplification of the genes coding for DHFR[61] and this has been shown in a number of experimental systems. Schimke et al[62] reported that in two sublines of the murine sarcoma 180, a 250-fold elevation of DHFR activity was accompanied by a proportional 250-fold increase in cellular DHFR mRNA content associated with genes coding for this enzyme. Melera et al[63] detected overproduction of DHFR accompanied by increased levels of DHFR-specific mRNA in a series of independently derived sublines of Chinese hamster cells.

Several cell systems which have acquired resistance to methotrexate subsequent to exposure to the drug have been shown to have altered forms of DHFR[64,65]. In 1977 Jackson and Niethammer[66] isolated the first human DHFR with altered kinetic properties and altered affinity for methotrexate from human lymphoblastic cells in vitro.

Since methotrexate is transported across cell membranes *via* an active carrier-mediated process[40,41], impaired transport will play an important role in resistance of neoplastic cells, with a resulting decreased permeability for the drug[67]. Evidence for an alteration in the carrier mechanism is corroborated by the fact that the uptake of N^5-methyl-THF is markedly reduced in methotrexate-resistant cell sublines[68]. A related mechanism of resistance that has been proposed is the protection of the cells against the non-lipophilic methotrexate by the development of lipophilic barriers. Studies by Burns *et al* demonstrate that lipid modifications in L1210 cells produced by diet are associated with changes in the plasma membrane fatty acid composition which would thus affect methotrexate transport[69].

It is evident that folate coenzymes exist intracellularly as polygammaglutamates and that these compounds are the natural cofactors for the one-carbon metabolism, thus being essential for cell growth[70]. It appears that methotrexate is also converted, by folylpolyglutamate synthetase, to polyglutamates[71] which are at least as potent at inhibiting DHFR as methotrexate[72]. Unlike methotrexate, the polyglutamyl derivatives are retained in the cell[73], thus prolonging the activity of the drug. However, evidence now suggests that defective polyglutamation may play a role in methotrexate resistance[74,75].

The development of resistance by more than one mechanism in a heterogeneous population of tumour cells has been observed[76]. Cowan *et al*[77] have characterised a human breast cell line with multiple defects.

1.4. Small Molecule or Non-Classical Inhibitors of Dihydrofolate Reductase

An approach to circumventing resistance of folate analogues has been the development of new non-classical small molecule inhibitors as antitumour agents. These would have a high lipid solubility so that cellular uptake may be increased and these compounds may then penetrate into the central nervous system (CNS) by simple passive diffusion rather than the carrier-mediated active process utilised by the reduced folates and methotrexate[40,41], Thus they may also be of use in the treatment of methotrexate-resistant tumours due to impaired transport of methotrexate[78,79], or defective polyglutamation since the absence of a glutamate residue precludes the formation of polygammaglutamates. These inhibitors may also have a role to play in the treatment of methotrexate-resistant tumours by virtue of an altered enzyme, as indicated by Hamrell[80] who demonstrated collateral sensitivity to several lipophilic inhibitors with a methotrexate-resistant 3T6 murine cell line characterised by an enzyme with altered affinity for the drug. Such inhibitors include 2,4-diaminopyrimidines[81-83], dihydrotriazines[84], quinazolines[85] and pyridopyrimidines[86] of which the first category will be considered in more detail.

Jonak et al[81,82] synthesised a number of pyrimidines with lipophilic substituents in the 5- and 6-positions. It was found that the 2,4-diaminopyrimidines with an adamantyl group in position 5 are good inhibitors of mammalian DHFR and show high inhibitory activity against the mouse mammary adenocarcinoma cells (TA3)[87]. The most effective adamantyl pyrimidines were found to be 2,4-diamino-5-(1-adamantyl)-6-ethylpyrimidine (DAEP) (6) and 2,4-diamino-5-(1-adamantyl)-6-methylpyrimidine (DAMP)[88] (7).

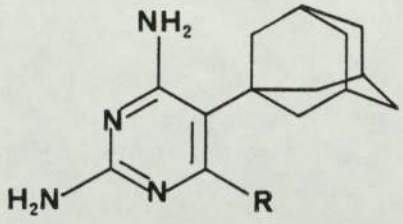

(6) DAEP R = Et

(7) DAMP R = Me

DAMP has an affinity for DHFR 100-fold lower than that of methotrexate but its activity in cell culture is equipotent to or greater than that of methotrexate[87], indicating that the lipophilic 5-substituent facilitates the passage of pyrimidines through the plasma cell membrane.

In a study of the correlation between the affinity of a series of 5-alkyl diaminopyrimidines for DHFR and their hydrophobicity, Ho et al[89] observed that the higher affinity of the adamantyl substituted pyrimidines may be due to the rigidity of these structures. Interestingly, the 5-(1-naphthyl) analogue of DAMP (DNMP) (8), which exhibits a similar lipophilicity to DAMP, is inactive against mammalian DHFR. In a structural comparison of these compounds it was shown that the 5-substituents occupy different regions in space, the volume of the naphthyl ring extending beyond that occupied by the adamantyl ring. In computer-modelling studies using the L.casei DHFR-methotrexate-NADPH ternary complex, Cody and Zakrzewski[90] went on to show that on superimposition of DAMP onto methotrexate in the active site of DHFR, the adamantyl ring occupied a hydrophobic pocket,

whilst a similar situation was not observed with DNMP and no single orientation was found to be satisfactory.

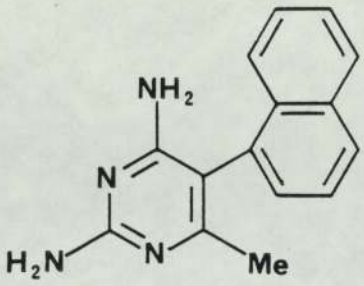

(8) DNMP

As far back as 1951 2,4-diamino-5-(3,4-dichlorophenyl)-6-methylpyrimidine (metoprine, DDMP) (9) and its 6-ethyl analogue (etoprine, DDEP) (10) were recognised, along with pyrimethamine (5), as antimalarial agents[83].

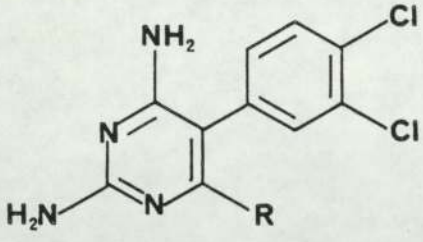

(9) Metoprine R = Me

(10) Etoprine R = Et

In an early study, the potential of using metoprine for the treatment of leukaemia was explored but results did not appear to be promising, with major toxicities to the bone marrow, gastrointestinal tract, and skin, and so interest in this compound declined[91]. In retrospect, the

toxicity observed in clinical studies with daily administration of small doses of the drugs was due to very long persistence in the body[92]. With the recognition of the need for the development of lipophilic folate antagonists interest in these pyrimethamine analogues was renewed. Geils et al[93] observed that pyrimethamine induced a complete remission of meningeal leukaemia for 6 months in an adult suffering from acute myeloblastic leukaemia. It was found that the more potent inhibitors of mammalian DHFR, metoprine (9) and etoprine (10), readily enter the cerebrospinal fluid (CSF) and penetrate into brain tumours in the rat[94]. However, clinical studies with metoprine have shown that its potential was limited by a long biological half-life (greater than 200 hours in man). It was found to be extensively bound to human plasma protein at therapeutic doses. Treatment with metoprine required simultaneous "rescue" therapy with calcium leucovorin to protect bone marrow and mucosal tissues[95]. An additional problem with metoprine was the neurological side-effects due possibly to inhibition, by DDMP, of histamine N-methyltransferase thus causing elevated histamine levels in the brain and other tissues[96].

2,4-Diamino-5-(3-azido-4-chlorophenyl)-6-ethylpyrimidine (MZP) (11), an azido analogue of pyrimethamine, was developed by Bliss[97]. Owing to its inherent antitumour activity, together with some favourable physicochemical characteristics (potent inhibition of mammalian DHFR (K_I 10^{-9} M), lipophilicity comparable to that of metoprine with a shorter half-life, a pKa of 7.19 which is close to physiological pH and easy formulation as the ethanesulphonate salt) it has warranted evaluation as a lipophilic inhibitor of DHFR[98]. It was proposed that with an azido substituent that is both lipophilic and readily degradable, these properties would provide a drug with a usefully short half-life.

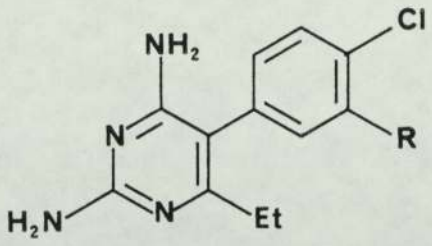

(11) MZP R = N_3

(12) MAP R = NH_2

It has been suggested that the bioreduction of MZP to the relatively polar arylamine (MAP) (12), which has been identified in the urine of mice following administration of MZP[99], should preclude any association with the hydrophobic domain of DHFR, resulting in a loss of activity. The formation of a basic centre at a site remote from the pyrimidine ring may result in protonation on the aromatic ring with subsequent loss of activity. However, results have shown that this amine does in fact exhibit weak inhibitory activity against DHFR[98]. This is supported by n.m.r studies which have since shown that the second protonation of this amine only takes place at high acid strengths[100].

MZP has entered the clinic as a lipophilic antifolate and has recently undergone Phase I evaluation as the ethanesulphonate salt[101]. The mean elimination half-life of MZP in man has been found to be approximately 34 hours which is indeed favourably shorter than metoprine with a half life of over 200 hours in man.

Other DHFR inhibitors that have elicited interest as non-classical antifolates include the quinazolinediamine trimetrexate (2,4-diamino-5-methyl-6-[(3,4,5-trimethoxyanilino)methyl]quinazoline)[85] (13) and

the pyridopyrimidine BW301U (piritrexim; 2,4-diamino-6-(2,5-dimethoxybenzyl)-5-methylpyrido-[2,3-d]pyrimidine)[86] (14).

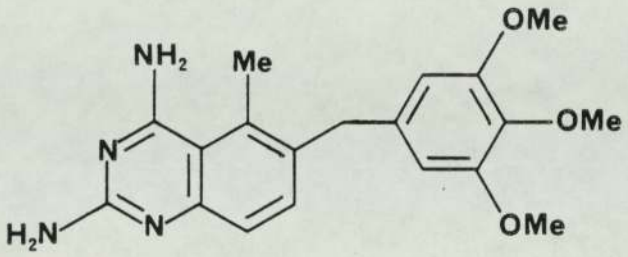

(13) Trimetrexate

Preliminary studies showed trimetrexate (13) to have a broad spectrum of antitumour effects against murine tumours in vivo[102]. Despite the fact that trimetrexate has been shown to inhibit histamine N-methyltransferase[96], this drug was chosen for clinical trial with the promise of showing a broader spectrum of activity in human tumours than methotrexate and being active against methotrexate-resistant tumours. On evaluation against a variety of methotrexate-resistant human tumour cell lines, trimetrexate showed activity against sublines with defective methotrexate transport, but, along with other lipophilic inhibitors, showed considerable cross-resistance to sublines with elevated levels of DHFR[78]. Phase I studies have shown definite antitumour activity, with some side-effects[103]. Phase II studies are now underway[104].

BW301U (14) was selected for evaluation as an antitumour agent as it has been found to be as active as methotrexate as an inhibitor of DHFR and mammalian cell growth in culture, with minimal effects on histamine metabolism[105].

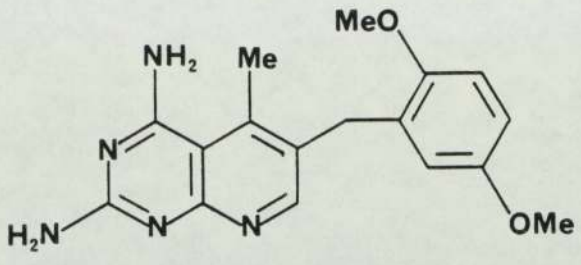

(14) BW301U

1.5. Activity of Diaminopyrimidines Unrelated to Inhibition of Dihydrofolate Reductase

The possibility that some of the growth inhibitory effects of diaminopyrimidines might be mediated through association with a locus or mechanism of action unrelated to DHFR was investigated by Griffin[98].

Hamrell and Sedwick[106] studied the action of equimolar concentrations of methotrexate and metoprine against the methotrexate-resistant (by virtue of elevated DHFR) mouse fibroblast 3T6 cell line. At concentrations of methotrexate that were found to be ineffectual, metoprine inhibited deoxyuridine incorporation into DNA by 80% compared to untreated control. It was suggested that sensitivity of deoxyuridine incorporation to metoprine was not fully explained by the ability of the drug to block DHFR. Greco and Hakala[88] have shown that the toxicity of a series of lipophilic diaminopyrimidines to various mammalian cell lines was not totally reversed by folinic acid, suggesting a second folate-independent site of action for these compounds. This was dissimilar to methotrexate, the activity of which was antagonised by folinic acid. However, cultured cell studies by Browman et al[107] on the intracellular mechanism of action of

metoprine have indicated DHFR to be the only cytotoxic locus of action of metoprine, but these studies were conducted at concentrations lower than those used by Greco and Hakala.

Further evidence for an alternative locus of action for diaminopyrimidines has been observed by Kavai et al[108]. They have shown that two chemically similar naphthyl derivatives of 2,4-diaminopyrimidine may have different mechanisms of action. Although the 2-naphthyl derivative is a competitive inhibitor of DHFR, results have shown the 1-naphthyl isomer to be a weak non-competitive inhibitor of DHFR. This isomer inhibits cell growth at substantially lower concentrations than it does DHFR, suggesting that this enzyme is not the only target of action of this compound.

Duch et al[105] have also observed that, unlike methotrexate, the cytotoxicity of the pyridopyrimidine BW310U cannot be completely reversed by the addition of hypoxanthine and thymidine to a standard culture medium containing glycine, but also requires the addition of nucleosides. However the biochemical basis for this difference between BW310U and methotrexate as yet remains unclear.

1.6 Rationale and Objectives

The previous sections have highlighted some of the problems associated with antifolate chemotherapy today and the need for the development of novel lipophilic antifolates.

As discussed in section 1.5 there is evidence to indicate a folate-independent site for the activity of 2,4-diaminopyrimidines. In an effort to develop biological probes for this folate-independent site Griffin[98] discovered a series of novel N-alkylbenzylaminopyrimidines which are potent inhibitors of DHFR, and of which (16) and (17), but

not (15), exhibit <u>in vivo</u> antitumour activity against the P388 lymphocytic leukaemia.

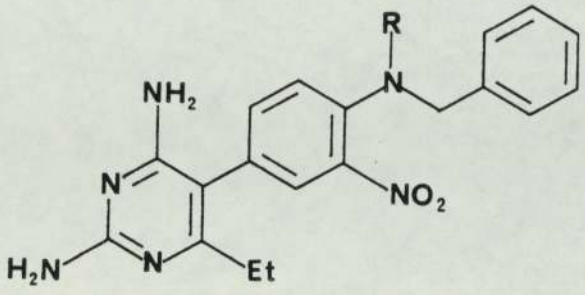

(15) Benzaprim R = H

(16) Methylbenzaprim R = Me

(17) Ethylbenzaprim R = Et

The binding of folates to DHFR is thought to involve association at a minimum of four regions with the enzyme active site[109] (figure 1.6):-

(i) a pteridyl or pyrimidine region;

(ii) the hydrophobic domain;

(iii) the p-aminobenzoyl region; and

(iv) the glutamate or polyglutamate region.

The high activity and lack of species selectivity of methotrexate has been attributed to association with all four binding regions while metoprine may only bind to regions (i) and (ii). The <u>N</u>-alkylbenzylaminopyrimidine, methylbenzaprim (MBP) (16), may be contorted to associate with binding regions (i), (ii) and (iii) on the enzyme and thus exhibit inhibitory properties intermediate between metoprine and methotrexate[98]. The object of this research was to design and synthesise analogues of MBP encompassing various substituents with the aim of developing a more potent, lipophilic, tight-binding inhibitor of DHFR. On the basis of the above hypothesis

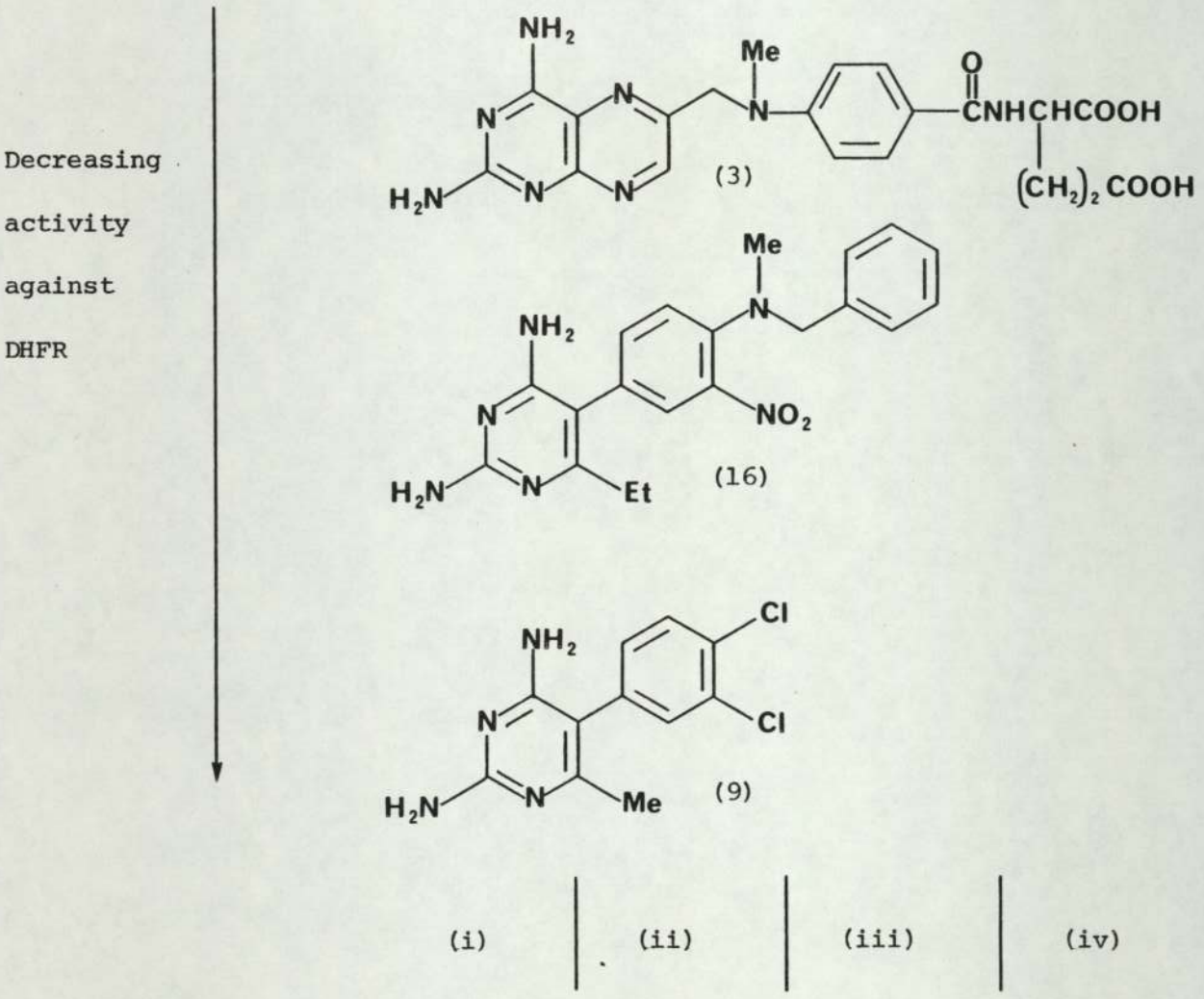

Figure 1.6 Structural similarities between methotrexate, methylbenzaprim and metoprine

an analogue of MBP embracing a glutamate residue in the 4-position of the benzyl ring (18) would also be of interest since, if indeed it is bound in the active site in a similar manner to methotrexate it would therefore be predicted to exhibit activity against DHFR comparable to that of methotrexate.

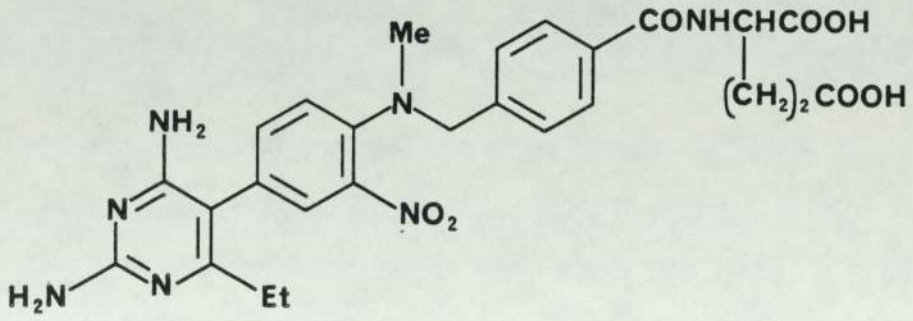

(18)

The compounds would be tested for <u>in vitro</u> activity against mammalian DHFR and then, for compounds exhibiting promising activity against DHFR, preliminary cytotoxicity studies <u>in vitro</u> against L1210 cells would be carried out. Taking the results of these studies into consideration, any promising compounds would then be screened for antitumour activity using murine tumour models.

Owing to the potent activity of the parent compound, methylbenzaprim, against mammalian DHFR, study of this compound in closer detail is warranted, with regard to its conformational and electronic characteristics. This requires the elucidation of the x-ray crystallographic structure of the compound. Accurately determined atomic co-ordinates would then be used to investigate the possible interactions of this type of compound with DHFR, applying quantum mechanical calculations to determine energetically favourable conformations and electronic distribution. Methylbenzaprim and the

analogues synthesised would also be tested against DHFR from E.coli since activity against the bacterial enzyme would justify study of these compounds, using molecular graphics, in the active site of this enzyme, for which the crystallographic co-ordinates are available.

CHAPTER 2

SYNTHESIS OF ANALOGUES OF METHYLBENZAPRIM

There are several possible approaches to the preparation of analogues of methylbenzaprim (16). Various retrosynthetic disconnections of the target structure can be made (scheme 2.1); for example, the 4-[N-(alkylbenzyl)-N-methylamino]-3-nitrophenyl portion of the molecule could be prepared initially, with subsequent synthesis of the 2,4-diaminopyrimidine (scheme 2.1.A). However, this requires conditions which may be too extreme for the survival of desired functional groups of the proposed analogues. The widely used method of Russell and Hitchings[110] for the preparation of 2,4-diaminopyrimidines requires the acylation of an arylacetonitrile followed by condensation with guanidine. This is achieved by heating the compounds under reflux in ethanolic sodium ethoxide for several hours. An alternative disconnection would be synthesis of 2,4-diamino-5-(4-methylamino-3-nitrophenyl)-6-ethylpyrimidine followed by alkylation with the required substituted benzyl halide or tosylate (scheme 2.1.B). However, the most obvious and useful disconnection is that described below, with treatment of nitropyrimethamine (2,4-diamino-5-(4-chloro-3-nitrophenyl)-6-ethylpyrimidine, MNP) (19) with the synthesised para-substituted benzyl-N-methylamino derivatives (scheme 2.1.C).

Bliss[97] treated pyrimethamine (5) with a mixture of concentrated nitric and sulphuric acids at 10°C for 12 hours to produce nitropyrimethamine (19). The electron-withdrawing nitro-substituent in the 3-position renders the aryl ring susceptible to nucleophilic attack in the 4-position, with displacement of the 4-chloro group, in a process known as aromatic nucleophilic substitution, S_NAr. As is

Scheme 2.1 Possible approaches to the preparation of analogues of methylbenzaprim

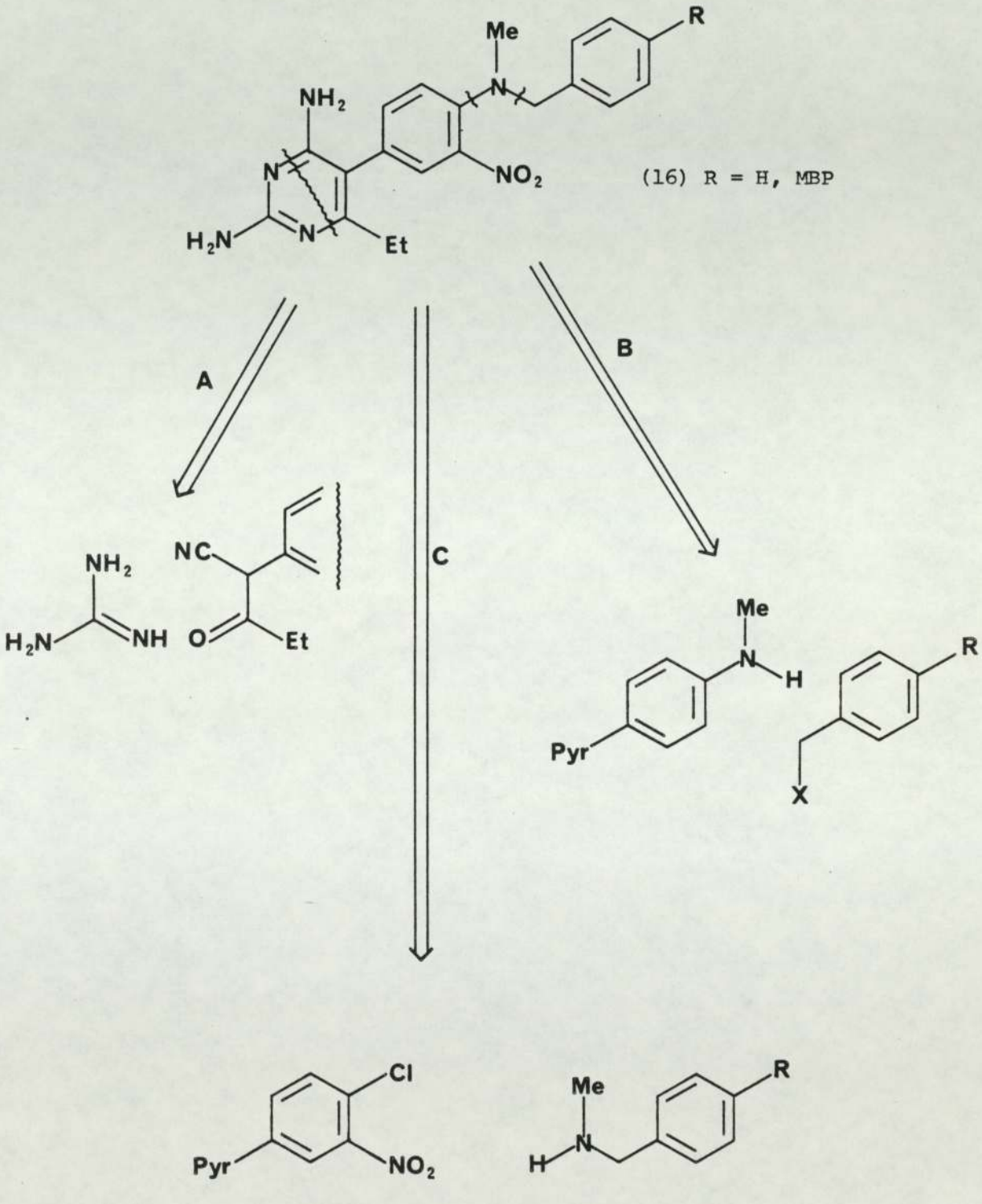

(19)

Pyr = 2,4-diamino-6-ethylpyrimidin-5-yl

the case here, the requirement for successful nucleophilic substitution at an aromatic centre is activation by an electron-withdrawing group ortho and/or para to the leaving group. This mechanism is sometimes called $S_N2(Ar)$ as evidence indicates it to be a bimolecular process (scheme 2.2)[111]. Griffin[98] recognised nitropyrimethamine to be a possible starting material for the N-alkylbenzylamino diaminopyrimidines that showed potent inhibitory activity against DHFR (15,16,17), finding that treatment of nitropyrimethamine with excess boiling benzylamine for 4 hours afforded 2,4-diamino-5-(4-benzylamino-3-nitrophenyl)-6-ethylpyrimidine (15) which was isolated by precipitation on addition of ether. Similar reactions with N-methylbenzylamine and N-ethylbenzylamine yielded the corresponding N-alkylbenzylamino diaminopyrimidines (16 and 17).

In considering the synthesis of analogues of methylbenzaprim, owing to the relative ease of the above reaction, nitropyrimethamine was again chosen as the starting point for reaction with the relevant amines.

Treatment of nitropyrimethamine (19) with an ester of 4-(methylaminomethyl)benzoic acid would thus furnish ester analogues of methylbenzaprim. This was of importance, not only for the compounds themselves, but also as a precursor for the synthesis of the benzoic acid analogue of MBP, which may subsequently lead onto the synthesis of the corresponding glutamic acid homologue (18).

Due to the therapeutic success of the lipophilic antifolates trimetrexate[85] (13) and BW301U[86] (14), both of which carry methoxy substituents on the terminal aromatic ring, it was considered that the enzyme inhibitory activity of analogues of MBP (16) and BZP (15) encompassing a 4-methoxy substituent would be extremely interesting.

Scheme 2.2 Mechanism of aromatic nucleophilic substitution onto an ortho-nitro-substituted benzene ring

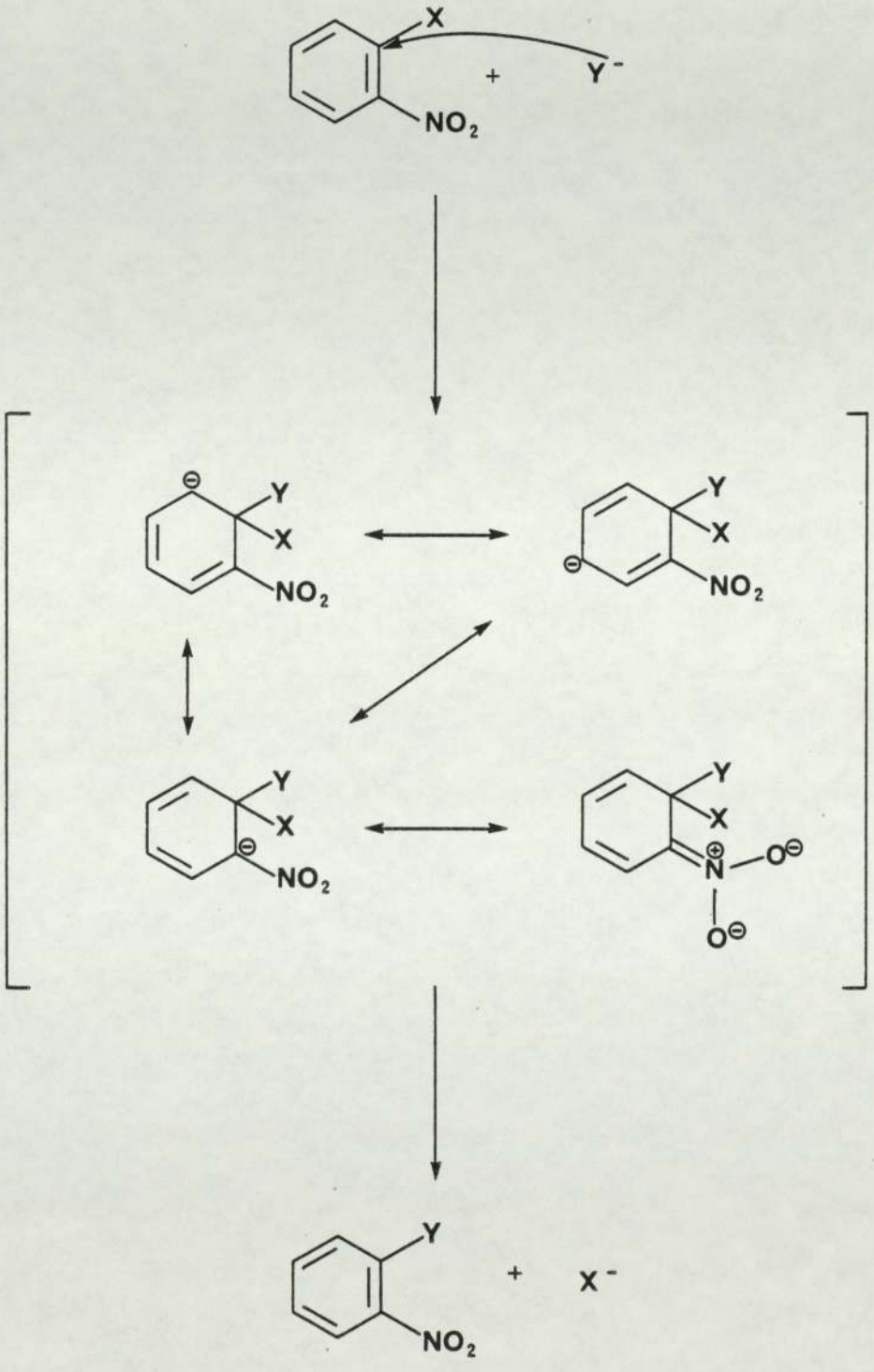

It can be seen that the anticancer drug methotrexate (3) has an amide group in the para-position on the terminal aromatic ring from the pteridine. Thus it was considered of interest to develop an analogue of MBP encompassing an amide substituent.

In preparation of an appropriate ester, 4-carboxybenzaldehyde (20) was treated with ethanol, utilising toluene-4-sulphonic acid as catalyst. This afforded a mixture of ethyl 4-formylbenzoate (21) (36%) and the corresponding diethyl acetal (22) (64%), shown to be so by comparison of the n.m.r spectrum with that reported in the literature[112]. The unwanted acetal was, however, converted by aqueous acid hydrolysis to give a good yield of the desired compound (21)(scheme 2.3). Synthesis of the secondary amine, ethyl 4-(methylaminomethyl)benzoate, required the reductive alkylation of the aldehyde to the amine via production of the imine ethyl 4-(methyliminomethyl)benzoate (23). Various methods are described for performing this reductive amination[113]. Initially, ethyl 4-formylbenzoate (21) was treated, in glacial acetic acid, with 40% aqueous methylamine to form the Schiff's base. This was followed by attempted reduction of the equilibrium amount of iminium ion by the addition of sodium cyanoborohydride. The reaction mixture was stirred at room temperature until the reaction had gone to completion (as indicated by the absence of starting material on t.l.c.). After the addition of excess sodium carbonate, the reaction mixture was extracted with ethyl acetate and the solvent was evaporated. However, spectral analysis (n.m.r, i.r, m.s) of the product showed it to be ethyl 4-(hydroxymethyl)benzoate (24), indicating that the Schiff's base had not in fact been formed in the first stage of the reaction. A two-step approach to form the substituted N-methylbenzylamine was therefore used. To prepare and isolate the intermediate imine (23), ethyl 4-formylbenzoate in toluene was treated with gaseous

Scheme 2.3 Synthetic route to ethyl 4-(methylaminomethyl)benzoate

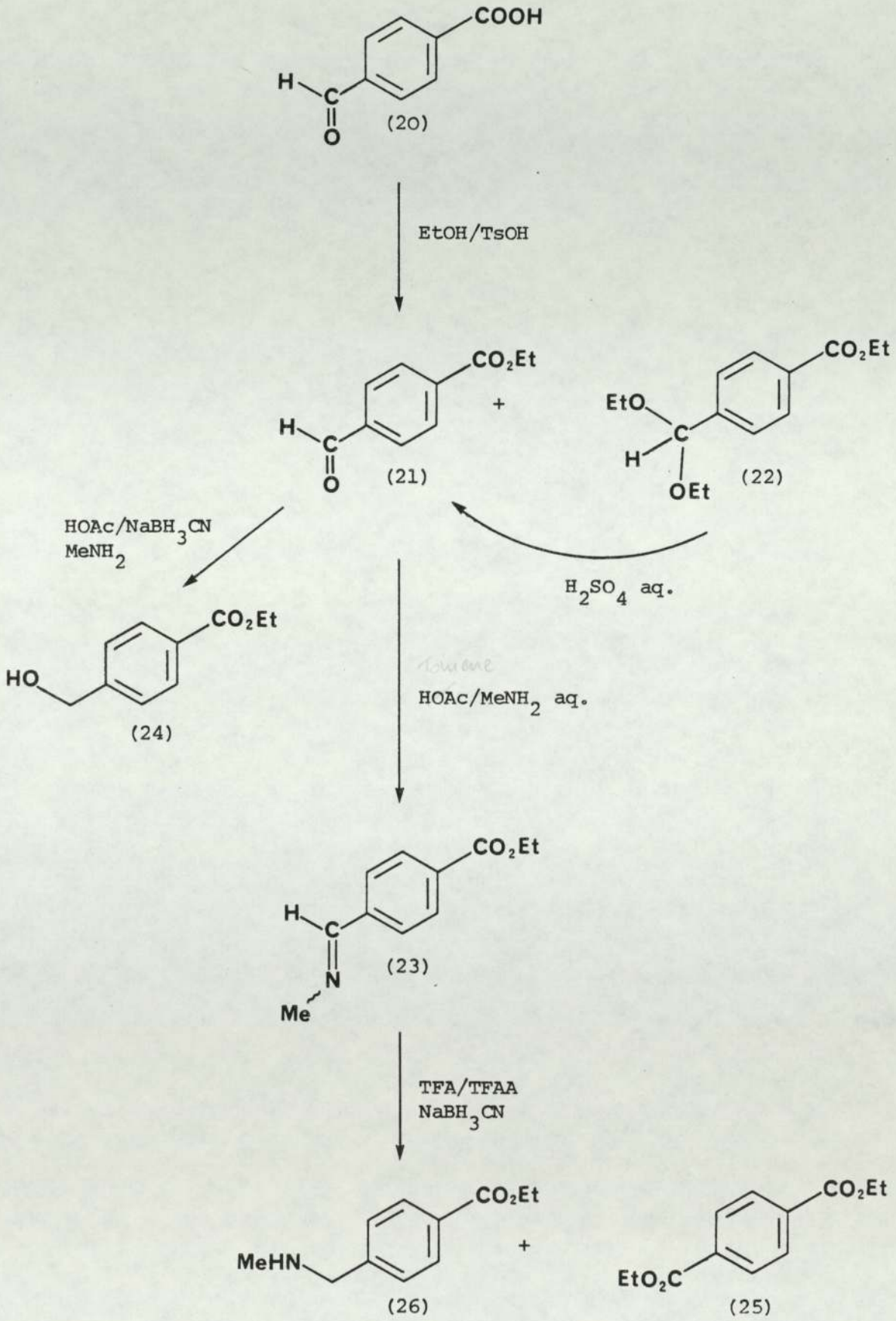

methylamine. Catalytic hydrogenation of (23) in ethanol with palladium/charcoal for 30 hours proved unsuccessful, spectral analysis indicating the presence of starting material only. The imine (23) was successfully reduced with sodium cyanoborohydride in trifluoroacetic acid (TFA) containing a small amount of trifluoroacetic anhydride (TFAA) to ensure anhydrous conditions. Separation of the product mixture by column chromatography afforded diethyl benzene-1,4-dicarboxylate (25) (6.5%), which had perhaps been formed in a possible Cannizzaro-like process, and the desired compound ethyl 4-(methylaminomethyl)benzoate (26) as a yellow oil (77%).

Owing to the difficulty of the above method, an alternative route (scheme 2.4) to the synthesis of an ester of 4-(methylaminomethyl)benzoic acid was considered, with the preparation of methyl 4-(methylaminomethyl)benzoate (27). Two synthetic routes were investigated. Firstly, 4-(chloromethyl)benzoic acid in methanol was treated with thionyl chloride to furnish methyl 4-(chloromethyl)benzoate (28) as a yellow liquid. This was heated under reflux with 40% aqueous methylamine in propan-2-ol, with sodium iodide as catalyst. ^{1}H n.m.r analysis of the product indicated the presence of the desired compound (27) and the corresponding N-methylamide (29) as a side product.

Alternatively, the following two-step reaction yielded the required ester (27). 4-(Chloromethyl)benzoic acid was heated under reflux in 40% aqueous methylamine to form 4-(methylaminomethyl)benzoic acid as the methylamine salt (30). The ^{1}H n.m.r spectrum of the crude product mixture from this reaction indicated that a minor side-product was N,N-bis(4-carboxybenzyl)methylamine (δ_H [60 MHz; D_2O] 2.35(3H, s, NCH_3), 3.86(4H, s, $ArCH_2N$), 7.26(4H, d, J 8.5 Hz, ArH) and 7.74(4H, d, J 8.5Hz, ArH)). However, this impurity was removed upon

Scheme 2.4 Synthetic route to the methyl- and 2-ethoxyethyl-esters of 4-(methylaminomethyl)benzoic acid

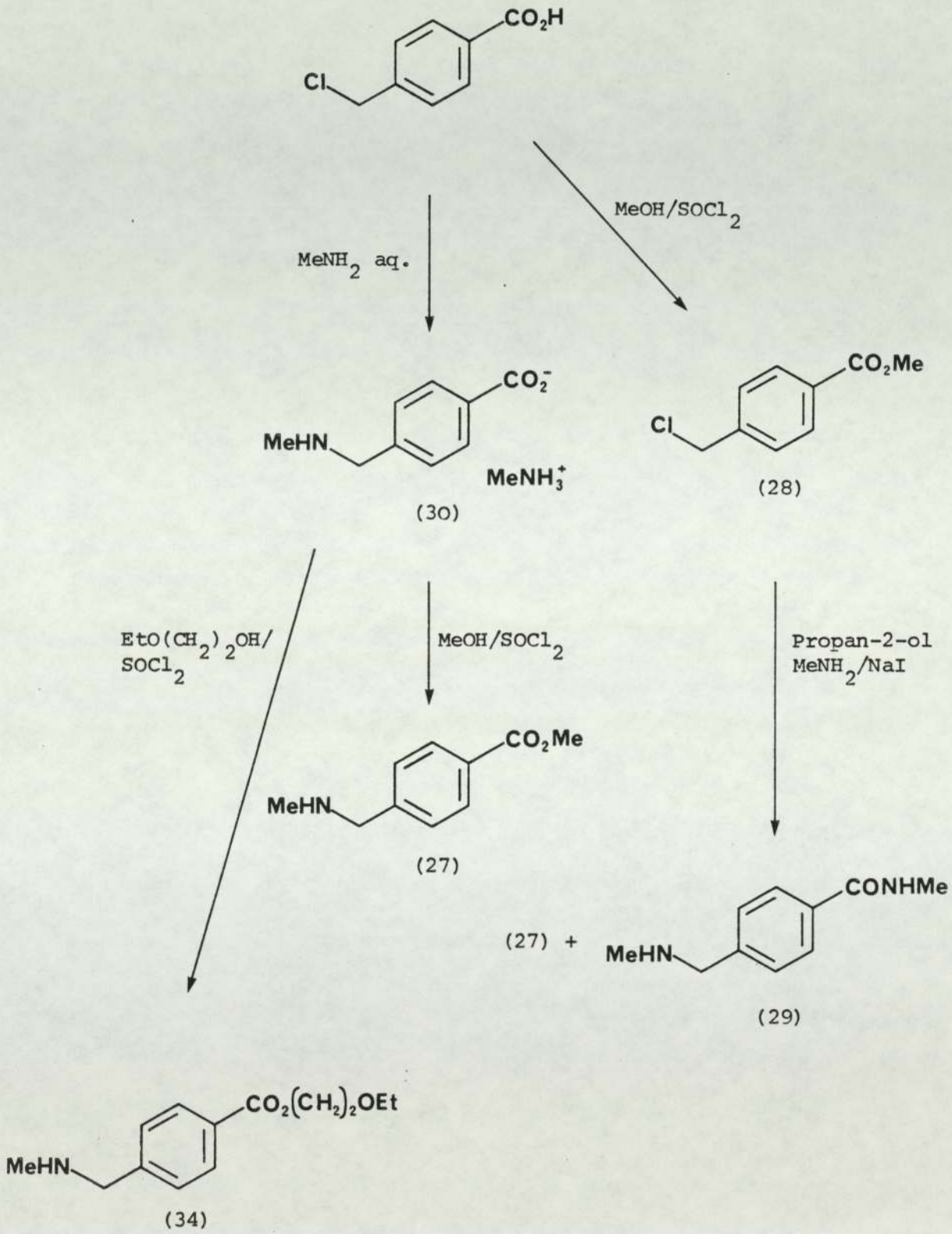

recrystallisation from aqueous ethanol. Esterification using methanol and thionyl chloride according to a general method for the preparation of amino-acid esters afforded methyl 4-(methylaminomethyl)benzoate (27) as the hydrochloride salt.

The nucleophilic substitution of ethyl 4-(methylaminomethyl)benzoate (26) onto MNP (19) was carried out by fusion of an intimate mixture of the two compounds under nitrogen at 180-190°C for several hours (scheme 2.5). Preparative-t.l.c. furnished a dark red viscous liquid, ^{1}H n.m.r analysis of which suggested that the required compound (31) may have been formed. Alternatively, the free base of methyl 4-(methylaminomethyl)benzoate (27) and MNP (19) were heated under reflux in 2-ethoxyethanol, in the presence of triethylamine, to form a deep red viscous liquid (2 major spots on t.l.c.) which was subjected to column chromatography (scheme 2.5). ^{1}H n.m.r analysis of the eluted product indicated the presence of two esters, the methyl ester (32) and also the 2-ethoxyethyl ester analogue of MBP (33). Trans-esterification of the mixture with methanol in the presence of concentrated sulphuric acid fully converted the mixture to the required methyl ester analogue (32).

In an attempt to find a more suitable non-hydroxylic medium for the above reaction, other high boiling solvents were investigated including dioxan, pyridine and diglyme (bis(2-methoxyethyl)ether). MNP (19), methyl 4-(methylaminomethyl)benzoate (27) and triethylamine were heated under reflux in dioxan but after 24 hours t.l.c. showed only the presence of starting materials. The boiling of the two reactants in pyridine afforded a number of products, whilst the use of diglyme as solvent yielded a brown intractable solid.

Since 2-ethoxyethanol was the most suitable solvent for the above reaction, but trans-esterified the synthesised esters, it seemed appropriate also to synthesise the 2-ethoxyethyl ester analogue of

Scheme 2.5 Treatment of nitropyrimethamine with substituted benzylamines

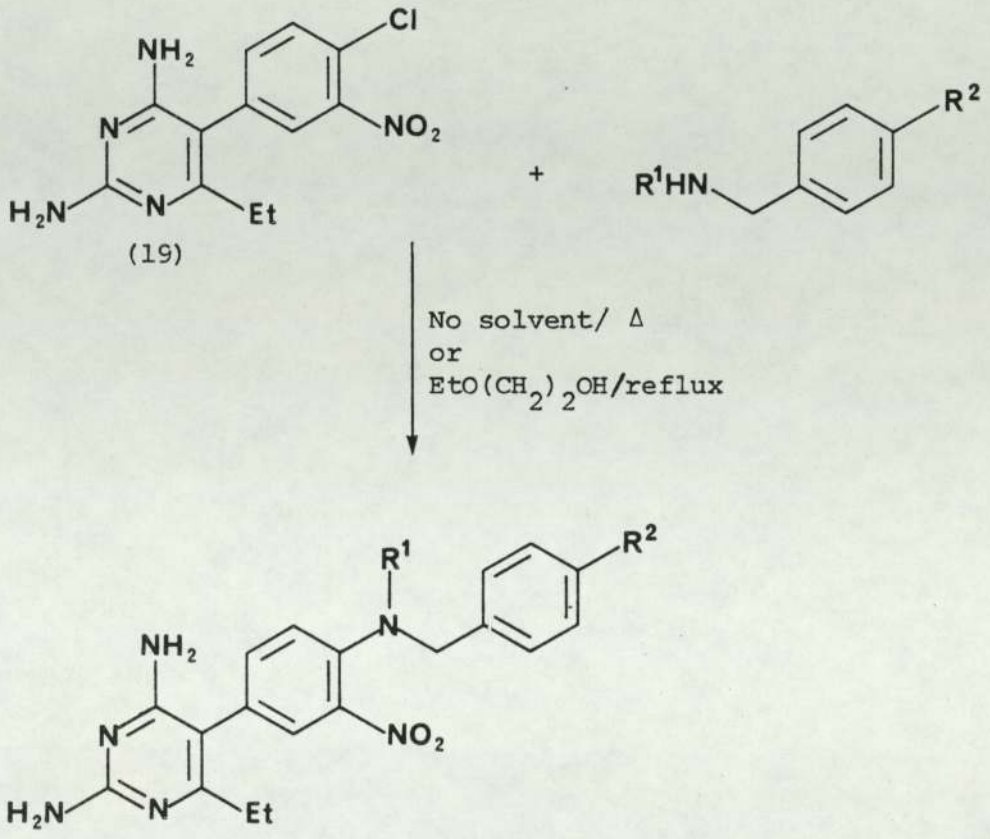

Methylbenzaprim Analogue	R^1	R^2
(31)	Me	CO_2Et
(32)	Me	CO_2Me
(33)	Me	$CO_2(CH_2)_2OEt$
(38)	H	OMe
(39)	Me	OMe
(40)	Me	CONHMe

MBP (33). The procedure was similar to that adopted for the methyl ester (27), treating 4-(methylaminomethyl)benzoic acid with 2-ethoxyethanol and thionyl chloride to furnish 2-ethoxyethyl 4-(methylaminomethyl)benzoate (34) (scheme 2.4). Excess amine (34) and MNP (19) were heated under reflux in 2-ethoxyethanol to form a deep red liquid. Separation by column chromatography afforded the 2-ethoxyethyl ester (33) as a yellow powder.

Griffin[98] observed that, following the nucleophilic substitution of MNP with dibenzylamine, in addition to formation of the desired dibenzylaminophenylpyrimidine, a second, less abundant component was observed. It was proposed that the corresponding benzimidazole-N-oxide had been formed in a base-catalysed cyclisation[114]. Therefore, prior to the base-catalysed hydrolysis of the methyl ester analogue of MBP (32), a sample of MBP and sodium hydroxide in methanol were heated together under reflux. T.l.c. analysis after 24 hours indicated only the presence of starting materials. Thus (32) was hydrolysed by sodium hydroxide in methanol to form the benzoic acid analogue of MBP (35) which was treated with ethanesulphonic acid to form the ethanesulphonate salt. However, crystallisation from water re-formed the free acid as the monohydrate, showing the pyrimidine to be a very weak base when compared with pyrimethamine and its close analogues[100] (scheme 2.6).

N-Methyl-4-methoxybenzylamine (36) was synthesised in a similar manner to the method used by Singer and Andrews[115]. 4-Methoxybenzylamine was treated with ethyl formate and sodium carbonate to form N-(4-methoxybenzyl)formamide (37). This was reduced by lithium aluminium hydride to produce the desired amine (36) (scheme 2.7).

The preparation of an analogue of benzaprim (15) encompassing a 4-methoxy substituent was carried out by boiling 4-methoxybenzylamine

Scheme 2.6 Base-catalysed hydrolysis of 2,4-diamino-5-{4-[N-(4-methoxycarbonylbenzyl)-N-methylamino]-3-nitrophenyl}-6-ethylpyrimidine

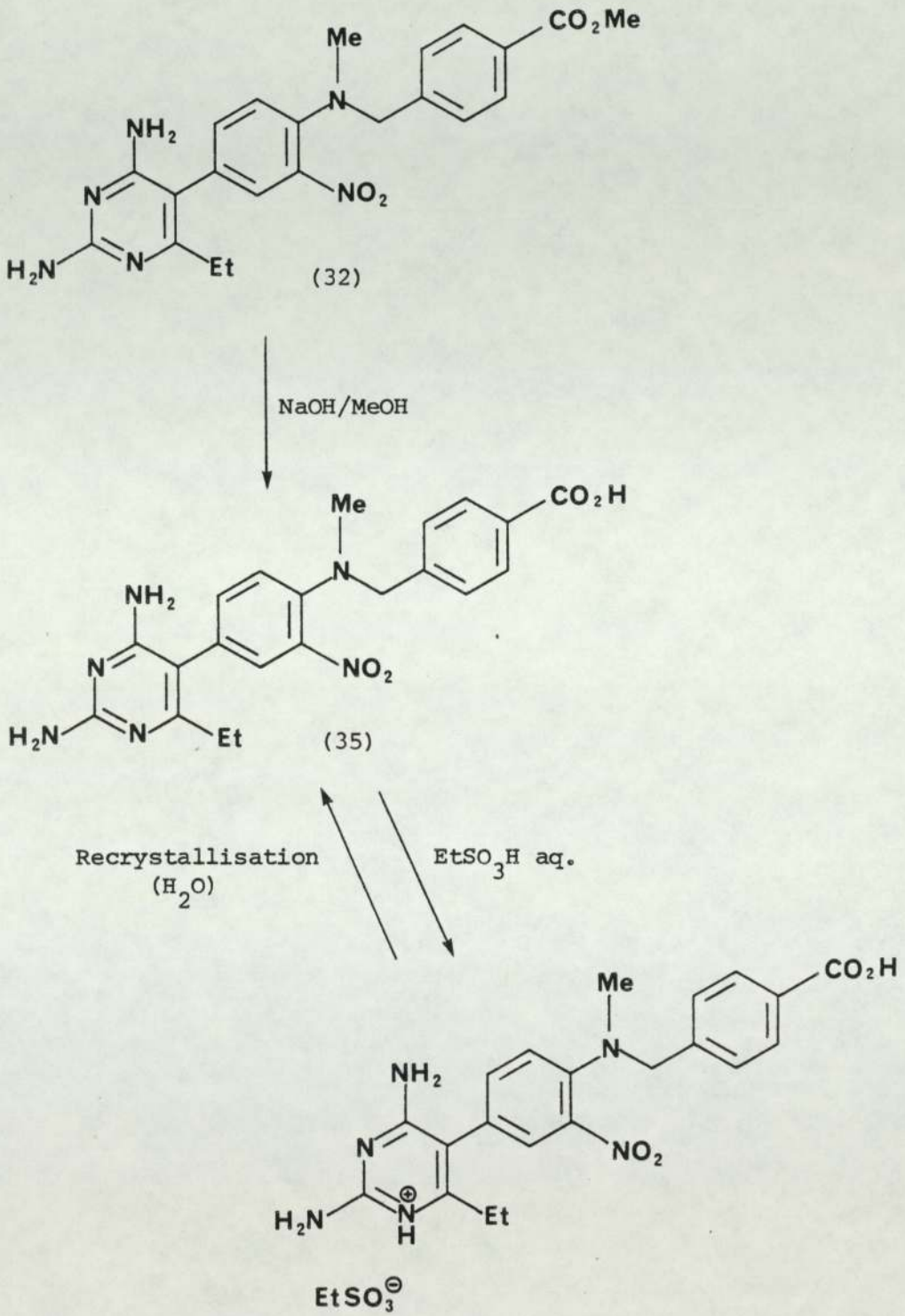

Scheme 2.7 Synthesis of N-methyl-4-methoxybenzylamine

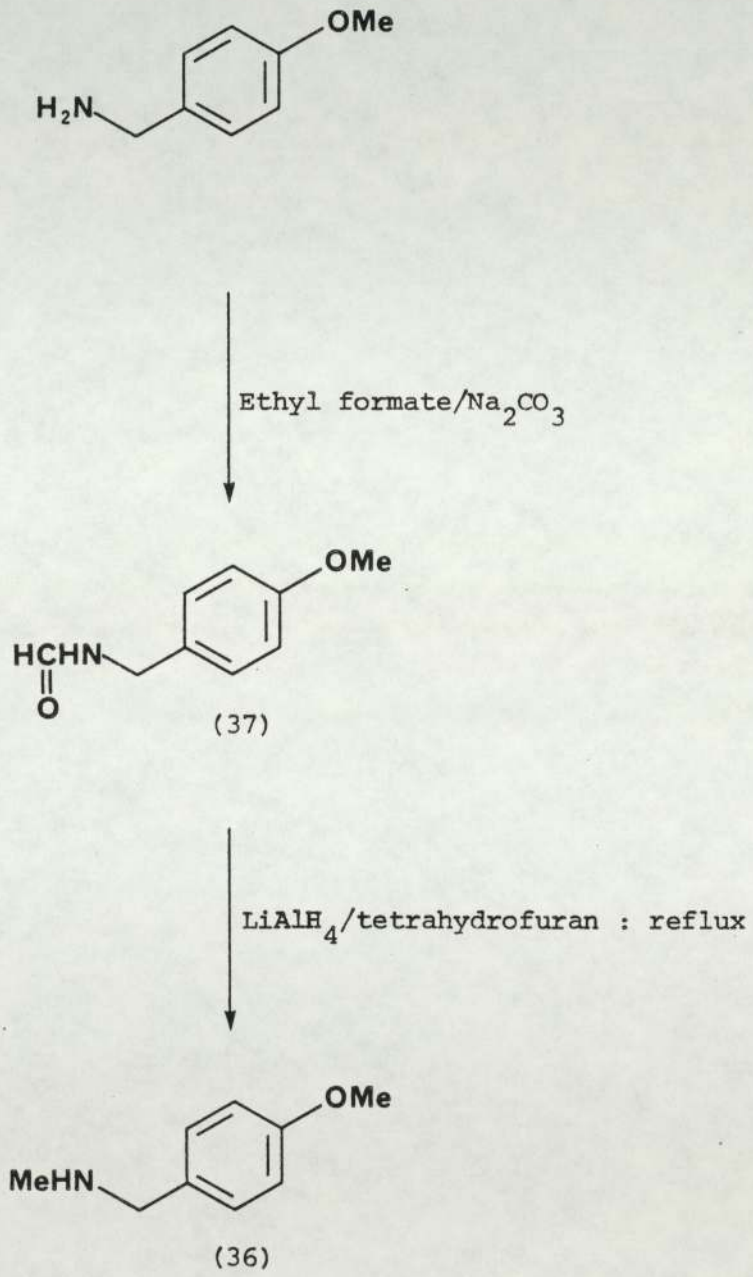

and MNP (19) in 2-ethoxyethanol under reflux for 12 hours. Precipitation in diethyl ether followed by crystallisation from 2-ethoxyethanol furnished the desired 2,4-diamino-5-{4-[N-(4-methoxybenzylamino)]-3-nitrophenyl}-6-ethylpyrimidine (38). By replacing 4-methoxybenzylamine with N-methyl-4-methoxybenzylamine (36) the 4-methoxy analogue of MBP (39) was prepared in a similar manner (scheme 2.5).

As described above, methyl 4-(chloromethyl)benzoate (28) was converted to N-methyl 4-(methylaminomethyl)benzamide (29) by treatment with aqueous methylamine, propan-2-ol and a catalytic amount of sodium iodide (scheme 2.4). This was then boiled under reflux in 2-ethoxyethanol with MNP (19), according to the general method developed here, to give the required N-methylcarboxamide (40) (scheme 2.5).

Owing to the antitumour activity of the lipophilic 3-azido analogue of nitropyrimethamine, MZPES (11), it was considered of interest to prepare the 3-azido analogue of methylbenzaprim. However Griffin[98] found that instead of the expected azide, treatment of the 3-amino analogue of MBP (41) with nitrous acid at 0°C and subsequent addition of sodium azide afforded the 1-alkylbenzotriazole (43). This constituted a novel reaction, the suggested mechanism being the formation of the N-alkyl-N-benzyltriazolium intermediate (44) by cyclisation of the diazonium species (45)[98]. Subsequent nucleophilic attack at the benzylic carbon by chloride, nitrite, water or azide may then furnish the corresponding benzotriazole with the production of benzyl chloride, benzyl alcohol, benzyl nitrite or benzyl azide (scheme 2.8).

It was proposed that, if the debenzylation occurred by this mechanism, then diazotisation with one molar equivalent of sodium nitrite in a relatively non-nucleophilic acid may afford the

Scheme 2.8

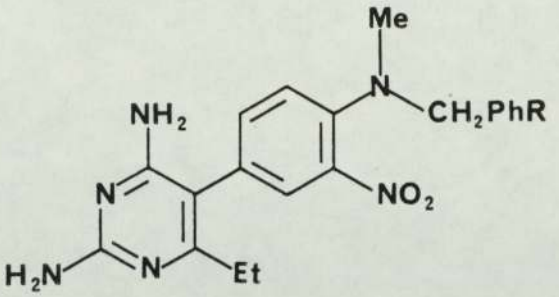

(16) R = H

(40) R = OMe

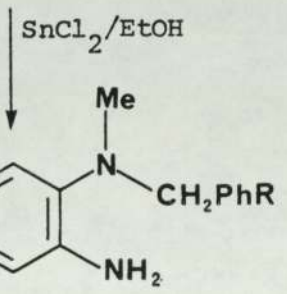

(41) R = H

(42) R = OMe

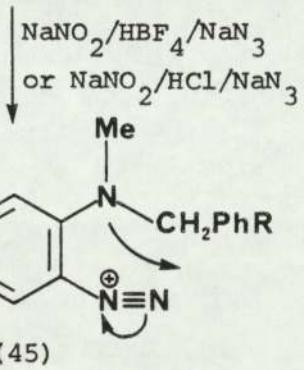

(45)

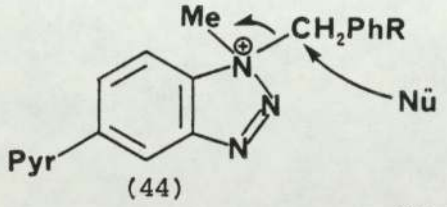

(44)

Nu = OH_2, ONO^-, Cl^-, N_3^-

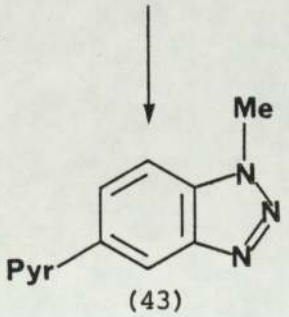

(43) + $PhCH_2Nu$

Pyr = 2,4-diamino-6-ethylpyrimidin-5-yl

benzotriazolium species possibly in equilibrium with the diazonium salt[98]. Evidence indicated that the diazonium or triazolium salts, or both, were formed by diazotisation of the amine (41) in glacial acetic acid, with sodium nitrite in sulphuric acid since, addition of an aliquot of this solution to alkaline 2-naphthol afforded a red azo-dye[98]. However, addition of excess sodium azide afforded only the N-methyl benzotriazole. This led to the suggestion that the nucleophilic azide ion attacks the benzylic carbon as opposed to the diazonium nitrogen[98].

In a further attempt to prepare the desired azide, it was decided to isolate the diazonium species with a non-nucleophilic counter ion, such as tetrafluoroborate. The 3-amino analogue of MBP (41) was prepared[98] and, employing the method used by Bliss[97], was diazotised in 40% aqueous tetrafluoroboric acid with an aqueous solution of sodium nitrite. However, yet again the sole isolable product was the N-methylbenzotriazole (43). It is possible that a totally non-aqueous system, such as sodium nitrite/ trifluoroacetic acid or alkyl nitrite/ dichloromethane may effect the diazotisation although these were not investigated.

It was considered that the electron-donating effect of the methoxy substituent on the p-methoxy analogue of MBP (39) may deactivate the benzylic CH_2 to S_N2 nucleophilic attack. Therefore, a suspension of (39) in ethanol was treated with tin (II) chloride dihydrate to form the 3-amino analogue (42). A solution of (42) in 5M aqueous hydrochloric acid was treated with sodium nitrite (1.1 molar equivalents) before addition of sodium azide. However, the product, a cream powder, was shown by mass spectrometry to be the N-methylbenzotriazole (43) (M^+ 269). The methoxybenzylium ion was also present in the spectrum (m/z 121).

2.1 Spectra

The ^{1}H n.m.r spectra of these MBP analogues are very characteristic. The hydrogen atoms of the amino-substituents resonate as 2 peaks, the peak of the amino group with the lower shift value always being broad, whilst the amino substituent with the higher shift appears as a much sharper singlet. However as yet, the assignment of each peak to a particular amino-substituent has not been possible.

In the aromatic region the resonances of the hydrogen atoms in the 5- and 6-positions of the nitrophenyl rings are superimposed to form a singlet. Likewise the hydrogen in the 2-position of the same ring occurs as a singlet. However an exception to this is the spectrum of the 4-methoxy analogue of benzaprim (38). Here coupling is not only observed between the hydrogen atoms in the 5- and 6-positions of the nitrophenyl ring, but also between the hydrogen in the 6-position and that in the 2-position. This meta-coupling is, as expected[116], approximately 1 Hz.

The infra-red (i.r) spectra are also characteristic with broad peaks occurring between 3000 and 3400 cm^{-1} corresponding to the amino groups on the pyrimidine ring. It was considered a possibility that the benzoic acid monohydrate (35) may occur as a zwitterion with the N-1 position on the diaminopyrimidine ring being protonated. Due to the presence of water this could not be resolved clearly using n.m.r analysis, but a band in the infra-red spectrum at 1700 cm^{-1} indicates that this acid is likely not to be present as the carboxylate.

^{1}H n.m.r analysis of 4-(methylaminomethyl)benzoic acid indicated it to be present as the methylamine salt (30). This was validated by the infra-red spectrum where a carboxylic acid at 1700 cm^{-1} was not observed.

In conclusion, using these approaches a series of novel p-substituted analogues of methylbenzaprim and a p-substituted derivative of benzaprim were synthesised.

2.2 Experimental

Infra-red spectra were determined as liquid films unless otherwise stated, using a Perkin-Elmer 1310 Spectrophotometer. ^1H n.m.r spectra were obtained at 60 MHz using a Varian EM360A spectrometer, at 300 MHz using a Bruker AC300 spectrometer and at 400 MHz using a Bruker WH400 spectrometer, with TMS as internal standard. Mass spectra were obtained using a VG Micromass 12B spectrometer, whilst high resolution mass spectra and FAB spectra were obtained using a VG Analytical ZAB-E spectrometer. Melting points were corrected.

Ethyl 4-formylbenzoate (21)

4-Carboxybenzaldehyde (20) (20g, 133mmol), toluene-4-sulphonic acid monohydrate (1g, 6mmol) and ethanol (200ml) were heated together under reflux for 48 h. The reaction was terminated by the addition of an excess of saturated aqueous sodium hydrogen carbonate. The mixture was extracted with successive volumes of chloroform (3 x 100ml). The solution was dried (Na_2SO_4) and filtered, and the solvent was evaporated under reduced pressure to yield a white solid (29.7g). N.m.r analysis indicated the presence of the aldehyde (21) (10.7g, 75mmol, 36%) and the diethylacetal (22) (19.0g, 60mmol, 64%), δ_H [60 MHz; $CDCl_3$] 1.24(6H, t, J 7 Hz, $ArCH(OCH_2\underline{C}H_3)_2$), 1.37(3H, t, J 7 Hz, $COOCH_2\underline{C}H_3$), 3.58(4H, q, J 7 Hz, $ArCH(O\underline{C}H_2CH_3)_2$), 4.28(2H, q, J 7 Hz, $COO\underline{C}H_2CH_3$), 5.52(1H, s, ArCH), 7.55(2H, d, J 8 Hz, ArH) and 8.05(2H, d, J 8 Hz, ArH). [Lit[112]: 1.18 and 1.30(apparent q consisting of 2 overlapping t with J 7 Hz (9H)), 3.52(q, J 7 Hz, 4H), 4.25(q, J 7 Hz, 2H), 5.50(s, 1H), AA'BB' system with signals at 7.47, 7.60, 7.97 and 8.10 p.p.m).].

1M Aqueous sulphuric acid (400ml) was added, with vigorous stirring, to the white solid (17.8g) and the reaction mixture was stirred at

room temperature for 48 h. The reaction was terminated with the addition of sodium hydrogen carbonate and the mixture was extracted with ethyl acetate (3 x 100ml). The solution was dried (Na_2SO_4) and filtered, and the solvent was evaporated under reduced pressure to give the aldehyde ester (21) (12.3g, 85%) as a white solid, $\nu_{max.}$ 2980, 1710, 1720 cm^{-1}; δ_H [60 MHz;$CDCl_3$] 1.41(3H, t, J 8 Hz, $CH_2\underline{CH_3}$), 4.40(2H, q, J 8 Hz, $\underline{CH_2}CH_3$), 7.95(2H, d, J 8 Hz, ArH), 8.20(2H, d, J 8 Hz, ArH) and 10.10(1H, s, COH).

Attempted synthesis of ethyl 4-(methylaminomethyl)benzoate (26)

Ethyl 4-formylbenzoate (21) (534mg, 3mmol) in glacial acetic acid was treated with 40% aqueous methylamine (1.0ml). After the addition of sodium cyanoborohydride (500mg, 8mmol) the solution was stirred for 1 h. The reaction was terminated with the addition of excess sodium carbonate and the reaction product was isolated by extraction into ethyl acetate (3 x 25ml). The combined extracts were dried (Na_2SO_4) and filtered and the solvent was evaporated under reduced pressure to give ethyl 4-(hydroxymethyl)benzoate (24) as a colourless liquid, [lit b.p.,[117] 161-163°C], $\nu_{max.}$ 3400(br.), 1720 cm^{-1}; δ_H [60 MHz; $CDCl_3$] 1.40(3H, t, J 7 Hz, $OCH_2\underline{CH_3}$), 3.61(1H, br.s, OH), 4.38(2H, q, J 7 Hz, $O\underline{CH_2}CH_3$), 4.70(2H, s, $ArC\underline{H_2}OH$), 7.37(2H, d, J 8 Hz, ArH) and 8.00(2H, d, J 8 Hz, ArH).

Ethyl 4-(methyliminomethyl)benzoate (23)

Toluene (400ml) was added to ethyl 4-formylbenzoate (21) (7.68g, 43mmol) and the mixture was stirred whilst gaseous methylamine was bubbled through for 30 min. The solution was stirred vigorously at room temperature for 1 h before being dried (Na_2SO_4) and filtered. The solvent was evaporated under reduced pressure to give the imine (23) (5.06g, 61%) as a yellow oil, $\nu_{max.}$ 2850-2700 (br.), 1650, 1210

cm^{-1}; δ_H [60 MHz; $CDCl_3$] 1.35(3H, t, J 7 Hz, $CH_2\underline{CH_3}$), 3.50(3H, d, J 2 Hz, NCH_3), 4.30(2H, q, J 7 Hz, $\underline{CH_2}CH_3$), 7.75(2H, d, J 9 Hz, ArH), 8.05(2H, d, J 9 Hz, ArH) and 8.25(1H, approx. q, J 2 Hz, ArCH). This compound was reported by Pitea et al[118] as yellow crystals, m.p. 251-252°C.

Ethyl 4-(methylaminomethyl)benzoate (26)

Trifluoroacetic acid (TFA) (50ml), containing trifluoroacetic anhydride (TFAA) (0.5ml), was added to ethyl 4-(methyliminomethyl)benzoate (23) (5.0g, 26mmol). Sodium cyanoborohydride (5.0g, 79mmol) was added to the mixture, with stirring, in several portions during 5 h. The mixture was then diluted with water (100ml), basified with anhydrous potassium carbonate and extracted with chloroform (3 x 100ml). The chloroform layer was dried (Na_2SO_4) and filtered. The solvent was evaporated under reduced pressure to yield a yellow oil. This product was then subjected to column chromatography (silica; chloroform with methanol increasing from 0 - 10%) to furnish diethyl benzene-1,4-dicarboxylate (25) (0.38g, 6.5%), δ_H [60 MHz; $CDCl_3$] 1.37(6H, t, J 7 Hz, $CH_2\underline{CH_3}$), 4.35(4H, q, J 7 Hz, $\underline{CH_2}CH_3$), 8.07(4H, s, ArH).

The combined fractions of the subsequent eluate were evaporated under reduced pressure to furnish ethyl 4-(methylaminomethyl)benzoate (26) as a yellow oil, $V_{max.}$ 2870, 2275, 1650, 1220 cm^{-1}; δ_H [60 MHz;$CDCl_3$] 1.38(3H, t, J 7 Hz, $CH_2\underline{CH_3}$), 2.43(3H, s, NCH_3), 3.25(1H, s, NH), 3.91(2H, s, $ArCH_2$), 4.36(2H, q, J 7 Hz, $\underline{CH_2}CH_3$), 7.32(2H, d, J 8 Hz, ArH) and 7.97(2H, d, J 8 Hz, ArH); m/z 193 (M^+), 192, 177, 164 and 148.

Attempted preparation of 2,4-diamino-5-{4-[N-(4-ethoxycarbonylbenzyl)-N-methylamino]-3-nitrophenyl}-6-ethylpyrimidine (31)

Ethyl 4-(methylaminomethyl)benzoate (26) (0.43g, 2.2mmol) and 2,4-diamino-5-(4-chloro-3-nitrophenyl)-6-ethylpyrimidine (nitropyrimethamine, MNP, 19) (0.10g, 0.34mmol) were stirred together at 180-190°C for 6 h under nitrogen, yielding a brown viscous gum. This was subjected to preparative-t.l.c.(silica; chloroform 80%: methanol 20%). The desired fraction was extracted with the chloroform-methanol solvent, which was then dried (Na_2SO_4) and filtered. The solvent was evaporated under reduced pressure yielding a deep red viscous oil (80mg). N.m.r analysis suggested this comprised mainly the desired compound (31), δ_H [60 MHz; $CDCl_3$] 1.06(3H, m, $CH_2C\underline{H}_3$), 1.40(3H, t, J 7 Hz, $COOCH_2C\underline{H}_3$), 2.18(2H, m, $C\underline{H}_2CH_3$), 2.82(3H, s, NCH_3), 3.54(2H, s, $ArCH_2N$), 4.37(2H, q, J 7 Hz, $COOC\underline{H}_2CH_3$), 4.89(2H, br., NH_2), 5.27(2H, br., NH_2), 7.25(1H, m, 6-H of $ArNO_2$ ring), 7.38(2H, d, J 8 Hz, 2-H and 6-H of $H_5C_2OOCC_6\underline{H}_4CH_2$ ring), 7.63(1H, d, J 1.5 Hz, 2-H of $ArNO_2$ ring), 8.02(1H, d, J 8 Hz, 5-H of $ArNO_2$ ring) and 8.05(2H, d, J 8 Hz, 3-H and 5-H of $H_5C_2OOCC_6\underline{H}_4CH_2$ ring).

4-(Methylaminomethyl)benzoic acid methylamine salt (30)

4-(Chloromethyl)benzoic acid (18.0g, 105.5mmol) and 40% aqueous methylamine (500ml, 6.5mol) were heated together under reflux for 24 h. The majority of solvent was evaporated under reduced pressure and the remainder was removed by freeze-drying overnight. Recrystallisation of the residue from aqueous ethanol yielded 4-(methylaminomethyl)benzoic acid methylamine salt (30) (9.0g, 44%) as white crystals, m.p. 227-9°C; $V_{max.}$ (KBr) 3350, 3100, 2870, 2450, 1650, 1540 cm^{-1}; δH [60 MHz; D_2O] 2.56(3H, s, NCH_3), 2.80(3H, s,

NCH_3), 4.19(2H, s, $ArCH_2$), 7.40(2H, d, J 9 Hz, ArH), and 7.78(2H, d, J 9 Hz, ArH); m/z 165.0770 (M^+) ($C_9H_{11}NO_2$ requires 165.0790), 164 (100%). This compound has been reported as the hydrochloride but not characterised[119].

Methyl 4-(chloromethyl)benzoate (28)

Thionyl chloride (3ml, 40mmol) was slowly added to 4-(chloromethyl)benzoic acid (5.0g, 29mmol) in methanol (300ml) and the reaction mixture was stirred for 24 h at room temperature. Following evaporation of the methanol under reduced pressure, the residue was taken up in dichloromethane and washed with saturated aqueous sodium hydrogen carbonate. The dichloromethane layer was dried (Na_2SO_4) and filtered, and the solvent was evaporated under reduced pressure to yield the ester (28) (4.9g, 91%) as a pale yellow liquid which crystallised overnight, m.p. 32-33°C (lit. b.p.[120] 86-90°C/1mm Hg); $\nu_{max.}$ 1720 cm^{-1}; δ_H [60 MHz; $CDCl_3$] 3.88(3H, s, OCH_3), 4.56(2H, s, $ArCH_2Cl$), 7.40(2H, d, J 8 Hz, ArH) and 7.98(2H, d, J 8 Hz, ArH); m/z 186, 184 (M^+).

Attempted synthesis of methyl 4-(methylaminomethyl)benzoate (27)

Methyl 4-(chloromethyl)benzoate (28) (1.9g, 10mmol), 40% aqueous methylamine (50ml, 645mmol), propan-2-ol (50ml) and sodium iodide (50mg) were heated together under reflux for 3 h to form a yellow solution. After removal of solvents under reduced pressure, ^1H n.m.r analysis indicated the presence of two compounds, methyl 4-(methylaminomethyl)benzoate (27) and N-methyl-4-(methylaminomethyl)benzamide (29), the n.m.r analyses corresponding to those reported for (27) above and (29) below.

Methyl 4-(methylaminomethyl)benzoate (27)

Thionyl chloride (6ml, 82mmol) was slowly added to 4-(methylaminomethyl)benzoic acid (30) (8.75g, 53mmol) and methanol (100ml). The reaction mixture was stirred for 48 h at room temperature and the solvent was evaporated under reduced pressure. The remaining white solid was dissolved in dichloromethane and washed with 10% aqueous potassium carbonate. The aqueous phase was extracted with a further three portions of dichloromethane (each 50ml). The combined extracts were then washed with saturated aqueous sodium hydrogen carbonate and this was again extracted with dichloromethane (3 x 50ml). The combined organic fractions were dried (Na_2SO_4) and filtered, and the solvent was evaporated under reduced pressure to yield methyl 4-(methylaminomethyl) benzoate (27) (6.63g, 70%) as a yellow liquid, $V_{max.}$ 3350, 2975, 1285 cm^{-1}; δ_H [60 MHz; $CDCl_3$] 1.42(1H, br.s, NH), 2.49(3H, s, NCH_3), 3.76(2H, s, $ArCH_2N$), 3.90(3H, s, OCH_3), 7.37(2H, d, J 9 Hz, ArH) and 7.95(2H, d, J 9 Hz, ArH).

2,4-Diamino-5-{4-[N-(4-methoxycarbonylbenzyl)-N-methylamino]-3-nitrophenyl}-6-ethylpyrimidine (32)

Methyl 4-(methylaminomethyl)benzoate (27) (1.06g, 6mmol), nitropyrimethamine (19) (860mg, 3mmol), triethylamine (0.8ml, 9mmol) and 2-ethoxyethanol (10ml) were boiled together under reflux for 72 h. The 2-ethoxyethanol was evaporated under reduced pressure. The dark red/brown viscous liquid was subjected to column chromatography (silica; chloroform 95%: methanol 5%) which, after removal of the solvent under reduced pressure, yielded a yellow oil. Trituration with light petroleum (b.p. 60-80°C) furnished an orange solid (190mg). N.m.r and m.s analysis indicated the presence of two compounds, the methyl- and 2-ethoxyethyl esters (32) and (33) respectively. This mixture was boiled under reflux in methanol (30ml)

with concentrated sulphuric acid (0.5ml) for 6 h. The methanol was evaporated under reduced pressure and the resulting solid was taken up in 10% aqueous potassium carbonate, and extracted with ethyl acetate (3 x 50ml). The combined ethyl acetate fractions were dried (Na_2SO_4) and filtered and the solvent was evaporated under reduced pressure to furnish the methyl ester (32) (160mg, 6%) as an orange powder, m.p. 198-200°C (Found: C, 60.34; H, 5.77; N, 18.90. $C_{22}H_{24}N_6O_4$ requires C, 60.55; H, 5.50; N, 19.27 %); $\nu_{max.}$ (nujol) 3490, 3320, 3150. 1720 cm^{-1}; δ_H [400 MHz; $(CD_3)_2SO$] 0.96(3H, t, J 7.5 Hz, CH_2CH_3), 2.11(2H, q, J 7.5 Hz, CH_2CH_3), 2.74(3H, s, NCH_3), 3.84(3H, s, OCH_3), 4.50(2H, br.s, $ArCH_2N$), 5.75(2H, br.s, NH_2), 5.92(2H, s, NH_2), 7.28(2H, s, 5-H and 6-H of $ArNO_2$ ring), 7.45(2H, d, J 8.2 Hz, 2-H and 6-H of $H_3COOCC_6H_4CH_2$ ring), 7.56(1H, s, 2-H of $ArNO_2$ ring) and 7.95(2H, d, J 8.2 Hz, 3-H and 5-H of $H_3COOCC_6H_4CH_2$ ring); m/z 436 (M^+), 419 (100%), 401.

2-Ethoxyethyl 4-(methylaminomethyl)benzoate (34)

Thionyl chloride (6ml, 82.5mmol) was slowly added to 4-(methylaminomethyl)benzoic acid (30) (4.5g, 27mol) and 2-ethoxyethanol (600ml). The mixture was stirred at 50°C for 16 h before evaporation of the excess reagent under reduced pressure. The white creamy solid was dissolved in 10% aqueous potassium carbonate and extracted with successive volumes of chloroform (3 x 100ml). The chloroform layer was dried (Na_2SO_4) and filtered, and the solvent was evaporated under reduced pressure to yield an oil (11.0g) which was shown by n.m.r analysis to comprise 3.5g 2-ethoxyethyl 4-(methylaminomethyl)benzoate (34) and 7.5g 2-ethoxyethanol, δ_H [60 MHz; $CDCl_3$] 2.41(3H, d, J 4.5 Hz, NCH_3), 7.35(2H, d, J 8 Hz, ArH), 7.98(2H, d, J 8 Hz, ArH); m/z 237.1360 (M^+) ($C_{13}H_{19}NO_3$ requires 237.1365), 236, 164, 148, 120 (100%).

2,4-Diamino-5-(4-{N-[4-(2-ethoxyethoxy)carbonylbenzyl]-N-methylamino}-3-nitrophenyl)-6-ethylpyrimidine (33)

The crude product (10.7g) from the reaction above, containing 2-ethoxyethyl 4-(methylaminomethyl)benzoate (34) (15mmol), nitropyrimethamine (19) (3.5g, 12mmol) and 2-ethoxyethanol (10ml) were boiled under reflux for 20 h before the solvent was evaporated under reduced pressure. The dark red oil was subjected to column chromatography (silica; chloroform 90%: methanol 10%) and the eluates were evaporated under reduced pressure. Trituration with diethyl ether furnished the 2-ethoxyethyl ester (33) (180mg, 3%) as a yellow powder, m.p. 114-6°C (Found: C, 60.55; H, 6.08; N, 17.17. $C_{25}H_{30}N_6O_5$ requires C, 60.73; H, 6.07; N, 17.00 %); $V_{max.}$ (nujol) 3400 (br.), 3170 (br.), 1620, 1540; δ_H [400 MHz; $(CD_3)_2SO$] 0.97(3H, t, J 7.5 Hz, CH_2CH_3), 1.11(3H, t, J 7 Hz, OCH_2CH_3), 2.11(2H, q, J 7.5 Hz, CH_2CH_3), 2.75(3H, s, NCH_3), 3.50(2H, q, J 7 Hz, OCH_2CH_3), 3.69(2H, m, $COOCH_2CH_2OCH_2CH_3$), 4.38(2H, m, $COOCH_2CH_2OCH_2CH_3$), 4.51(2H, br.s, $ArCH_2N$), 5.69(2H, br.s, NH_2), 5.88(2H, s, NH_2), 7.28(2H, ca. d, J 1.2 Hz, 5-H and 6-H of $ArNO_2$ ring), 7.46(2H, d, J 8.4 Hz, 2-H and 6-H of $H_5C_2O(H_2C)_2OOCC_6H_4CH_2$ ring), 7.56(1H, ca. t, 2-H of $ArNO_2$ ring) and 7.95(2H, d, J 8.4 Hz, 3-H and 5-H of $H_5C_2(H_2C)_2OOCC_6H_4CH_2$ ring); m/z 494.2273 (M+) ($C_{25}H_{30}N_6O_5$ requires 494.2278) (100%).

2,4-Diamino-5-{4-[N-(4-carboxybenzyl)-N-methylamino]-3-nitrophenyl}-6-ethylpyrimidine monohydrate (35)

The methyl ester (32) (0.92mg, 2.11mmol) and sodium hydroxide (500mg, 12.5mmol) in methanol (25ml) were boiled under reflux for 16 h. The mixture was allowed to cool to room temperature before concentrated hydrochloric acid was added dropwise to approximate pH 6.0. The precipitate formed was filtered and washed with methanol to furnish an orange powder (720mg) which was suspended in an aqueous solution

of ethanesulphonic acid (0.21g, 1.88mmol) and gently boiled. On cooling a yellow precipitate was formed which, after filtration, was recrystallised from water to yield the benzoic acid monohydrate (35) (410mg, 44%) as a yellow powder, m.p. 244-6°C (Found: C, 56.88; H, 5.43; N, 18.90. $C_{21}H_{22}N_6O_4.H_2O$ requires C, 57.27; H, 5.45; N, 19.10 %); $\nu_{max.}$ 3475, 3400-3200 (br.), 2850 (br.), 1695 cm^{-1}; δ_H [300 MHz; $(CD_3)_2SO$] 0.96(3H, t, J 7.5 Hz, $CH_2\underline{CH_3}$), 2.12(2H, q, J 7.5 Hz, $\underline{CH_2}CH_3$), 2.74(3H, s, NCH_3), 4.49(2H, s, $ArCH_2N$), 5.86(2H, br.s, NH_2), 6.10(2H, s, NH_2), 7.27(2H, s, 5-H and 6-H of $ArNO_2$ ring), 7.40(2H, d, J 8.1 Hz, 2-H and 6-H of $HOOCC_6\underline{H_4}CH_2$ ring), 7.56(1H, s, 2-H of $ArNO_2$ ring) and 7.91(2H, d, J 8.1 Hz, 3-H and 5-H of $HOOCC_6\underline{H_4}CH_2$ ring); m/z (FAB) 423($M+1^+$).

N-(4-methoxybenzyl)formamide (37)

Ethyl formate (30ml) was added to 4-methoxybenzylamine (20g, 146mmol) and sodium carbonate (5.0g), and the suspension was stirred for 48 h. The solvents were removed under reduced pressure, the residue was suspended in chloroform (200ml) and sodium carbonate was removed by filtration. The chloroform was evaporated under reduced pressure to furnish a white crystalline solid which was recrystallised from ethyl acetate-light petroleum (b.p. 60-80°C) to give the N-(4-methoxybenzyl)formamide (37) (21.5g, 90%) as white needle prisms, m.p. 80-81°C (lit.,[121] 75-6°C); δ_H [60 MHz; $CDCl_3$] 3.75(3H, s, OCH_3), 4.32(2H, d, J 6 Hz, $ArCH_2$), 6.80(2H, d, J 9 Hz, ArH), 6.80(1H, br., NH), 7.17(2H, d, J 9 Hz, ArH) and 8.12(1H, d, J 2 Hz, COH); m/z 165.

N-methyl-4-methoxybenzylamine (36)

A solution of N-(4-methoxybenzyl)formamide (37) (15.0g, 91mmol) in tetrahydrofuran (100ml) was added dropwise to a solution of lithium aluminium hydride (2.0g, 105mmol) in tetrahydrofuran (200ml) during

30 min. The mixture was boiled gently under reflux for 3 h, then cooled. After addition of water (5g), 2M aqueous sodium hydroxide (15g) and water (5g) the mixture was stirred for 5 min and filtered through diatomaceous earth. The solvent was evaporated under reduced pressure to yield a yellow oil (14.0g) which was purified by vacuum distillation to furnish the desired product (36) (4.07g, 30%) as a colourless liquid, b.p. 80-84°C/1mm Hg (lit.,[122] 88-96°C/2mm Hg); δ_H [60 MHz; $CDCl_3$] 1.33(1H, s, NH), 2.35(3H, s, NCH_3), 3.55(2H, s, $ArCH_2$), 3.70(3H, s, OCH_3), 6.73(2H, d, J 8 Hz, ArH), 7.13(2H, d, J 8 Hz, ArH).

2,4-Diamino-5-{4-[N-(4-methoxybenzyl)-N-methylamino]-3-nitrophenyl}-6-ethylpyrimidine (39)

N-Methyl-4-methoxybenzylamine (36) (4.07g, 27mmol), nitropyrimethamine (2.0g, 6.8mmol) and 2-ethoxyethanol (20ml) were boiled under reflux for 12 h. After the mixture was poured into diethyl ether and allowed to cool, filtration furnished an orange powder. This was washed with water, dried and recrystallised from aqueous 2-ethoxyethanol to yield the pyrimidine (39) (680mg, 24.5%) as an orange powder, m.p. 201-3°C (Found: C, 61.61; H, 5.97; N, 20.44. $C_{21}H_{24}N_6O_3$ requires C, 61.76, H, 5.88, N, 20.59 %); $\nu_{max.}$ (nujol) 3450, 3425, 3300, 3100, 1630, 1540, 1345 cm^{-1}; δ_H [400 MHz; $(CD_3)_2SO$] 0.97(3H, t, J 7.5 Hz, CH_2CH_3), 2.12(2H, q, J 7.5 Hz, CH_2CH_3), 2.68(3H, s, NCH_3), 3.73(3H, s, OCH_3), 4.31(2H, br.s, $ArCH_2N$), 5.72(2H, br., NH_2), 5.90(2H, s, NH_2), 6.91(2H, d, J 8.6 Hz, 3-H and 5-H of $H_3COC_6H_4CH_2$ ring), 7.21(2H, d, J 8.6 Hz, 2-H and 6-H of $H_3COC_6H_4CH_2$ ring), 7.27(2H, s, 5-H and 6-H of $ArNO_2$ ring) and 7.54(1H, s, 2-H of $ArNO_2$ ring); m/z 408.1906 (M^+) ($C_{21}H_{24}N_6O_4$ requires 408.1910), 121 (100%).

2,4-Diamino-5-{4-[N-(4-methoxybenzyl)amino]-3-nitrophenyl}-6-ethylpyrimidine (38)

4-Methoxybenzylamine (3.6g, 27.2mmol), nitropyrimethamine (19) (2.0g, 6.8mmol) and 2-ethoxyethanol (15ml) were heated together under reflux for 12 h. The solution was poured into diethyl ether, filtered and washed with water. The resulting orange powder crystallised from aqueous 2-ethoxyethanol to yield the pyrimidine (38) (930mg, 35%) as red crystals, m.p. 241-2°C (Found: C, 60.76; H, 5.74; N, 21.59. $C_{20}H_{22}N_6O_3$ requires C, 60.91; H, 5.58; N, 21.32 %); $\nu_{max.}$ (nujol) 3450, 3350, 3300, 3150 (br.), 1540, 1340 cm^{-1}; δ_H [400 MHz; $(CD_3)_2SO$] 0.95(3H, t, J 7.5 Hz, CH_2CH_3), 2.10(2H, q, J 7.5 Hz, CH_2CH_3), 3.73(3H, s, OCH_3), 4.55(2H, d, J 5.9 Hz, $ArCH_2N$), 5.69(2H, br.s, NH_2), 5.86(2H, s, NH_2), 6.93(2H, d, J 8.7 Hz, 3-H and 5-H of $H_3COC_6H_4CH_2$ ring), 7.03(1H, d, J 8.9Hz, 5-H of $ArNO_2$ ring), 7.27(1H, dd, J 8.8 and 2.1 Hz, 6-H of $ArNO_2$ ring), 7.36(2H, d, J 8.7 Hz, 2-H and 6-H of $H_3COC_6H_4CH_2$ ring), 7.81(1H, d, J 2.1 Hz, 2-H of $ArNO_2$ ring) and 8.65(1H, t, J 5.9 Hz, NH); m/z 394 (M^+) (100%), 121.

N-methyl-4-(methylaminomethyl)benzamide (29)

Methyl 4-(chloromethyl)benzoate (28) (4.8g, 26mmol), 40% aqueous methylamine (300ml, 3.9mmol), propan-2-ol (100ml) and sodium iodide (50mg) were stirred at room temperature for 72 h and then boiled under reflux for 1 h. After the volume had been reduced to approximately 100ml by distillation, the colourless solution was extracted with dichloromethane (3 x 100ml). The combined extracts were dried (Na_2SO_4) and filtered and the solvent was evaporated under reduced pressure to yield N-methyl 4-(methylaminomethyl)benzamide (29) (3.32g, 72%) as a white powder, m.p. 57-9°C; $\nu_{max.}$ (nujol) 3350, 2925, 1620, 1540, 1300 cm^{-1}; δ_H [60 MHz; $CDCl_3$] 1.48(1H, s, $ArCH_2NHCH_3$), 2.35(3H, s, $ArCH_2NHCH_3$), 2.87(3H, d, J 5 Hz, $CONHCH_3$),

3.68(2H, s, $ArCH_2N$), 7.20(1H, br., $ArCONHCH_3$), 7.23(2H, d, J 8 Hz, ArH) and 7.72(2H, d, J 8 Hz, ArH); m/z 178.1096 (M^+) ($C_{10}H_{14}N_2O$ requires 178.1098), 177, 163, 148, 136, 120 (100%).

2,4-Diamino-5-(4-{N-[4-(N-methylcarbamoyl)benzyl]-N-methylamino}-3-nitrophenyl)-6-ethylpyrimidine (40)

N-Methyl-4-(methylaminomethyl)benzamide (29) (2.56g, 14.4mmol), nitropyrimethamine (19) (2.1g, 7.2mmol) and 2-ethoxyethanol (25ml) were boiled under reflux for 6 h. The reactant mixture was then poured into water and cooled to 4°C. The resulting precipitate was collected by filtration and recrystallised from ethyl acetate-light petroleum (b.p. 60-80°C) to furnish the N-methylamide (40) (800mg, 26%) as a pale orange powder, m.p. 235-7°C (Found: C, 60.37; H, 5.70; N, 22.50. $C_{22}H_{25}N_7O_3$ requires C, 60.69; H, 5.75; N, 22.53 %); $\nu_{max.}$ (nujol) 3400, 3300, 3150, 2940, 1615, 1540 cm^{-1}; δ_H [300 MHz; $(CD_3)_2SO$] 0.97(3H, t, J 7.5 Hz, CH_2CH_3), 2.12(2H, q, J 7.5 Hz, CH_2CH_3), 2.73(3H, s, NCH_3), 2.78(3H, d, $CONHCH_3$), 4.47(2H, br.s, $ArCH_2N$), 5.70(2H, br.s, NH_2), 5.89(2H, s, NH_2), 7.28(2H, s, 5-H and 6-H of $ArNO_2$ ring), 7.38(2H, d, J 8.2 Hz, 2-H and 6-H of $H_3CHNOCC_6H_4CH_2$ ring), 7.56(1H, s, 2-H of $ArNO_2$ ring) and 7.81(2H, d, J 8.2 Hz, 3-H and 5-H of $H_3CHNOCC_6H_4CH_2$ ring); m/z 435.2104 (M^+) ($C_{22}H_{25}N_7O_3$ requires 435.2019), 418, 400 (100%).

Attempted synthesis of 2,4-diamino-5-[3-yl-4-(N-methylbenzylamino)]-6-ethylpyrimidine diazonium tetrafluoroborate

To a suspension of methylbenzaprim (16) (10.0g, 26mmol) in ethanol (250ml), tin (II) chloride dihydrate (30g) was slowly added and the mixture was stirred at 50°C. After 3 h a pale yellow solution had formed which was refluxed for a further 3 h before evaporation of the ethanol under reduced pressure. The ensuing yellow syrup was

dissolved in hot water and basified to pH 14 with 10M aqueous sodium hydroxide. The precipitate was collected by filtration and washed with water to furnish a crude cream powder containing 2,4-diamino-6-ethyl-5-{4-(N-methylbenzylamino)-3-aminophenyl]pyrimidine (41) (6.7g, 73%), δ_H [300 MHz; $(CD_3)_2SO$] 0.98(3H, t, J 7.5 Hz, $CH_2\underline{CH_3}$), 2.15(2H, q, J 7.5 Hz, $\underline{CH_2}CH_3$), 2.49(3H, s, NCH_3), 3.99(2H, s, $ArCH_2N$), 4.88(2H, s, $ArNH_2$), 5.32(2H, br., NH_2), 5.78(2H, s, NH_2), 6.34(1H, dd, J 1.8 and 7.9 Hz, 6-H of $ArNO_2$ ring), 6.53(1H, d, J 1.8 Hz, 2-H of $ArNO_2$ ring), 6.95(1H, d, J 7.9 Hz, 5-H of $ArNO_2$ ring), 7.29(5H, m, C_6H_5), [lit.,[98] δ_H [400 MHz; $(CD_3)_2SO$] 1.00(3H, t, CH_3), 2.20(2H, q, CH_2), 2.53(3H, s, NCH_3), 3.98(2H, s, $\underline{CH_2}Ph$), 4.73(2H, NH), 5.48(2H, NH), 5.73(2H, NH), 6.38(1H, dd, 6-H of $ArNO_2$ ring), 6.56(1H, d, 2-H of $ArNO_2$), 6.96(1H, d, 5-H of $ArNO_2$), 7.30(5H, brs, C_6H_5).]

This material (41) (2.0g, 5.7mmol) was diazotised during 0.5 h, at 0°C with stirring, in 40% aqueous tetrafluoroboric acid (30ml) with an aqueous solution of sodium nitrite (0.48g in 1ml). The orange reaction mixture was left to stand at 4°C in the dark overnight. The yellow precipitate that had formed was poured into iced water and basified to pH 9 with aqueous ammonia solution, filtered and washed with water to give a cream powder, indicated to be 1-methyl-5-(2,4-diamino-6-ethylpyrimidin-5-yl)benzotriazole (43), m.p. 256-7°C (sinters) (lit.,[98] 255-256°C (sinters)); δ_H [300 MHz; $(CD_3)_2SO$] 0.94(3H, t, J 7.5 Hz, $CH_2\underline{CH_3}$), 2.09(2H, q, J 7.5 Hz, $\underline{CH_2}CH_3$), 4.32(3H, s, NCH_3), 5.65(2H, br., NH_2), 5.95(2H, s, NH_2), 7.31(1H, d, J 8.5 Hz, 6-H of $ArNO_2$ ring), 7.79(1H, s, 2-H of $ArNO_2$ ring), 7.88(1H, d, J 8.5 Hz, 5-H of $ArNO_2$ ring).

CHAPTER 3

BIOCHEMICAL STUDIES ON METHYLBENZAPRIM AND ANALOGUES

3.1 Introduction

As discussed in chapter 1, dihydrofolate reductase catalyses the NADPH-dependent reduction of 7,8-dihydrofolate (DHF) to 5,6,7,8-tetrahydrofolate (THF) (figure 3.1.).

Figure 3.1

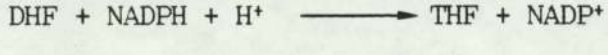

The most commonly used method for assaying this reaction is the UV spectrophotometric assay developed by Osborn and Huennekens[123] in which a decrease in absorbance at 340 nm is measured over a five to ten minute time period as DHF and NADPH are converted to THF and $NADP^+$. The change in absorbance at 340nm records the loss of NADPH. This method was adopted for evaluation of the I_{50} values for potential inhibitors of DHFR. The diminution in the velocity of the reaction at a particular inhibitor concentration was expressed as a percentage of the uninhibited reaction rate. The I_{50} value is defined as the concentration of inhibitor in the assay system necessary to reduce the reaction rate to 50% of the uninhibited rate, and was obtained graphically from a plot of $\log_{10}$ concentration of inhibitor versus percentage inhibition of enzyme activity.

The problems of comparing I_{50} values from different laboratories and using different enzyme sources are well known[124]. However, under standardised conditions using an enzyme from a single source and with

identical experimental conditions, the I_{50} value is useful for comparing the inhibitory potency of potential inhibitors of DHFR[124], assuming inhibition is competitive.

Most studies with reversible, competitive enzyme inhibitors have been performed under steady state conditions where the concentration of the inhibitor is much greater than that of the enzyme ($[I_t] >> [E_t]$) and where all equilibria involving the enzyme and reactants are set up rapidly. Such compounds demonstrate linearity when subjected to the Lineweaver and Burk plot, as described by equation 1[125].

$$\frac{1}{V} = \frac{K_m(1 + [I]/K_I)}{V_{max}[S]} + \frac{1}{V_{max}} \qquad (1)$$

These are known as Zone A conditions[126].

There are compounds which inhibit enzyme-catalysed reactions at concentrations comparable to that of the enzyme and under conditions where the equilibria are set up rapidly[127]. It has been shown that for these tight-binding inhibitors, the dissociation constant, K_I, is small and only a very low concentration of inhibitor is required to demonstrate inhibition[128]. Cha has shown that as the strength of interaction between an enzyme and tight-binding inhibitor increases, a stage is reached where the equilibrium of the reaction cannot be established rapidly[128]. This slow establishment of inhibition can be circumvented by pre-incubation of the enzyme with the inhibitor before the addition of substrate[129]. Morrison[127] showed that, in the presence of tight-binding inhibitors, the usual Lineweaver and Burk double reciprocal plot becomes non-linear. Thus analysis of kinetic data by conventional methods is complicated and Zone B kinetics apply[126].

To account for the depletion of free inhibitor by binding, Henderson[130] presented equation 2 below:-

$$\frac{I_t}{1 - (V_i/V_o)} = K_{Iapp}(V_o/V_i) + Et \qquad (2)$$

Equation 2 allows the determination of K_{Iapp}, the apparent dissociation constant, from which, assuming competitive inhibition, the true dissociation constant can be calculated[130] (equation 3).

$$K_{Iapp} = K_I (1 + S/K_m) \qquad (3)$$

Hart[131,132] has written a modification of a FORTRAN computer programme developed by Henderson[133] which uses equation 2 to generate the K_{Iapp} by a statistical method. This then allows the calculation of K_I values from equation 3.

The N-methylbenzylaminopyrimidine methylbenzaprim (16) was shown to have a K_I value of 0.009 nM for rat liver DHFR[98]. This value is only ten-fold less than that quoted for methotrexate[98] and methylbenzaprim can therefore be classed as a tight-binding inhibitor. Thus this compound and the six novel analogues of methylbenzaprim described in chapter 2, as well as pyrimethamine (5), were selected for determination of I_{50} values against DHFR from rat liver and also from E.coli. Apart from pyrimethamine, these results were also subjected to the equation for Zone B inhibition, as described above, to determine the K_{Iapp} and K_I values.

From the results obtained it was also considered worth investigating the in vitro cytotoxicity of these compounds. The six analogues of methylbenzaprim were thus subjected to preliminary cytotoxicity

studies against L1210 murine leukaemia cells over a range of concentrations, from 5×10^{-6} M to 1×10^{-9} M.

Having determined the I_{50} values of these compounds against DHFR from rat liver and the cytotoxicity against L1210 cells in vitro, the two compounds that appeared to be promising candidates for antitumour activity were selected for screening against the M5076 reticulum cell sarcoma. This is a particularly relevant model to choose since it has been shown to be intrinsically resistant to methotrexate although highly responsive to the lipophilic antifolate metoprine[134]. The insensitivity of this tumour to methotrexate appears to be explained by a reduced capacity for carrier-mediated entry into the cell. Werbel et al[135] have evaluated a series of 5-[4-(substituted aryl)-1-piperazinyl]-6-alkyl-2,4-pyrimidinediamines as antitumour agents against the M5076 sarcoma. Results showed that this tumour responded to only the more lipophilic of these compounds. This sarcoma has been shown to be one of the slowest growing experimental murine tumours which is a favourable characteristic since most intractable human tumours are slow-growing[136]. Thus it was considered of interest to study the effects of these antifolates against the M5076 sarcoma.

3.2 Materials and Methods

3.2.1 Source of Reagents and Enzymes Used in Assays

The following reagents were purchased from or supplied by the sources indicated.

BDH Chemicals Ltd., Atherstone

Potassium dihydrogen orthophosphate

Potassium hydroxide

2-Mercaptoethanol

Ammonium sulphate (enzyme grade)

Sigma Chemical Company, Poole, Dorset

Dihydrofolic acid

NADPH (tetrasodium salt)

Pyrimethamine

Dr. R. J. Griffin, Department of Pharmaceutical Sciences, Aston University, Birmingham

Methylbenzaprim and benzaprim

Nitropyrimethamine

Microbial Technology Laboratory, Centre for Applied Microbiology and Research, Porton Down, Salisbury

Frozen cell paste of E.coli MRE 600 (EC/600/38, Lot 5). Cells were grown aerobically by continuous culture at 37°C under conditions of glycerol limitation at a dilution rate of 0.78 hr^{-1}.

Source of Enzymes

Partially purified DHFR from rat liver, prepared by the method of Bertino and Fischer[137], was supplied by the Biochemical Pharmacology Section of the Institute for Cancer Research, Sutton, Surrey. Partially purified DHFR from E.coli was prepared by the method described in section 3.2.2.

3.2.2 Preparation of Partially Purified DHFR from E.coli

Partially purified DHFR was prepared using the procedure of Burchall and Hitchings[19]. Cells from 10 g of frozen paste of E.coli MRE 600 were suspended in 400 ml of 0.01M sodium phosphate buffer, pH 7.0, containing 1 mM EDTA. After centrifuging (12100 g for 10 min at 4°C) the supernatant was discarded and the washed cells (ca. 10 g wet weight) were resuspended in 20 ml of the same buffer. The cells were then broken by sonication (5 cycles of 30 sec maximum power on MSE

Soniprep with 20 sec intervening cooling on ice), and centrifuged at 4°C (48400 g for 5 min). The pellet was discarded and the supernatant (32 ml) retained at 4°C. All subsequent stages were carried out at 4°C. Streptomycin sulphate (Glaxo) was added to 1% w/v, the suspension was centrifuged (48400 g for 5 min) and the pellet discarded. The supernatant was diluted to 100 ml with the buffer and solid ammonium sulphate (35.1 g) was added to give a concentration of 55.1%. The suspension was then centrifuged (12100 g for 5 min) and the pellet was discarded. Ammonium sulphate (25.6 g) was added to the supernatant to 90% and the suspension was again centrifuged (12100 g for 5 min). The supernatant was discarded. The pellet was redissolved in 0.001 M sodium phosphate buffer, pH 7.0, containing 1 mM EDTA to 11.5 ml. This enzyme solution was dialysed with 0.001 M phosphate buffer, pH 7.0, containing 1 mM EDTA to give a final volume of 20 ml. A Lowry protein assay[138] was carried out to determine the protein content of the enzyme preparation. The specific activity of the preparation of DHFR was 9.587 nmoles.min^{-1}.mg^{-1} of protein.

3.2.3 Compound Dissolution

Stock inhibitor solutions were prepared by dissolving the appropriate compound in 0.1 M hydrochloric acid, 0.01 M sodium hydroxide, ethanol or methanol to give a final concentration of 1×10^{-4} M or 5×10^{-4} M. Some of the compounds required heating in a water bath at 40°C for dissolution before they were made up to the desired volume. All solutions were prepared on the day before the experiment and stored at 4°C in the dark.

The stock solutions were diluted as necessary to produce the required inhibitor concentration. The concentrations chosen were those that would inhibit the reaction by between 20 and 80% of the uninhibited

rate. At the concentrations used for the reaction, the solvents were shown to have no effect on the activity of DHFR.

3.2.4 Preparation of Reagent Solutions

0.15 M Phosphate buffer (pH 7.0) was prepared by dissolving potassium dihydrogen orthophosphate (10.21 g) in water (ca. 300 ml), adjusting the solution to pH 7.0 with potassium hydroxide pellets, and diluting to 500 ml with water. The buffer was kept at 4°C to prevent bacterial growth.

2-Mercaptoethanol solution (0.25 M) was prepared by diluting 2-mercaptoethanol (1.75 ml) with water (to 100 ml) and the solution was kept in the dark at 4°C prior to use.

A solution of dihydrofolate (1 $mg.ml^{-1}$, 2 mM) was prepared immediately before use by suspending dihydrofolate in 2-mercaptoethanol solution (0.25 M) and adding 1 M sodium hydroxide dropwise with vigorous agitation until dissolution had occurred. The solution was maintained at 0°C and protected from light.

An aqueous solution of NADPH (2 $mg.ml^{-1}$, 2 mM) was prepared immediately prior to use and again maintained at 0°C.

3.2.5 Assay for Inhibitor Activity

The spectrophotometric assay was carried out using a Perkin-Elmer Lambda 7 UV/VIS Spectrophotometer with a thermostatted cell compartment capable of accommodating six sample and six reference cuvettes. Reaction rates were recorded on a Perkin-Elmer chart recorder, at a chart speed of 1 $cm.min^{-1}$ and a full scale deflection of 1 absorbance unit. The cuvettes were read sequentially at one

minute time intervals over 10 min. Plastic disposable cuvettes (3 ml, 1 cm x 1 cm) were used throughout.

The assay was carried out as follows[98]:

NADPH (0.1 ml) and the enzyme preparation (0.1 ml) were incubated at 30°C for 5 min in phosphate buffer (total volume 2.9 ml). The reaction was initiated by the addition of dihydrofolate (0.1 ml) and monitored by following the decrease in absorbance at 340 nm. Parallel assays were carried out where the reaction mixture contained 0.1 ml of the inhibitor at the required concentration and the volume of buffer was adjusted accordingly to give a final volume of 3 ml in the cuvette after the addition of 0.1 ml dihydrofolate.

Reference cuvettes were set up containing NADPH, buffer, inhibitor, if appropriate, and dihydrofolate, but without enzyme (table 3.1.).

In all cases the reaction rate was linear over the time course (10 min) of the assay. Enzyme activity was taken as the slope of the change in absorbance with time and this was arbitrarily designated as 100% for the uninhibited enzyme. The observed decrease in activity in the presence of inhibitor was expressed as a percentage of the uninhibited enzyme activity.

Inhibitory activity at a minimum of five inhibitor concentrations was evaluated, in duplicate, in order to determine the I_{50} values. From this data, K_I values were determined by Zone B analysis. A K_m value of 0.2 μM for dihydrofolate[139] for DHFR from rat liver was adopted for the calculation of the K_I.

Table 3.1 DHFR assay; volumes of reagents, inhibitor and enzyme used

Nature of Assay	NADPH (ml)	Enzyme (ml)	Buffer (ml)	Inhibitor (ml)	DHF (ml)	Final Vol. (ml)
Uninhibited enzyme	0.1	0.1	2.7	-	0.1	3
Reference	0.1	-	2.8	-	0.1	3
Inhibited enzyme	0.1	0.1	2.6	0.1	0.1	3
Reference	0.1	-	2.7	0.1	0.1	3

3.2.6 *In Vitro* Cytotoxicity Studies

Cultures of L1210 murine leukaemia cells were grown as a suspension in RPMI 1640 medium (with 20 mM HEPES and L-glutamine) and donor horse serum (Flow Laboratories). Using an initial concentration of 5 x 10^4 cells.ml^{-1}, the suspension was incubated for 48 h at 37°C with the appropriate concentration of drug, and then the cells were counted using a Coulter counter. Eight concentrations of drug were chosen: 5 x 10^{-6}, 1 x 10^{-6}, 5 x 10^{-7}, 1 x 10^{-7}, 5 x 10^{-8}, 1 x 10^{-8}, 5 x 10^{-9}, and 1 x 10^{-9} M. The solutions were prepared in a similar manner to those used for the DHFR assay, with the same solvents.

Control experiments with these solvents were also implemented. All incubations were carried out in duplicate and the cell number in the presence of inhibitor after 48 h was expressed as a percentage of the control cell count.

3.2.7 Antitumour Screening

The following experiments were carried out by Mr. D. Chubb, Department of Pharmaceutical Sciences, Aston University. The experimental protocol was as follows[140]:

Fragments of the M5076 reticulum cell sarcoma were obtained from donor mice. The solid was homogenised in RPMI 1640, and the homogenate was tested for viability and counted using a Coulter counter. BDF_1 female mice, divided into groups of 5, were each injected i.m. in the left hind leg, with 1×10^6 cells. The compounds were administered i.p., at the appropriate concentration, daily for 17 days, starting on day 1. Tumour volume was measured on days 0, 5, 10, 17 and 24. Measurement was made with vernier calipers and the tumour volume calculated by the standard method[141].

3.3 Results and Discussion

The results of the determination of the I_{50} values for inhibition against DHFR from rat liver and E.coli are outlined in table 3.2. To validate this assay procedure the I_{50} of pyrimethamine (5) against DHFR from rat liver was determined and was found to be 1.0 μM. This compares favourably with the 1.4 μM value obtained by Griffin[98] using the same procedure, and is also of a similar order of magnitude to the I_{50} values reported by other workers[142,143]. However the I_{50}

value for methylbenzaprim (16) against DHFR from rat liver was found, on two different occasions, from two different stock solutions, to be 1.5 nM which is nearly seven-fold lower than the 10 nM value reported previously[98].

Using I_{50} values it is not possible to compare directly the differential activities of the inhibitors against microbial and mammalian enzymes since the Michaelis-Menten parameters of the enzymes (e.g. K_m and V_{max}) are different. However the general trend in activities is similar, i.e. the rank order of inhibitory activity of the compounds is the same: (40) > (35) > (16) > (38) > (39) (where > = shows greater inhibitory potency than). Further, the compounds are all ten to a thousand times more active against the mammalian enzyme than the microbial enzyme.

Due to solubility problems, the ester analogues of methylbenzaprim (32) and (33), were not evaluated against E.coli DHFR for which higher concentrations, compared to the rat liver assay, were required. In these assays, the inhibition of DHFR from rat liver by the compounds was measured using concentrations that would inhibit the enzyme by between 20 and 80% of the uninhibited reaction rate. However this occurred over such a narrow concentration range, with a very steep plot of percentage inhibition of enzyme activity versus $\log_{10}$ concentration of inhibitor, that it proved difficult to determine the I_{50} for the 2-ethoxyethyl ester (33). Therefore, in assaying this compound, the concentration of dihydrofolate was increased to 2 $mg.ml^{-1}$ (4 mM). Also, when this compound was subjected to the equation for Zone B inhibition, as described above, a K_{Iapp} could not be determined. This equation is based on the assumption of competitive inhibition and so it is a possibility that this compound might not behave in a competitive manner.

Table 3.2 shows that three of the compounds tested against DHFR from rat liver, methylbenzaprim (16), (35) and (40) have I_{50} values in the nanomolar concentration range. Methotrexate has been demonstrated to inhibit DHFR from rat liver with reported I_{50} values of 90 nM[19], 1.9 nM[98] and 0.2 nM[142] respectively, which indicates the variations in I_{50} values which can be obtained from different laboratories. However, this does show that the inhibitory potency of these compounds approaches that of methotrexate.

The K_{Iapp} and K_I values that were determined are listed in table 3.3. It is clear that the two compounds bearing a 4-methoxy substituent on the benzyl ring, (38) and (39), are much poorer inhibitors of DHFR than compounds (16),(32), (35) and (40). The two most potent inhibitors of DHFR were found to be (35) and (40) whose K_I values lie in the range 6×10^{-14} M to 7×10^{-13} M. This is significantly lower than the K_I value of the parent compound, methylbenzaprim (16). These three compounds all have K_I values at the picomolar concentration level and lower, which is comparable to the K_I of 2.2×10^{-12} M reported by Maag et al[144] for inhibition of rat liver DHFR by methotrexate. Werkheiser[25] estimated the dissociation constant of the methotrexate-DHFR complex to be less than 3×10^{-11} M and consequently described this inhibition as "stoichiometric". From the K_I values of (16), (35) and (40) calculated from these experiments it may therefore be assumed that these compounds are also effectively stoichiometric inhibitors of DHFR.

Results of the preliminary cytotoxicity studies carried out against L1210 murine leukaemia cells are shown in table 3.4. Previously reported results have shown benzaprim to have an I_{50} of less than 1.0 nM against L1210 cells[98]. Thus, as expected, all the compounds tested were found to have sub-micromolar I_{50} concentrations. The results for the 2-ethoxyethyl ester (33) show a particularly large variation. It

is interesting to note that although (38), the 4-methoxy analogue of benzaprim, is more potent an inhibitor of rat liver DHFR than (39), the 4-methoxy analogue of methylbenzaprim, their approximate I_{50} values against L1210 cells are of a similar magnitude.

On the basis of these results and the K_I values obtained against mammalian DHFR, two compounds were selected for antitumour testing. These were the benzoic acid (35) and the N-methylcarboxamide (40) analogues of methylbenzaprim, which had significantly lower K_I values compared to the other inhibitors. Griffin[98] has already reported the results of the screening of benzaprim and methylbenzaprim against P388 lymphocytic leukaemia in mice. Methylbenzaprim exhibited activity whilst benzaprim, which gave an identical I_{50} to methylbenzaprim against rat liver DHFR, and which was cytotoxic to L1210 cells *in vitro*, was inactive *in vivo*[98]. Thus, the minor transformation of benzaprim to form methylbenzaprim has led to a major effect in antitumour activity. This is possibly due to lack of uptake of the N-demethylated benzaprim. The results of the screening of the two analogues of methylbenzaprim, (35) and (40), against the M5076 reticulum cell sarcoma are provided in table 3.5. Antitumour activity is expressed as a measure of inhibition of tumour volume by the value T/C (%). The criterion for antitumour activity is for the T/C to be less than or equal to 42%[145]. These results show that at the optimum dose of 12 $mg.kg^{-1}$, the N-methylcarboxamide (40) was active at three doses with a T/C at the optimum dose of 15%. However the benzoic acid (35), the optimum dose of which was also 12 $mg.kg^{-1}$ proved to be inactive. Both compounds were toxic at 25 $mg.kg^{-1}$. The polar nature of the benzoic acid substituent probably rendered (35) inactive against the tumour due to lack of uptake. These results are consistent with the studies by Werbel *et al*[135] where only the more lipophilic compounds exhibited activity against the M5076 sarcoma.

From these results the N-methylcarboxamide analogue of methylbenzaprim (40) has emerged as the most promising candidate for evaluation as a lipophilic antitumour agent and further studies are warranted. These include evaluation against a wider range of tumours and examination of the physicochemical characteristics of the compound.

Table 3.2 Inhibition of DHFR from rat liver and E.coli

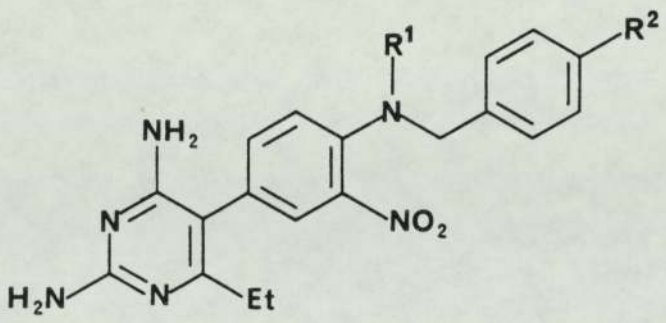

Compound Number	R^1	R^2	I_{50} E.coli DHFR (μM)	I_{50} Rat Liver DHFR (nM)
(16)[a]	Me	H	1.6	1.5
(32)[b]	Me	COOMe	n.d	10.0
(33)[c]	Me	$COO(CH_2)_2OC_2H_5$	n.d	5.0[e]
(35)[d]	Me	$COOH.H_2O$	1.4	1.0
(38)[a]	H	OMe	3.3	21.0
(39)[a]	Me	OMe	5.0	380.0
(40)[a]	Me	CONHMe	0.4	0.9

a solvent = 0.1 M hydrochloric acid

b solvent = methanol

c solvent = ethanol

d solvent = 0.01 M sodium hydroxide

e assay carried out using DHF 2 $mg.ml^{-1}$, 4 mM.

n.d I_{50} not determined.

Table 3.3 K_{Iapp} and K_I values determined for methylbenzaprim and analogues

Compound Number	R^1	R^2	K_{Iapp} (nm)	K_I (nm)
16	Me	H	0.79 ± 0.27[a]	0.0021 ± 0.007
32	Me	COOMe	5.4 ± 4.2	0.014 ± 0.011
35	Me	$COOH.H_2O$	0.15 ± 0.11	0.0004 ± 0.0003
38	H	OMe	33 ± 7	0.088 ± 0.019
39	Me	OMe	590 ± 100	1.6 ± 0.3
40	Me	CONHMe	0.13 ± 0.011	0.00035 ± 0.00029

a 95% confidence limits

Table 3.4 Cytotoxicity of analogues of methylbenzaprim against L1210 cells in vitro

Compound Number	Inhibitor Concentration (μM)	Percentage Growth Inhibition	IC_{50}[a] (μM)
32	5.0	91, 90	~0.1
	1.0	87, 92	
	0.5	85, 87	
	0.1	45, 55	
	0.05	2, 13	
	0.01	(+15[b]), 27	
	0.005	(+15[b]), (+10[b])	
	0.001	(+10[b]), 91	
33	5.0	89, 90	~0.05
	1.0	87, 87	
	0.5	75, 81	
	0.1	73, 82	
	0.05	32, 84	
	0.01	4, 99	
	0.005	38, 66	
	0.001	(+22[b]), 53	

Table 3.4 continued

Compound Number	Inhibitor Concentration (μM)	Percentage Growth Inhibition	IC_{50}[a] (μM)
35	5.0	92, 93	~0.02
	1.0	93, 93	
	0.5	92, 93	
	0.1	91, 92	
	0.05	89, 89	
	0.01	(+12[b]), 6	
	0.005	(+9[b]), 0	
	0.001	0, 0	
38	5.0	91, 91	~0.05
	1.0	89, 89	
	0.5	87, 89	
	0.1	70, 67	
	0.05	51, 66	
	0.01	(+16[b]), 19	
	0.005	(+6[b]), 19	

Table 3.4 continued

Compound Number	Inhibitor Concentration (μM)	Percentage Growth Inhibition	IC_{50}[a] (μM)
39	5.0	92, 92	~0.08
	1.0	89, 90	
	0.5	84, 88	
	0.1	53, 69	
	0.05	15, 26	
	0.01	0, 36	
	0.005	3, 7	
	0.001	(+3[b]), 12	
40	5.0	92, 91	~0.015
	1.0	91, 89	
	0.5	89, 91	
	0.1	87, 87	
	0.05	80, 83	
	0.01	31, 34	
	0.005	3, 23	
	0.001	(+7[b]), 14	

a the inhibitor concentration necessary to reduce the 48 h cell count to 50% of control

b no inhibition of cell growth evident

Table 3.5 Antitumour activity of two analogues of methylbenzaprim against the M5076 reticulum cell sarcoma

Compound Number	R	Dose ($mg.kg^{-1}$)	T/C (%)[a]
40	CONHMe	12.5[b]	15
		6.25	30
		3.125	41
		1.5	59
		0.75	67
35	$COOH.H_2O$	12.5[b]	100
		6.25	89
		3.125	107
		1.5	115
		0.75	100

a T = mean tumour volume of treated mice, and C = mean tumour volume of control mice. Thus 0% refers to complete absence of tumour and 100% refers to no difference between the volumes of treated and control mice

b The optimum dose; this is the dose nearest in value to the LD_{10} value

CHAPTER 4

CRYSTALLOGRAPHIC INVESTIGATION OF METHYLBENZAPRIM

4.1 Introduction

With the development of analogues of 2,4-diamino-5-[4-*N*-methylbenzylamino]-3-nitrophenyl]-6-ethylpyrimidine (methylbenzaprim) (16) as potential antitumour agents, it was considered of interest to study the crystal structure of the parent compound. Andrews *et al*[146] have used theoretical methods to establish preferred conformations of DHFR inhibitors, also using electrostatic potentials and conformational energy data to account for the species specificity of inhibitors to mammalian, bacterial and protozoal DHFRs. Crystallographic analysis of the lipophilic antifolates 2,4-diamino-5-(1-adamantyl)-6-methylpyrimidine (DAMP) (7) and 2,4-diamino-5-(1-naphthyl)-6-methylpyrimidine (DNMP) (8) allowed Cody and Zakrzewski[90] to examine the conformational aspects of drug specificity. They found that the two compounds occupied different regions in space and suggested that this may account for the reduced effectiveness of DNMP, since DNMP may not be able to fit into the active site of DHFR. Thus the elucidation of the structure of methylbenzaprim would aid the determination of the conformational and electronic properties of this compound.

4.2 Experimental

2,4-Diamino-5-[4-(*N*-methylbenzylamino)-3-nitrophenyl]-6-ethylpyrimidine (methylbenzaprim, 16) crystallised from aqueous 2-ethoxyethanol as hexagonal plates. A specimen 0.80 x 0.45 x 0.20 mm

was chosen for crystallographic analysis. The data were collected from an Enraf-Nonius CAD4 diffractometer with monochromated Mo-Kα radiation, lambda = 0.71069 Å.

4.2.1 Crystal Data

Methylbenzaprim, $C_{20}H_{22}N_6O_2$, M = 378.44, triclinic, a = 10.563(2), b = 11.842(6), c = 16.158(3) Å, α = 76.35(3), β = 89.53(2), γ = 78.13(3)°, V = 1930.5 Å^3, Z = 4, D_x = 1.303 Mg m^{-3}, D_m = 1.30 Mg m^{-3} (flotation in carbon tetrachloride/ light petroleum), F(000) = 800.00, μ = 0.52 cm^{-1}, space group $P\bar{1}$.

4.2.2 Structural Analysis

Unit cell dimensions were obtained from least squares analysis of setting angles of 25 reflections, $9.71 \leq \theta \leq 14.08°$. Intensity data were collected by the ω-2θ scan technique with ω scan range 1.35 + 0.35tanθ and ω scan speed 0.83 to 3.33 deg min^{-1}. The 7849 reflections were measured for $-12 \leq h \leq 12$, $-14 \leq k \leq 14$, $-19 \leq l \leq 2$, in the range $2 \leq \theta \leq 25°$ and were merged to give 6745 independent reflections (R_{int} = 0.095) of which 4467 were deemed observed with $F > 3\sigma$. Normalised structure factors were calculated and phases were determined by the MULTAN-80 programme[147] with default options. The distribution of intensities was found to be hypercentric. The phase set with the best combined figure of merit yielded an E-map in which both independent molecules were located, except for C(10), C(23), C(24), C(25), C(26), C(27), C(28) and C(10'). Apart from C(10'), the remaining atoms were located, using SHELX[148], in an electron density map following calculation of structure factors. With least squares refinement of positions and isotropic temperature factors it was

found that the terminal carbon of the ethyl group in the primed molecule did not occupy one position in the rigid molecule. To enable refinement of this group, site occupancy factors were assigned to the two positions, C(10') and C(10'').

Difference electron density synthesis located some of the hydrogen atoms whilst the remainder, excepting four of the hydrogen atoms attached to the ethyl group of the primed molecule, were fixed in calculated positions according to the AFIX procedure in SHELX. These were H(7), H(9), H(18), H(19), H(21), H(19') and H(21'). Further refinement of co-ordinates and anisotropic temperature factors for non-hydrogen atoms, and co-ordinates and isotropic temperature factors for hydrogen atoms was carried out with SHELX.

In the weighting scheme $w = k/[\sigma^2(F_o) + gF_o^2]$, the parameters converged to give $k = 7.8704$ and $g = 0.000235$ at discrepancy indices $R = 0.0761$ and $R_g = 0.1004$. The final maximum shift/ e.s.d ratio was 0.151 and the maximum and minimum features on a difference Fourier map were +0.32 and -0.39 e $Å^{-3}$.

4.3 Results and Discussion

Final atomic co-ordinates and equivalent isotropic temperature factors are given in Table 4.1, atomic nomenclature in figure 4.1 and plates 4.1.a and 4.1.b, and bond lengths and angles in Tables 4.2 and 4.3. Torsion angles are given in Table 4.4 and important intermolecular contacts are presented in Table 4.5. Observed and calculated structure factors are given in Appendix 1.

Results show the crystal to be triclinic with two independent molecules in the asymmetric unit. Like pyrimethamine hydrochloride[149], the ethyl group of the primed molecule shows disorder and so the C(10) atom was refined in the two positions as

Figure 4.1 PLUTO[161] drawing, with numbering scheme, of the two independent molecules of methylbenzaprim in the asymmetric unit

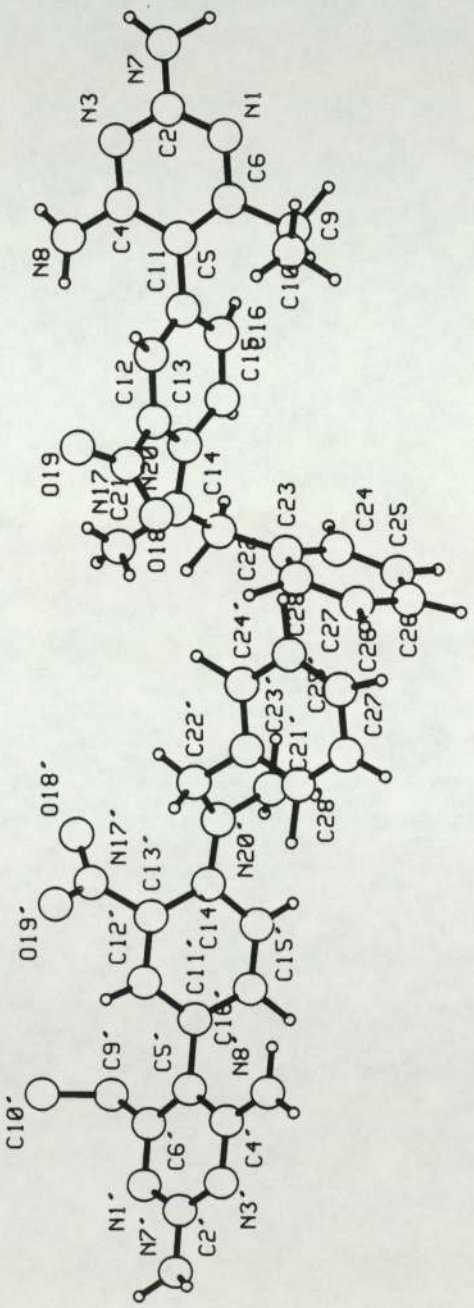

Plate 4.1.a Unprimed molecule of methylbenzaprim with numbering scheme, as drawn by CHEM-X[152]

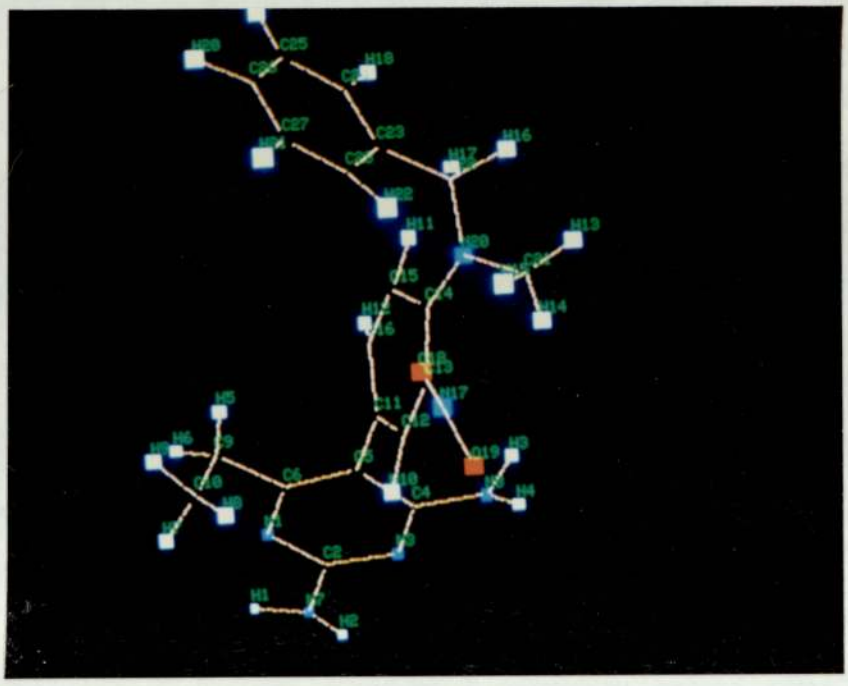

Plate 4.1.b Primed molecule of methylbenzaprim with numbering scheme, as drawn by CHEM-X[152]

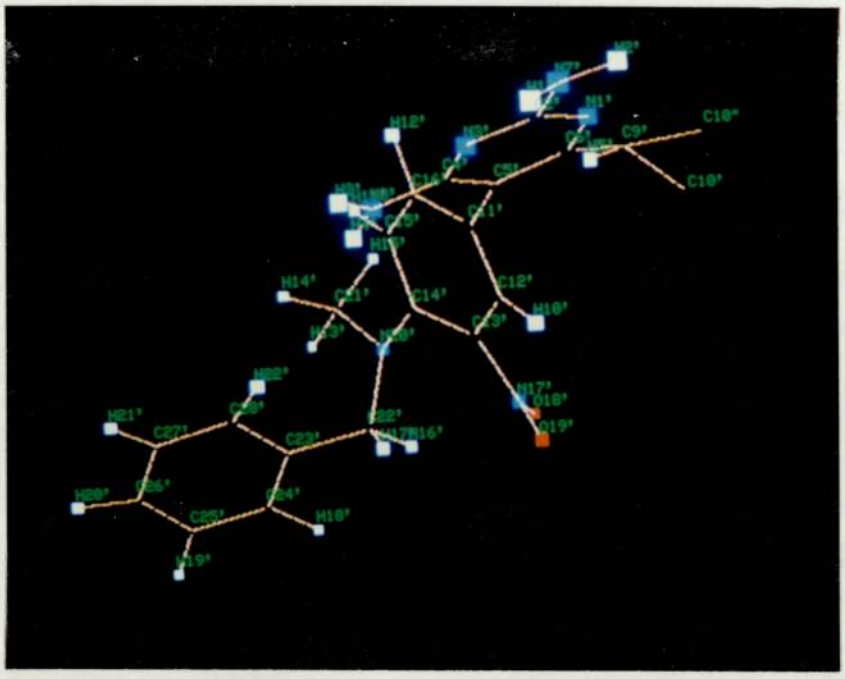

described. A significant difference (standard deviation > 3σ) between the two molecules was seen between the bond distance N(20)-C(21). Likewise, significant differences in bond angles between the two molecules occur between C(5)-C(6)-N(1), C(5)-C(11)-C(12), C(13)-N(17)-O(19), C(13)-C(14)-N(20), C(14)-N(20)-C(21), C(14)-N(20)-C(22) and O(18)-N(17)-O(19). Excepting the angle C(5)-C(6)-N(1), these differences may be expected as they occur in parts of the molecule capable of free rotation. In their study of the adamantyl pyrimidine DAMP (7), Cody and Zakrzewski[90] noted that due to steric interactions, the pyrimidine ring and its 4,6 substituents were severely distorted from coplanarity. A small distortion of this kind may account for the difference between the two angles of C(5)-C(6)-N(1). The narrow range of C-N bond distances [1.323(6)-1.352(7) Å] indicates that the p-electrons from every nitrogen atom in the pyrimidine participate in the delocalised π system.

Figure 4.2 shows the packing of the molecules in the unit cell. Antifolate drugs are found to associate in the crystalline state via dimeric N-H....N interactions with exocyclic amino groups as proton donors and endocyclic nitrogen atoms as proton acceptors[150]. Unprotonated diaminopyrimidine antifolates normally form two such base-pairs around centres or pseudo-centres of inversion, the 2-amino groups and N(1) atoms linking one pair of molecules and the 4-amino groups and N(3) atoms linking the other[151]. This pattern is indeed observed for the title compound. A pseudo-centre of inversion relating the atoms of the 2,4-diaminopyrimidine can be defined at x = 0.923, y = 0.399 and z = 0.165. Using the molecular modelling package CHEM-X[152] the planes of the pyrimidine rings of the primed and unprimed molecules, defined by N(1), C(2), N(3), C(4), C(5) and C(6), were calculated. If there were a true centre of symmetry, the angle between the planes would be expected to be 0°. However, this was not

Figure 4.2 PLUTO[161] drawing of the packing of the molecules of methylbenzaprim in the unit cell, viewed along the a-axis

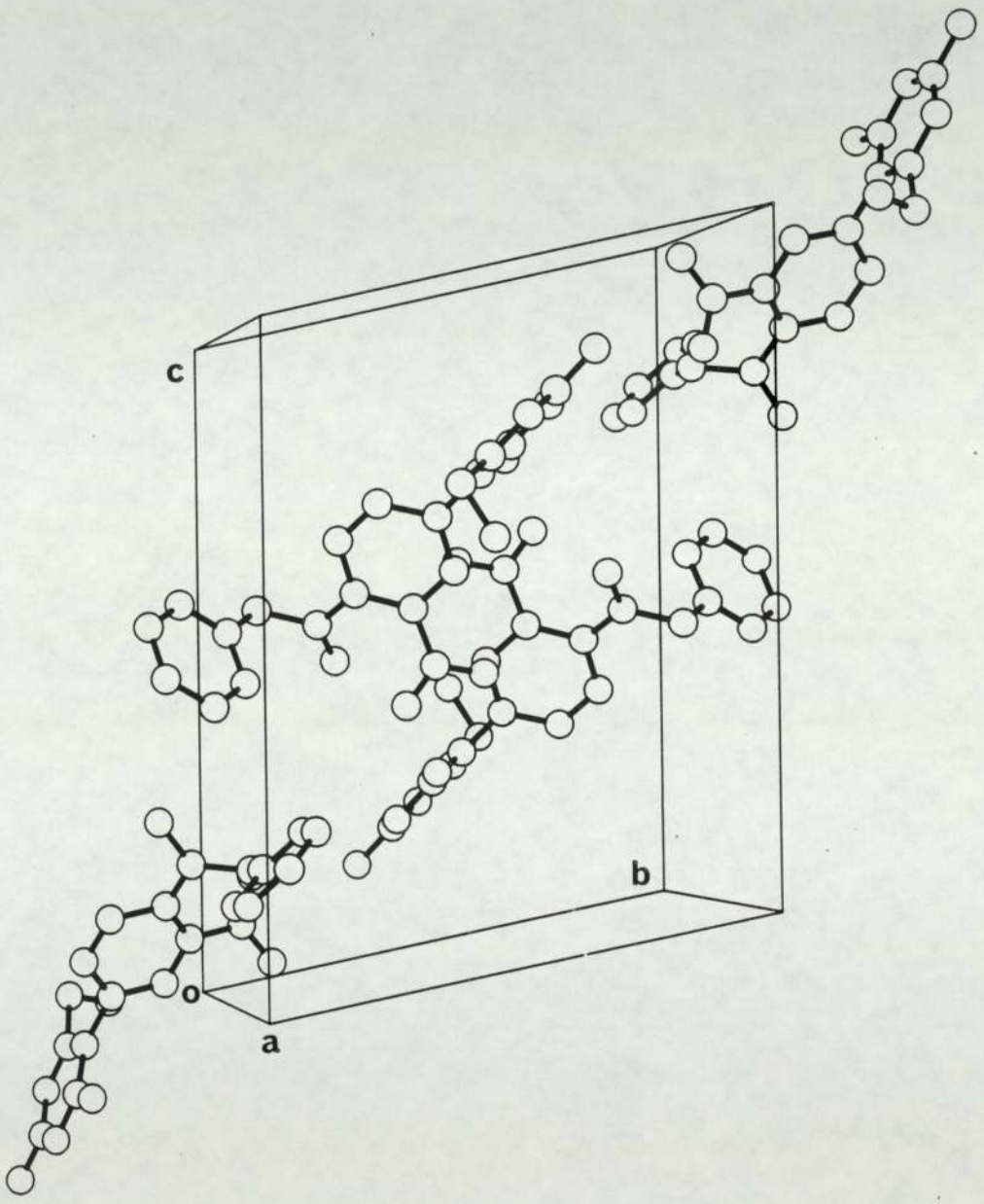

the case, the angle being 32°. The two independent molecules are associated not only by hydrogen-bonding between the amino groups and the nitrogen atoms but also by a weaker hydrogen-bond between the nitro group of the unprimed molecule and the N(7') amino group.

The differences between the two molecules lie, as expected, in the flexible N-methylbenzylamino region of the molecule. The C(13)-C(14)-N(20)-C(22), C(14)-N(20)-C(22)-C(23) and the N(20)-C(22)-C(23)-C(24) torsion angles are -170.1 and 37.4°, 79.9 and 117.8°, and -153.5 and 128.1° for the unprimed and primed molecules respectively. These both differ from benzaprim (15) whose three torsion angles are 175.8,-174.9 and 111.5 respectively[153]. This difference is probably due to the steric hindrance of the N-methyl group in methylbenzaprim. Plate 4.2 shows the two crystallographically independent molecules of methylbenzaprim and benzaprim, modified with a N-methyl at N(20) instead of N-H, superimposed onto one another to show the various conformations. It is interesting to note that the p-aminobenzoylglutamate moiety of methotrexate can be orientated to adopt several low energy conformations and can therefore readily accommodate itself to the requirements of the active site of the enzyme DHFR[154].

From the C(12)-C(13)-N(17)-O(18) and C(12)-C(13)-N(17)-O(19) torsion angles it can be seen that the nitro group is not coplanar with the benzene ring. By calculation of the planes of the nitro group, defined by N(17), O(18) and O(19), and the benzene ring, defined by C(11), C(12), C(13), C(14), C(15) and C(16), it was shown that the plane of the nitro group intersects the plane of the benzene ring at 30° and 33° respectively for the unprimed and primed molecules. This is less than the average 40° for non-interacting ortho-nitro groups[155]. The measured distances of N(17) and N(17') from the plane of the benzene ring were found to be 0.306 and 0.257 Å respectively.

Plate 4.2 The two crystallographically independent molecules of methylbenzaprim superimposed onto a modified benzaprim

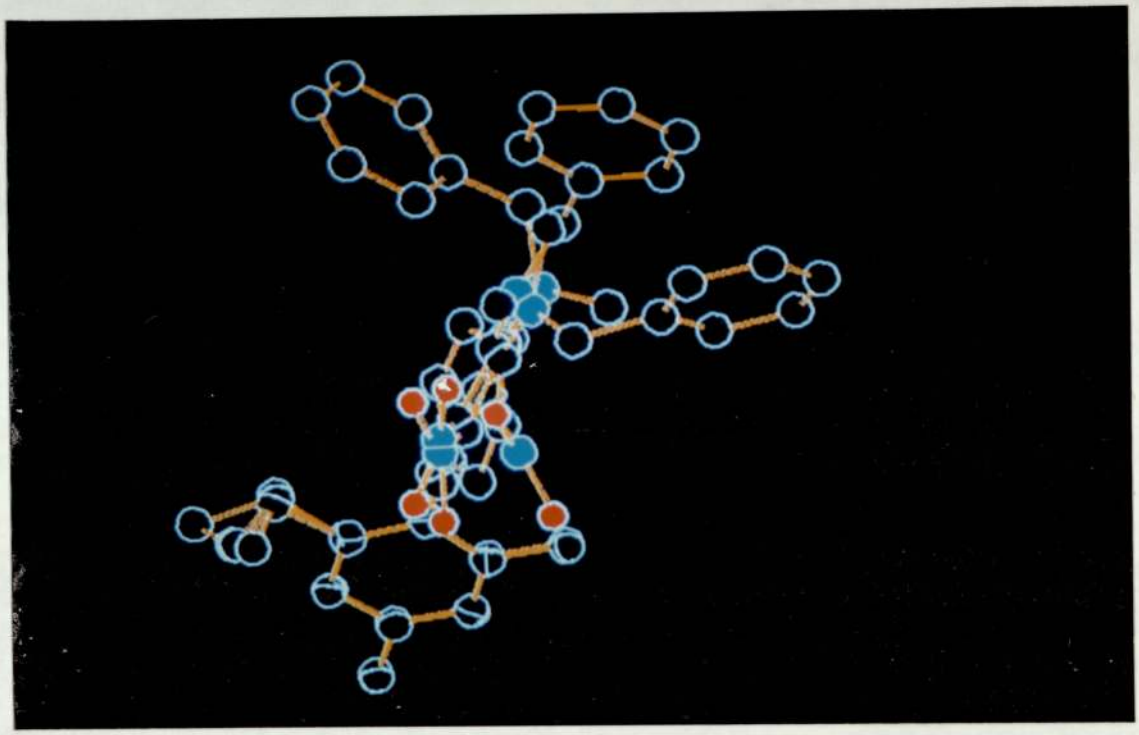

This deviation from coplanarity probably compensates for the reduced angle of intersection of the two planes, as described above, thus reducing the steric hindrance.

In order to map the region around the active site of DHFR, Hansch and coworkers have formulated QSARs (quantitative structure-activity relationships) from ligand interactions with DHFR for various compounds[156]. In their study of a series of Baker's triazines against bovine liver DHFR, Fukunaga et al[157] were able to show the main features of substituent interactions with the enzyme (figure 4.3).

Figure 4.3 Main features of substituent interactions of Baker's triazines with bovine liver DHFR

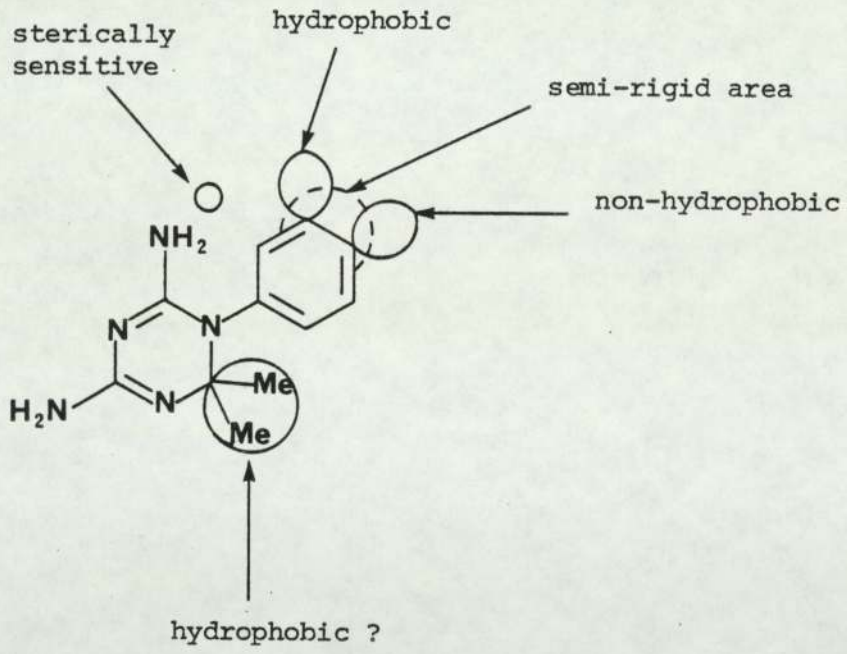

QSAR studies on a series of 6-substituted 2,4-diaminopyrimidines have shown that there is little to be gained with large groups in this 6-position, with ethyl or propyl substituents appearing to yield maximum activity through hydrophobic interaction[158]. Methylbenzaprim bears a resemblance to the triazine structure in the respect that the pyrimidine ring has a phenyl ring substituent in the 5-position which

in turn is p-substituted with a non-hydrophobic amino group. However this 5-phenyl ring is also meta-substituted with a non-hydrophobic nitro group. Figure 4.4 shows a possible resonance structure which indicates how the basicity of the N-methylbenzylamino portion of the molecule can be suppressed by the electron-withdrawing nitro group.

Figure 4.4 Possible resonance structure for methylbenzaprim.

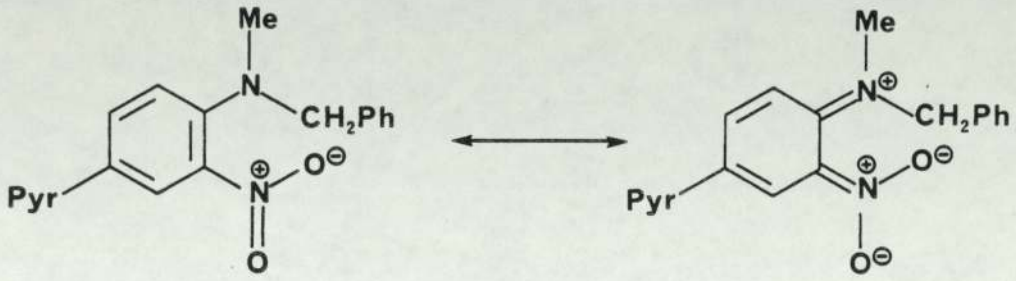

(I) (II)

Analysis of the bond distances shows that the C(13)-N(17) and C(14)-N(20) bond distances for the unprimed and primed molecules are 1.464(6), 1.462(5) and 1.365(6), 1.347(7) Å respectively. The C(14)-N(20) distances are appreciably shorter than those reported for aniline[159], being more comparable with the 1.352(5) bond length reported for 2,4-dinitroaniline[160]. The C13-N17 bond lengths come in between those reported for the C-N distances to the 2-nitro and 4-nitro substituents. This leads to the suggestion that resonance structure (II) may be very significant, thus reducing the hydrophilicity of this component. To substantiate this possibility, it was decided to study this portion of the molecule in more detail, and also to look at the flexibility of the N-methylbenzylamino group with respect to finding the lowest energy conformation. In order to do this, using the molecular modelling programme CHEM-X[152], the unprimed and primed molecules were modified by removal of the

pyrimidine ring and replacement with a hydrogen atom to form 2-(N-methylbenzylamino)nitrobenzene. These molecules were subjected to geometry optimisation using the semi-empirical MNDO programme[161] in MOPAC under CHEM-X. The three relevant torsion angles of the primed and unprimed molecules after MOPAC optimisation are given in Table 4.6. It can be seen that the geometry of the optimised structures does not vary greatly from those of the crystallographic structures. A map of the electrostatic potentials of the optimised structures, created by VSS in CHEM-X, at levels of -45 (red), 1000 (yellow) and 2000 (light blue) kcal.mol^{-1}, shows an area of electronegativity around the oxygen atoms of the nitro group but not around N20 (Plates 4.3.a and 4.3.b) thus supporting the resonance structure II shown in figure 4.4. This is not however consistent with the QSAR for triazines[157] but biological results have shown methylbenzaprim and some of its analogues to be potent inhibitors of DHFR (see Chapter 3).

Thus it can be seen that the combination of crystallography with theoretical calculations has provided some interesting information about methylbenzaprim. In the study described by Andrews *et al*[146] on the conformational energy of various inhibitors of DHFR, geometry optimisation of these molecules yielded a number of low energy conformations. Where the crystal structures of these free inhibitors were available, they fell in or near one of these low energy regions. Geometry optimisation of the flexible portion of the unprimed and primed molecules of methylbenzaprim has indeed shown the optimised structures to be very close to the crystallographic conformations.

Plate 4.3.a Electrostatic potential map of the optimised unprimed molecule of 2-(N-methylbenzylamino)nitrobenzene

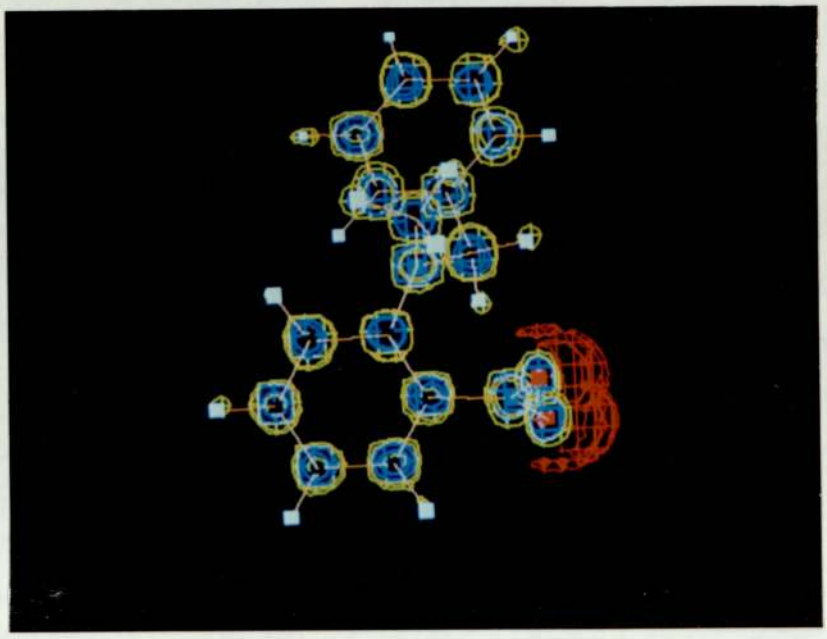

Plate 4.3.b Electrostatic potential map of the optimised primed molecule of 2-(N-methylbenzylamino)nitrobenzene

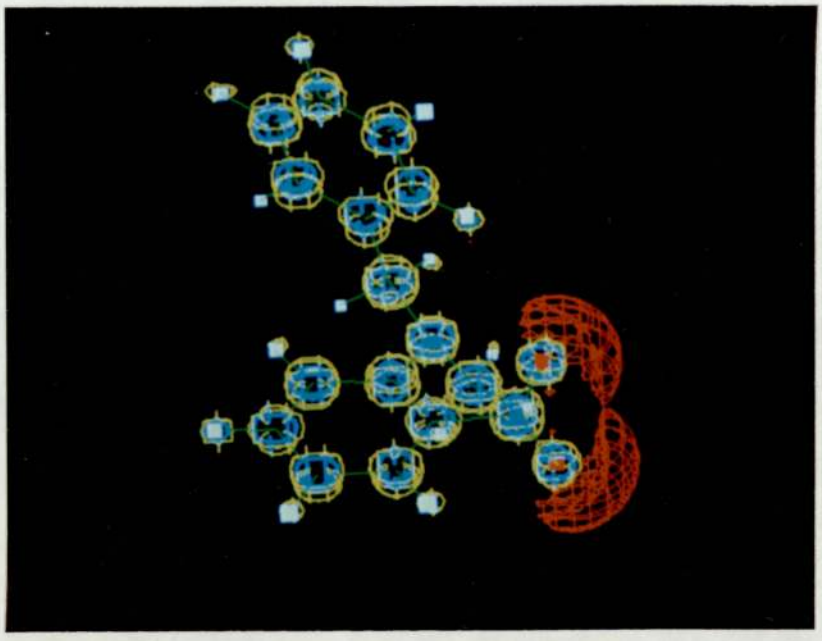

Table 4.1 Positional parameters (fractional co-ordinates x 10^4) and equivalent isotropic temperature factors for non-hydrogen atoms (x 10^4) with estimated standard deviations (e.s.d's) in parentheses

Atom	x	y	z	U_{iso}($Å^2$)
N(1)	300(3)	4691(3)	2226(3)	393(21)
C(2)	1279(4)	3958(4)	1963(3)	404(26)
N(3)	2545(3)	3849(3)	2125(2)	394(63)
C(4)	2861(4)	4549(4)	2592(3)	339(23)
C(5)	1911(4)	5360(3)	2904(3)	340(70)
C(6)	656(4)	5385(3)	2687(3)	344(69)
N(7)	940(3)	3259(4)	1488(3)	607(28)
N(8)	4134(3)	4427(3)	2768(3)	486(23)
C(9)	-489(4)	6182(4)	2993(3)	462(28)
C(10)	-890(6)	5609(5)	3843(4)	728(39)
C(11)	2325(4)	6143(4)	3393(3)	352(24)
C(12)	2771(4)	5736(3)	4231(3)	350(24)
C(13)	3209(4)	6494(4)	4656(3)	350(24)
C(14)	3296(4)	7662(4)	4251(3)	371(25)
C(15)	2717(4)	8084(4)	3430(3)	443(27)
C(16)	2260(4)	7354(4)	3017(3)	437(27)
N(17)	3456(3)	6015(3)	5564(3)	436(23)
O(18)	3121(4)	6671(3)	6051(2)	659(24)
O(19)	3938(3)	4938(3)	5845(2)	602(23)
N(20)	3970(3)	8328(3)	4600(3)	438(22)
C(21)	5028(5)	7803(4)	5210(3)	550(32)
C(22)	3819(4)	9595(4)	4192(3)	473(28)
C(23)	2626(5)	10381(4)	4404(3)	461(28)

Table 4.1 continued

Atom	x	y	z	U_{iso}(Å^2)
C(24)	2108(5)	11418(5)	3838(4)	632(34)
C(25)	1067(7)	12188(5)	4049(5)	849(45)
C(26)	504(6)	11922(5)	4832(5)	831(46)
C(27)	1018(7)	10883(6)	5399(4)	913(48)
C(28)	2077(6)	10098(5)	5181(4)	732(40)
N(1')	8064(3)	13711(3)	10817(2)	436(22)
C(2')	7199(4)	13892(4)	11408(3)	393(25)
N(3')	5998(3)	13720(3)	11428(2)	391(21)
C(4')	5614(4)	13290(4)	10790(3)	370(25)
C(5')	6455(4)	13027(3)	10152(3)	378(24)
C(6')	7681(4)	13266(4)	10192(3)	432(27)
N(7')	7592(3)	14354(4)	12037(3)	508(25)
N(8')	4400(3)	13104(4)	10816(3)	550(27)
C(9')	8630(5)	13114(6)	9497(4)	686(39)
C(10')	9674(12)	12123(17)	9796(9)	795(107)
C(10'')	10004(13)	13072(22)	9611(9)	943(127)
C(11')	5993(4)	12493(3)	9486(3)	371(24)
C(12')	6444(4)	11298(4)	9501(3)	375(24)
C(13')	5972(4)	10805(4)	8895(3)	394(25)
C(14')	5000(4)	11434(4)	8275(3)	369(24)
C(15')	4620(4)	12653(4)	8264(3)	453(26)
C(16')	5106(4)	13159(4)	8833(3)	420(26)
N(17')	6660(3)	9598(3)	8903(3)	476(24)
O(18')	6915(3)	9338(3)	8217(3)	614(23)
O(19')	7008(4)	8912(3)	9590(3)	808(28)

Table 4.1 continued

Atom	x	y	z	U_{iso}(Å^2)
N(20')	4452(4)	10946(3)	7725(2)	452(23)
C(21')	3715(4)	11706(4)	6969(3)	511(30)
C(22')	4171(5)	9743(4)	7992(3)	478(28)
C(23')	2777(4)	9701(4)	7948(3)	475(28)
C(24')	2391(6)	8929(5)	7521(4)	703(38)
C(25')	1102(8)	8861(6)	7496(6)	1037(57)
C(26')	233(7)	9539(9)	7900(8)	1271(70)
C(27')	594(7)	10311(7)	8316(6)	1090(62)
C(28')	1877(5)	10386(5)	8346(4)	754(41)
H(1)	-17	3552	1197	
H(2)	1484	2761	1223	
H(3)	4590	4952	3011	
H(4)	4679	4127	2363	
H(5)	-390	6861	2972	
H(6)	-1165	6401	2402	
H(7)	-1456	4998	3684	
H(8)	-390	5175	4352	
H(9)	-1574	6318	4052	
H(10)	2496	4863	4610	
H(11)	3045	8824	3072	
H(12)	2204	7677	2335	
H(13)	5863	8140	4980	
H(14)	5245	7002	5362	
H(15)	4627	7730	5841	
H(16)	4819	9836	4333	

Table 4.1 continued

Atom	x	y	z	$U_{iso}(Å^2)$
H(17)	3854	9739	3616	
H(18)	2525	11605	3217	
H(19)	651	13010	3602	
H(20)	-452	12514	4955	
H(21)	619	10682	6024	
H(22)	2720	9388	5696	
H(1')	7108	14177	12551	
H(2')	8611	14464	12058	
H(3')	3837	13319	11198	
H(4')	4057	12732	10412	
H(10')	7000	10756	9961	
H(11')	4093	13137	7765	
H(12')	4792	14150	8799	
H(13')	3277	11245	6608	
H(14')	2843	12115	7079	
H(15')	4369	12342	6738	
H(16')	4830	9326	7601	
H(17')	4369	9394	8567	
H(18')	3214	8392	7156	
H(19')	838	8223	7118	
H(20')	-781	9641	8006	
H(21')	-153	10751	8627	
H(22')	2328	10827	8844	

Table 4.2 Bond distances (Å) of the two molecules in the asymmetric unit (unprimed and primed) with e.s.d's in parentheses

Bond	Bond distance (Å)	
	Unprimed	Primed
N(1)-C(2)	1.334(5)	1.333(6)
C(2)-N(3)	1.338(5)	1.323(6)
C(2)-N(7)	1.336(7)	1.352(7)
N(3)-C(4)	1.318(6)	1.336(6)
C(4)-C(5)	1.406(6)	1.396(6)
C(4)-N(8)	1.348(5)	1.342(6)
C(5)-C(6)	1.365(6)	1.384(6)
C(5)-C(11)	1.465(7)	1.484(7)
C(6)-N(1)	1.323(6)	1.330(7)
C(6)-C(9)	1.520(6)	1.511(7)
C(9)-C(10)	1.498(8)	1.441(15)
C(9')-C(10'')		1.453(15)
C(5)-C(11)	1.465(7)	1.484(7)
C(11)-C(12)	1.392(6)	1.393(6)
C(12)-C(13)	1.383(7)	1.381(7)
C(13)-N(17)	1.464(6)	1.462(5)
N(17)-O(18)	1.216(6)	1.223(7)
N(17)-O(19)	1.262(5)	1.241(6)
C(13)-C(14)	1.424(6)	1.417(6)
C(14)-C(15)	1.413(6)	1.413(6)
C(15)-C(16)	1.355(7)	1.352(7)
C(16)-C(11)	1.425(6)	1.409(6)
C(14)-N(20)	1.365(6)	1.347(7)

Table 4.2 continued

Bond	Bond distance (Å)	
	Unprimed	Primed
N(20)-C(21)	1.445(6)	1.478(6)
N(20)-C(22)	1.487(5)	1.489(6)
C(22)-C(23)	1.487(6)	1.485(7)
C(23)-C(24)	1.385(6)	1.375(9)
C(24)-C(25)	1.367(8)	1.380(10)
C(25)-C(26)	1.396(10)	1.347(13)
C(26)-C(27)	1.387(8)	1.353(16)
C(27)-C(28)	1.393(9)	1.377(10)
C(28)-C(23)	1.383(8)	1.364(8)
N(7)-H(1)	1.08	0.98
N(7)-H(2)	0.91	1.11
N(7)-H(3)	1.00	0.89
N(8)-H(4)	0.94	0.97
C(9)-H(5)	0.83	1.31
C(9)-H(6)	1.15	
C(10)-H(7)	1.10	
C(10)-H(8)	0.97	
C(10)-H(9)	1.10	
C(12)-H(10)	1.18	0.98
C(15)-H(11)	1.06	0.99
C(16)-H(12)	1.09	1.14
C(21)-H(13)	1.07	1.04
C(21)-H(14)	0.91	0.98
C(21)-H(15)	1.09	1.13

Table 4.2 continued

Bond	Bond distance (Å)	
	Unprimed	Primed
C(22)-H(16)	1.18	1.05
C(22)-H(17)	0.91	0.94
C(24)-H(18)	1.09	1.19
C(25)-H(19)	1.10	1.14
C(26)-H(20)	1.15	1.07
C(27)-H(21)	1.09	1.04
C(28)-H(22)	1.16	1.19

Table 4.3 Bond angles (°) for the two molecules in the asymmetric unit (unprimed and primed) with e.s.d's in parentheses

Atoms	Bond angle (°)	
	Unprimed	Primed
C(6)-N(1)-C(2)	114.6(4)	115.6(4)
N(1)-C(2)-N(3)	127.2(5)	127.6(5)
N(1)-C(2)-N(7)	115.4(4)	115.3(4)
C(2)-N(3)-C(4)	116.5(4)	116.3(4)
N(3)-C(4)-C(5)	121.4(4)	121.0(4)
N(3)-C(4)-N(8)	116.6(4)	116.2(4)
C(4)-C(5)-C(6)	116.2(4)	117.3(5)
C(4)-C(5)-C(11)	118.8(4)	118.4(4)
C(5)-C(6)-N(1)	124.2(4)	122.1(4)
C(5)-C(6)-C(9)	122.9(4)	121.8(5)
C(5)-C(11)-C(12)	121.3(4)	119.5(4)
C(6)-C(9)-C(10)	110.9(4)	109.9(7)
C(6')-C(9')-C(10'')		122.6(8)
N(7)-C(2)-N(3)	117.4(4)	117.0(4)
N(8)-C(4)-C(5)	122.1(4)	122.7(5)
C(6)-C(5)-C(11)	125.0(4)	124.3(4)
C(9)-C(6)-N(1)	112.8(4)	116.0(4)
C(11)-C(12)-C(13)	119.3(4)	118.8(4)
C(12)-C(13)-C(14)	122.3(4)	123.6(4)
C(12)-C(13)-N(17)	113.5(4)	113.2(4)
C(13)-N(17)-O(18)	118.2(3)	117.0(4)
C(13)-N(17)-O(19)	121.6(4)	119.6(5)
C(13)-C(14)-C(15)	116.6(4)	115.1(4)

Table 4.3 continued

Atoms	Bond angle (°)	
	Unprimed	Primed
C(13)-C(14)-N(20)	112.7(4)	124.4(4)
C(14)-C(15)-C(16)	120.8(4)	121.9(4)
C(14)-N(20)-C(21)	122.1(4)	119.9(4)
C(14)-N(20)-C(22)	117.9(4)	120.6(4)
C(15)-C(14)-N(20)	120.6(4)	120.5(4)
C(15)-C(16)-C(11)	121.7(4)	121.7(4)
C(16)-C(11)-C(12)	118.5(4)	118.5(4)
C(16)-C(11)-C(5)	120.1(4)	122.0(4)
N(17)-C(13)-C(14)	124.0(4)	123.0(4)
O(18)-N(17)-O(19)	120.2(4)	123.3(4)
N(20)-C(22)-C(23)	115.3(4)	114.4(3)
C(21)-N(20)-C(22)	118.3(4)	116.2(4)
C(22)-C(23)-C(24)	119.7(5)	119.4(5)
C(22)-C(23)-C(28)	119.8(4)	121.3(5)
C(23)-C(24)-C(25)	120.3(5)	119.8(6)
C(24)-C(25)-C(26)	120.1(5)	119.8(8)
C(25)-C(26)-C(27)	119.8(6)	121.2(8)
C(26)-C(27)-C(28)	120.0(6)	119.5(8)
C(27)-C(28)-C(23)	119.4(5)	120.4(7)
C(28)-C(23)-C(24)	120.4(5)	119.3(5)

Table 4.4 Torsion angles (°) of the two molecules (unprimed and primed) in the asymmetric unit

Atoms	Torsion Angle (°)	
	Unprimed	Primed
C(2)-N(1)-C(6)-C(5)	-1.4	1.1
C(2)-N(1)-C(6)-C(9)	-178.5	177.1
C(6)-N(1)-C(2)-N(3)	1.1	-2.6
C(6)-N(1)-C(2)-N(7)	-179.3	-179.4
N(1)-C(2)-N(3)-C(4)	-0.6	1.6
N(7)-C(2)-N(3)-C(4)	179.8	178.4
C(2)-N(3)-C(4)-C(5)	0.3	0.9
C(2)-N(3)-C(4)-N(8)	178.9	179.3
N(3)-C(4)-C(5)-C(6)	-0.7	-2.1
N(3)-C(4)-C(5)-C(11)	-177.8	176.8
N(8)-C(4)-C(5)-C(6)	-179.2	179.6
N(8)-C(4)-C(5)-C(11)	3.7	-1.5
C(4)-C(5)-C(6)-N(1)	1.3	1.1
C(4)-C(5)-C(6)-C(9)	178.1	-174.7
C(4)-C(5)-C(11)-C(12)	-76.2	-105.2
C(4)-C(5)-C(11)-C(16)	104.6	74.9
C(6)-C(5)-C(11)-C(12)	106.9	73.7
C(6)-C(5)-C(11)-C(16)	-72.2	-106.2
C(11)-C(5)-C(6)-N(1)	178.2	-177.8
C(11)-C(5)-C(6)-C(9)	-5.0	6.4
N(1)-C(6)-C(9)-C(10)	91.2	74.1
N(1')-C(6')-C(9')-C(10'')		19.6
C(5')-C(6')-C(9')-C(10'')		-164.3

Table 4.4 continued

Atoms	Torsion Angle (°)	
	Unprimed	Primed
C(5)-C(6)-C(9)-C(10)	-85.9	-109.8
C(5)-C(11)-C(12)-C(13)	177.0	177.8
C(5)-C(11)-C(16)-C(15)	-175.4	-175.3
C(12)-C(11)-C(16)-C(15)	5.4	4.8
C(16)-C(11)-C(12)-C(13)	-3.8	-2.3
C(11)-C(12)-C(13)-C(14)	-4.0	-3.1
C(11)-C(12)-C(13)-N(17)	170.9	171.4
C(12)-C(13)-C(14)-C(15)	10.1	5.8
C(12)-C(13)-C(14)-N(20)	-165.8	174.2
C(12)-C(13)-N(17)-O(18)	-138.5	-137.8
C(12)-C(13)-N(17)-O(19)	37.7	38.9
C(14)-C(13)-N(17)-O(18)	36.4	36.8
C(14)-C(13)-N(17)-O(19)	-147.5	-146.5
N(17)-C(13)-C(14)-C(15)	-164.3	-168.2
N(17)-C(13)-C(14)-N(20)	19.8	11.8
C(13)-C(14)-C(15)-C(16)	-8.4	-3.2
C(13)-C(14)-N(20)-C(21)	24.6	-163.9
C(13)-C(14)-N(20)-C(22)	-170.1	37.4
C(15)-C(14)-N(20)-C(21)	-151.1	16.1
C(15)-C(14)-N(20)-C(22)	14.2	-142.5
N(20)-C(14)-C(15)-C(16)	167.5	176.8
C(14)-C(15)-C(16)-C(11)	1.0	-1.9
C(14)-N(20)-C(22)-C(23)	79.9	117.8
C(21)-N(20)-C(22)-C(23)	-114.3	-41.6

Table 4.4 continued

Atoms	Torsion Angle (°)	
	Unprimed	Primed
N(20)-C(22)-C(23)-C(24)	-153.5	128.1
N(20)-C(22)-C(23)-C(28)	29.5	-54.1
C(22)-C(23)-C(24)-C(25)	-175.4	178.3
C(22)-C(23)-C(28)-C(27)	175.2	-178.3
C(24)-C(23)-C(28)-C(27)	-1.8	-0.4
C(28)-C(23)-C(24)-C(25)	1.7	0.4
C(23)-C(24)-C(25)-C(26)	-1.3	-0.9
C(24)-C(25)-C(26)-C(27)	1.1	1.5
C(25)-C(26)-C(27)-C(28)	-1.3	-1.6
C(26)-C(27)-C(28)-C(23)	1.6	1.0

Table 4.5 Contacts related to hydrogen bonds in the packing of the molecules of methylbenzaprim

	Distance (Å) X....Y	Angle (°) X-H....Y
N(7)-H(1)....N(1')^{i}	3.135	165
N(8)-H(4)....N(3')^{ii}	3.040	171
N(7')-H(2')....N(1)^{iii}	2.991	173
N(8')-H(3')....N(3)^{iv}	3.009	177
N(7')-H(1')....O(18)^{v}	3.219	155

Symmetry code: (i) 1+x, 1+y, 1+z; (ii) x, 1+y, 1+z; (iii) -1+x, -1+y, -1+z; (iv) x, -1+y, -1+z; (v) 1-x, 2-y, 2-z.

Table 4.6 Important torsion angles (°) of 2-(N-methylbenzylamino)-nitrobenzene after MOPAC optimisation

Atoms	Torsion Angle (°)	
	Unprimed	Primed
C(13)-C(14)-N(20)-C(22)	-164.2 (-170.1)[a]	46.9 (37.4)[a]
C(14)-N(20)-C(22)-C(23)	66.6 (79.9)[a]	125.8 (117.8)[a]
N(20)-C(22)-C(23)-C(24)	-147.0 (-153.5)[a]	127.6 (128.1)[a]

[a] The figures in brackets are the corresponding torsion angles for the unoptimised structures as shown on Table 4.4

CHAPTER 5

CONCLUSIONS AND FUTURE OBJECTIVES

Several analogues of the lead compound methylbenzaprim (16), encompassing a range of substituents, were synthesised. Assessment of these compounds for activity against DHFR from rat liver revealed that two of the compounds, (35) and (40), had K_I values that were significantly lower than that of methylbenzaprim. These two compounds were then screened for antitumour activity against the M5076 reticulum cell sarcoma, the results showing that the N-methylcarboxamide (40) was active *in vivo* as well as *in vitro*, whilst the M5076 sarcoma was refractory to inhibition by the benzoic acid (35). This is possibly due to the decreased lipophilicity of the benzoic acid over the N-methylcarboxamide, thus affecting the uptake of the compound into the tumour cells. From these preliminary studies compound (40) exhibits promise as a candidate lipophilic antitumour agent.

Due to the inhibitory potency of compounds (16), (35), and (40) against DHFR, it would be of interest to study the interaction of these compounds with the enzyme at a molecular level. To this end, the crystal structure of the parent compound methylbenzaprim (16) was elucidated, and analysis of preferred conformations and electrostatic potentials of the flexible portion of methylbenzaprim, 2-(N-methylamino)nitrobenzene, were carried out. Knowledge of the structure of methylbenzaprim thus allows investigation of the possible interactions of this compound with DHFR. Ideally, this would be carried out using molecular graphics by fitting MBP into the active site of the mammalian enzyme. However, presently the crystallographic coordinates of mammalian DHFR are not yet available,

although those of the E.coli DHFR-methotrexate binary complex, and the L.casei DHFR-methotrexate-NADPH ternary complex are available. Since these compounds have been shown to have inhibitory activity against DHFR from E.coli the studies could be carried out using the crystal structure of the E.coli DHFR-methotrexate binary complex.

Recent preliminary high-field n.m.r experiments with MBP bound to L.casei DHFR in a binary complex indicate that the benzylic ring does not occupy the same region in the active site as the p-aminobenzoylglutamate moiety of methotrexate[162] as predicted earlier by comparison of the relative activities of metoprine, MBP and methotrexate (figure 1.6). This may be the reason that methylbenzaprim does not fit the structure-activity relationship developed for the triazines, with possible differences in the mode of binding to DHFR.

Therefore, future work could involve the modelling of MBP with L.casei DHFR in order to determine the possible position of the benzylic moiety. With the knowledge of the residues surrounding the molecule, with which it interacts, and the space occupied by this region, it may be possible then to explain the high activity of the N-methylcarboxamide (40). Thus it may also be possible to rationally design and synthesise analogues of methylbenzaprim which will further probe this site.

APPENDIX 1

Observed and Calculated Structure Factors for Methylbenzaprim

(see microfiche in rear cover)

REFERENCES

1. Rader, J.I. and Huennekens, F.M. In "The Enzymes"; Boyer, P., Ed; Academic Press, New York, 1973, 3rd ed., Vol. 9, p. 197

2. Huennekens, F.M. In "Biological Oxidations"; Singer, T.P., Ed.; Wiley, New York, p.439

3. Kisliuk, R.L. In "Folate Antagonists as Therapeutic Agents"; Sirotnak, F.M., Burchall, J.J., Ensminger, W.D. and Montgomery, J.A., Eds.; Academic Press, New York, Vol. 1, p.19

4. Freidkin, M. Adv. Enzymol., **1973**, 38, 235

5. McDougall, B.M. and Blakley, R.L. J. Biol. Chem., **1961**, 236, 832

6. Cohen, S.S. Ann. N. Y. Acad. Sci., **1971**, 186, 292

7. Angier, R.B., Boothe, J.H., Hutchings, B.L., Mowat, J.H., Semb, J., Stokstad, E.L.R., SubbaRow, Y., Walker, C.W., Cosulich, D.B., Fahrenbach, M.J., Deeger, D.R., Sickels, J.P., and Smith, J.M., Jr. Science, **1946**, 103, 667

8. Seeger, D.R., Smith, J.M., Jr. and Hultquist, M.E. J. Am. Chem. Soc., **1947**, 69, 2567

9. Seeger, D.R., Cosulich, D.B., Smith, J.M., Jr. and Hultquist, M.E. J. Am. Chem. Soc., **1949**, 71, 1753

10. Farber, S., Diamond, L.K., Mercer, R.D., Sylvester, R.F. and Wolff, J.A. N. Engl. J. Med., **1948**, 238, 787

11. Burchenal, J.H., Karnofsky, D.A., Southam, C.M., Myers, P.L.I., Carrer, L.F., Dargeon, H.W. and Rhoads, C.P. Am. J. Med., **1949**, 7, 420

12. Futterman, S. J. Biol. Chem., **1957**, 228, 1031

13. Osborn, M.J., Freeman, M. and Huennekens, F.M. Proc. Soc. Exp. Biol. Med., **1958**, 97, 429

14. Zakrzewski, S. F. and Nichol, C. A. Biochim. Biophys. Acta, **1958**, 27, 425

15. Roth, B. and Cheng, C.C. Prog. Med. Chem., **1982**, 19, 269

16. Baker, B. R. "Design of Active-Site-Directed Irreversible Enzyme Inhibitors"; Wiley, New York, 1967, p. 192

17. "Folate Antagonists as Therapeutic Agents. Vol. 1. Biochemistry, Molecular Action and Synthetic Design"; Sirotnak, F.M., Burchall, J.J., Ensminger, W.B. and Montgomery, J.A., Eds.; Academic Press, New York, 1984

18. Hitchings, G.H. and Roth, B. In "Enzyme Inhibitors as Drugs"; Sandler, M., Ed.; Macmillan, London, 1980, chapter 17, p. 263

19. Burchall, J.J. and Hitchings, G.H. Mol. Pharmacol., **1965**, 1, 126

20. Blakley, R.L. "The Biochemistry of Folic Acid and Related Pteridines"; North-Holland, Amsterdam, 1969

21. "Folate Antagonists as Therapeutic Agents. Vol. 2."; Sirotnak, F.M., Burchall, J.J., Ensminger, W.B. and Montgomery, J.A., Eds.; Academic Press, New York, 1984

22. Philips, F.S., Thiersch, J.B. and Ferguson, F.C., Jr. Ann. N. Y. Acad. Sci., **1950**, 52, 1349

23. Johns, D.G., Ianotti, A.C., Sartorelli, A.C. and Bertino, J.R. Biochem. Pharmacol., **1966**, 15, 555

24. Sirotnak, F.M. and Donsbach, R.C. Cancer Res., **1976**, 36, 1151

25. Werkheiser, W.C. J. Biol. Chem., **1961**, 236, 888

26. Baker, B.R. Cancer Chemother. Rep., **1959**, 4, 1

27. Perault, A.M. and Pullman, B. Biochim. Biophys. Acta, **1961**, 52, 266

28. Matthews, D.A., Alden, R.A., Bolin, J.T., Freer, S.T., Hamlin, R., Xuong, N., Kraut, J., Poe, M. and Hoogsteen, K. Science (Washington D.C.), **1977**, 197, 452

29. Matthews, D.A., Alden, R.A., Bolin, J.T., Filman, D.J., Freer, S.T., Hamlin, R., Hol, W.G.J., Kisliuk, R.L., Pastore, E.J., Plante, L.T., Xuong, N.H. and Kraut, J. J. Biol. Chem., **1978**, 253, 6946

30. Bolin, J.T., Filman, D.J., Matthews, D.A., Hamlin, R.C. and Kraut, J. J. Biol. Chem., **1982**, 257, 13650

31. Filman, D.J., Bolin, J.T., Matthews, D.A. and Kraut, J. J. Biol. Chem., 1982, 257, 13663

32. Volz, K., Matthews, D.A., Alden, R., Freer, S.T., Hansch, C., Kaufman, B. and Kraut, J. J. Biol. Chem., 1982, 257, 2528

33. Gready, J.E. Adv. Pharmacol. Chemother., 1980, 17, 37

34. Cocco, L., Roth, B., Temple, C., Jr., Montgomery, J.A., London, R.E. and Blakley, R.L. Arch. Biochem. Biophys., 1983, 226, 567

35. Fontecilla-Camps, J.C., Bugg, C.E., Temple, C., Jr., Rose, J.D., Montgomery, J.A. and Kisliuk, R.L. J. Am. Chem. Soc., 1979, 101, 6114

36. Charlton, P.A., Young, D.W., Birdsall, B., Feeney, J. and Roberts, G.C.K. J. C. S. Chem. Commun., 1979, 922

37. Montgomery, J.A. and Piper, J.R. In "Folate Antagonists as Therapeutic Agents. Vol. 1"; Sirotnak, F.M., Burchall, J.J., Ensminger, W.D. and Montgomery, J.A., Eds.; Academic Press, New York, 1984, p. 219

38. Bertino, J.R. Cancer Res., 1979, 39, 293

39. Kessel, D., Hall, J.C., Roberts, D. and Wodinsky, I. Science, 1965, 150, 752

40. Goldman, I.D., Lichenstein, N.S. and Oliverio, V.T. J. Biol. Chem., 1968, 243, 5007

41. Goldman, I.D. Ann. N. Y. Acad. Sci., 1971, 186, 400

42. Sirotnak, F.M. Cancer Res., 1985, 45, 3992

43. Tattersall, M.H.N. In "Folate Antagonists as Therapeutic Agents. Vol. 2"; Sirotnak, F.M., Burchall, J.J., Ensminger, W.B. and Montgomery, J.A., Eds.; Academic Press, New York, 1984, p. 165

44. Selawry, O. S. J. Am. Med. Assoc., 1965, 194, 75

45. Burchenal, J.H., Kushida, M.N., Johnston, S.F. and Cremer, M.A. Proc. Soc. Exp. Biol. Med., 1949, 71, 559

46. Goldin, A., Mantel, N., Greenhouse, S.W., Venditti, J.M. and Humphreys, S.R. Cancer Res., 1953, 13, 843

47. Goldin, A., Venditti, J.M., Kline, I. and Mantel, N. Nature, 1966, 212, 1548

48. Bertino, J.R. Seminars Oncol., 1977, 4, 203

49. Borsa, J. and Whitmore, G.F. Cancer Res., 1969, 29, 737

50. Nederbragt, H., Uitendaal, M.P., van der Grint, L., Levya, A. and Pinedo, H.M. Cancer Res., 1981, 41, 1193

51. Chabner, B.A.,Johns, D.G. and Bertino, J.R. Nature, 1972, 239, 395

52. Capizzi, R.L., Handschumaker, R.E. In "Cancer Medicine"; Holland, J.F. and Frei, E., Eds.; Lea and Fabinger, Philadelphia, 1973, p.920

53. Capizzi, R.L. Cancer. Chemother. Rep., 1975, 6, 37-41

54. Shapiro, W.R., Young, D.F. and Mehta, B.M. N. Engl. J. Med., 1975, 293, 161

55. Wang, J.O., Freeman, J.I. and Sinks, L.F. Cancer Res., 1976, 36, 1441

56. Rosowsky, A., Freisheim, J.H., Bader, H., Forsch, R.A., Susten, S.S., Cucchi, C.A. and Frei III, E. J. Med. Chem., 1985, 28, 660

57. Rosowsky, A., Beardsley, G.P., Ensminger, W.D., Lazarus, H. and Yu, C-S. J. Med. Chem., 1978, 21, 380

58. Piper, J.R. and Montgomery, J.A. Devl. Biochem., 1979, 4, 261

59. Rosowsky, A., Bader, H., Radike-Smith, M., Cucchi, C.A., Wick, M.M. and Freisheim, J.H. J. Med. Chem., 1986, 29, 1703

60. Albrecht, A.M. and Biedler, J.L. In "Folate Antagonists as Therapeutic Agents. Vol. 1"; Sirotnak, F.M., Burchall, J.J., Ensminger, W.B. and Montgomery, J.A., Eds.; Academic Press, New York, 1984, p. 319

61. Alt, F., Kellems, R.E., Bertino, J.R. and Schimke, R.T. J. Biol. Chem., 1978, 253, 1357

62. Schimke, R.T., Kaufman, R.J., Alt, F.W. and Kellems, R.F. Science, 1978, 202, 1051

63. Melera, P.W., Hession, C.A., Davide, J.P., Scotto, K.W., Biedler, J.L., Meyers, M.B. and Schanske, S. J. Biol. Chem., 1982, 257, 12939

64. Flintoff, W.F. and Essani, K. Biochemistry, 1980, 19, 4321

65. Goldie, J.H., Dedhar, S. and Krystal, G. J. Biol. Chem., 1981, 256, 11629

66. Jackson, R.C. and Niethammer, D. Eur. J. Cancer, 1977, 13, 567

67. Fischer, G.A. Biochem. Pharmacol., 1962, 11, 1233

68. Galivan, J. Cancer Res., 1981, 41, 1757

69. Burns, C.P., Lutteneger, D.G., Dudley, D.T., Buettner, G.R. and Spector, A.A. Cancer Res., 1979, 39, 1726

70. Taylor, R.T. and Hanna, M.L. Arch. Biochem. Biophys., 1977, 181, 331

71. Baugh, C.M., Krumdieck, C.L. and Nair, M.G. Biochem. Biophys. Res. Commun., 1973, 52, 27

72. Jacobs, S.A., Adamson, R.H., Chabner, B.A., Derr, C.J. and Johns, D.G. Biochem. Biophys. Res. Commun., 1975, 63, 692

73. Galivan, J., Inglese, J., McGuire, J.J., Nimec, Z. and Coward, J.G. Proc. Natl. Acad. Sci., 1985, 82, 2598

74. Cowan, J.H. and Jolivet, J. Clin. Res., 1983, 31, 508A

75. Curt, G., Carney, D., Jolivet, J., Bailey, B., Schepartz, S. and Chabner, B. Proc. Am. Assoc. Cancer Res., 1983, 24, 283

76. Mini, E., Moroson, B.A., Franco, C.T. and Bertino, J.R. Cancer Res., 1985, 45, 325

77. Cowan, K.H. and Jolivet, J. J. Biol. Chem., 1984, 259, 10793

78. Diddens, H., Niethammer, D. and Jackson, R.C. Cancer Res., 1983, 43, 5286

79. Kamen, B.A., Eibl, B., Cashmore, A. and Bertino, J. Biochem. Pharmacol., 1984, 33, 1697

80. Hamrell, M.R. Oncology, 1984, 41, 343

81. Jonak, J.P., Zakrzewski, S.F. and Mead, L.H. J. Med. Chem., 1971, 14, 408

82. Jonak, J.P., Zakrzewski, S.F. and Mead, L.H. J. Med. Chem., 1972, 15, 662

83. Russell, P.B. and Hitchings, G.H. J. Am. Chem. Soc., 1951, 73, 3763

84. Baker, B.R. and Ashton, W.T. J. Med. Chem., 1973, 16, 209

85. Elslager, E.F., Johnson, J.L. and Werbel, L.M. J. Med. Chem., 1983, 26, 1753

86. Grivsky, E.M., Lee, S., Sigel, C.W., Duch, D.S. and Nichol, C.A. J. Med. Chem., 1980, 23, 327

87. Ho, Y.K., Hakala, M.T. and Zakrzewski, S.F. Cancer Res., 1972, 32, 1023

88. Greco, W.R. and Hakala, M.T. Mol. Pharmacol., 1980, 18, 521

89. Ho, Y.K., Zakrzewski, S.F. and Mead, L.H. Biochemistry, 1973, 12, 1003

90. Cody, V. and Zakrzewski, S.F. J. Med. Chem., 1982, 25, 427

91. Murphy, M.I., Ellison, R.R., Karnofsky, D.A. and Burchenal, J.H. J. Clin. Invest., 1954, 33, 1388

92. Nichol, C.A., Cavallito, J.C., Woolley, J.L. and Sigel, C.W. Cancer Treat. Rep., 1977, 61, 559

93. Geils, G.F., Scott, C.W., Jr., Baugh, C.M. and Butterworth, C.E., Jr. Blood, 1971, 38, 131

94. Denlinger, R.H., Nichol, C.A., Cavallito, J.C. and Sigel, C.W. Proc. Am. Assoc. Cancer Res., 1976, 17, 379

95. Cavallito, J.C., Nichol, C.A., Brenckman, W.D., Jr., DeAngelis, R.L., Stickney, D.R., Simmons, W.S. and Sigel, C.W. Drug Metab. Disp., 1978, 6, 329

96. Duch, D.S., Edelstein, M.P. and Nichol, C.A. Mol. Pharmacol., 1980, 18, 100

97. Bliss, E.A. PhD Thesis, Aston University, 1980

98. Griffin, R.J. PhD Thesis, Aston University, 1986

99. Pashley, S.G.H., Slack, J.A., Stevens, M.F.G. and Bliss, E.A. J. Pharm. Pharmacol., 1984, 36(S), 69P

100. Threadgill, M.D., Griffin, R.J., Stevens, M.F.G. and Wong, S.K. J. Chem. Soc. Perkin Trans. 1, in press

101. Slack, J.A., Blackledge, G.R.P., Newlands, E.S., Stuart, N., Crawford, S.M., Wong, S.K., Pashley, S.H., Brindley, C.J. and Hoffman, R. Proc. Am. Assoc. Cancer Res., 1987, 28, 746

102. Bertino, J., Sawicki, W.L., Moroson, B.A., Cashmore, A.R. and Elslager, E.F. Biochem. Pharmacol., 1979, 28, 1983

103. Weiss, R.B., James, W.D., Major, W.B., Porter, M.B., Allegra, C.J. and Curt, G.A. Invest. New Drugs, 1986, 4, 159

104. Leiby, J., Goldberg, D., Stewart, D., Martelo, O., Stewart, J., Bergsagel, D., Capizzi, R., Robert, N., Jolivet, J., Ballaire, B., Grillo, A. and Grove, W. Proc. Am. Soc. Clin. Oncol., 1987, 6, 210

105. Duch, D.S., Edelstein, M.P., Bowers, S.W. and Nichol, C.A. Cancer Res., 1982, 42, 3987

106. Hamrell, M.R. and Sedwick, W.D. Proc. Amer. Assoc. Cancer Res., 1979, 20, 247

107. Browman, G.P., Calvert, A.H.,, Taylor, G.A., Hart, L.I. and Harrap, K.R. Eur. J. Cancer, 1980, 16, 1547

108. Kavai, I., Mead, L.H., Drobniak, J. and Zakrzewski, S.F. J. Med. Chem., 1975, 18, 272

109. Hitchings, G.H. and Burchall, J.J. Adv. Enzymol., 1965, 27, 417

110. Russell, P.B. and Hitchings, G.H. J. Am. Chem. Soc., 1951, 73, 3763

111. Bunnett, J.F. and Zahler, R.E. Chem. Rev., 1951, 49, 273

112. Anderson, E. and Capon, B. J. Chem. Soc. Perkin Trans. 2, 1972, 515

113. Emerson, W.S. Organic Reactions, 1948, 4, 174

114. Preston, P.N. and Tennant, G. Chem Rev., 1972, 72, 627

115. Singer, G.M. and Andrews, A.W. J. Med. Chem., 1983, 26, 309

116. Williams, D.H. and Fleming, I. In "Spectroscopic Methods in Organic Chemistry", 3rd ed., McGraw-Hill, London, 1980, p.74

117. Case, F.H. J. Am. Chem. Soc., 1925, 47, 1143

118. Pitea, D., Grasso, D. and Favini, G. J. Mol. Struct., 1971, 10, 101

119. Hoefnagel, A.J., Hoefnagel, M.A. and Webster, B.M. J. Org. Chem., 1978, 43, 4720

120. Benjamins, H. and Chandler, W.D. Can. J. Chem., 1974, 52, 597

121. Sekiya, M., Yanaihara, N. and Masui, T. Chem. Pharm. Bull., 1961, 9, 945

122. Lutz, R.E., Bailey, P.S., Rowlett, R.J., Jr., Wilson, III, J.W., Allison, R.K., Clark, M.T., Leake, N.H., Jordan, R.H., Keller, III, R.J. and Nicodemus, K.C. J. Org. Chem., 1947, 12, 760

123. Osborn, M.J. and Huennekens, F.M. J. Biol. Chem., 1958, 233, 969

124. Roth, B. Handb. Exp. Pharmakol., 1983, 64, 107

125. Engel, P.C. "Enzyme Kinetics: The Steady State Approach"; Chapman and Hall, London, 1977

126. Goldstein, A. J. Gen. Physiol., 1944, 27, 529

127. Morrison, J.F. Biochim. Biophys. Acta, 1969, 185, 269

128. Cha, S. Biochem. Pharmacol., 1975, 24, 2177

129. Morrison, J.F. Trends in Biochemical Sciences, 1982, 182

130. Henderson, P.J.F. Biochem. J., 1972, 127, 321

131. Jackson, R.C., Hart, L.I. and Harrap, K.R. Cancer Res., 1976, 36, 1991

132. BMD Biomedical Computer Programs, X-Series Supplement; Dixon, W.J., ed.; University of California Press, Berkeley, California, 1970, pp. 177-186. Modified by L. Hart - V3.6, 1985

133. Henderson, P.L. Biochem. J., 1973, 135, 101

134. Sirotnak, F.M., Moccio, D.M., Goutas, L.J., Kellener, L.E. and Montgomery, J.A. Cancer Res., 1982, 42, 924

135. Werbel, L.M., Hung, J., Besserer, J.A., Boritzki, T.J., Leopold, W.R. and Fry, D.W. In "Chemistry and Biology of Pteridines"; Cooper, B.A. and Whitehead, V.M., eds.; Walter de Gruyter & Co., Berlin, 1986, p. 69

136. Langdon, S.P. PhD Thesis, Aston University, 1983

137. Bertino, J.R. and Fischer, G.A. Meth. Med. Res., 1964, 10, 297

138. Lowry, O.H., Rosebrough, N.J., Farr A.L. and Randall, R.J. J. Biol. Chem., 1951, 193, 265

139. Webber, S. and Whiteley, J.M. Arch. Biochem. Biophys., 1985, 236, 681

140. Langdon, S.P., Gescher, A., Hickman, J.A. and Stevens, M.F.G. Eur. J. Cancer Clin. Oncol., 1984, 20, 699

141. Geran, R.I., Greenberg, N.H., MacDonald, M.M., Schumacher, A.M. and Abbott, B.J. Cancer. Chemother. Rep., 1972, 3, 1

142. Burchall, J.J. Handb. Exp. Pharmakol., 1983, 64, 60

143. Burchall, J.J. and Smith, S.L. Adv. Enz. Regul., 1980, 18, 349

144. Maag, H., Locher, R., Daly, J.J. and Kompis, I. Helv. Chim. Acta, 1986, 69, 887

145. Chubb, D., personal communication.

146. Andrews, P.R., Sadek, M., Spark, M.J. and Winkler, D.A. J. Med. Chem., 1986, 29, 698

147. Main, P., Fiske, S.J., Hull, S.E., Lessinger, L., Germain, P., Declercq, J.-P. and Woolfson, M.M. "MULTAN80. A System of Computer Programs for the Automated Solution of Crystal Structures from X-ray Diffraction Data", Univs. of York, England and Louvain, Belgium, 1980.

148. Sheldrick, G.M. "SHELX-76. Program for Crystal Structure Determination", Univ. of Cambridge, England, 1976.

149. Jencks, R.G. B.Sc. Project Report, The Polytechnic, Wolverhampton

150. Schwalbe, C.H. and Williams, G.J.B. Acta Cryst., **1982**, B38, 1840

151. Schwalbe, C.H. and Williams, G.J.B. Acta Cryst., **1987**, C43, 1097

152. CHEM-X, Chemical Design Ltd., Unit 12, 7 West Way, Oxford

153. Bryant, P.K., personal communication

154. Sutton, P.A. and Cody, V. In "The Chemistry and Biology of Pteridines", Walter de Gruyter & Co., Berlin, 1986, p. 969

155. Holden, J.R. and Dickinson, C. J. Phys. Chem., **1969**, 73, 1199

156. Blaney, J.M., Hansch, C., Silipo, C. and Vittoria, A. Chem. Rev., **1984**, 84, 333

157. Fukunaga, J.Y., Hansch, C. and Steller, E.E. J. Med. Chem., **1976**, 19, 605

158. Hansch, C., Silipo, C. and Steller, E.E. J. Pharm. Sci., **1975**, 64, 1186

159. Fukuyo, M., Hirotsu, K. and Higuchi, T. Acta Cryst., **1982**, B38, 640

160. Prasad, L., Gabe, E.J. and Le Page, Y. Acta Cryst., 1982, B38, 674

161. Dewar, M.J.S. and Thiel, W. J. Am. Chem. Soc., 1977, 99, 4899

161. Motherwell, W.D.S. and Clegg, W. "PLUTO78. Program for Plotting Molecular and Crystal Structures. Univ. of Cambridge, England, 1978

162. Tendler, S.J.B., personal communication.